TECHNISCHE UNIVERSITÄT MÜNCHEN

Lehrstuhl für Entwicklungsgenetik

Developmental wiring and adaptive plasticity of peripheral sensorimotor circuitry

Heidi Söllner

Vollständiger Abdruck der von der Fakultät Wissenschaftszentrum Weihenstephan für Ernährung, Landnutzung und Umwelt der Technischen Universität München zur Erlangung des akademischen Grades eines

Doktors der Naturwissenschaften

genehmigten Dissertation.

Vorsitzender: Univ.-Prof. Dr. E. Grill

Prüfer der Dissertation:

1. Univ.-Prof. Dr. W. Wurst
2. Univ.-Prof. Dr. M. Götz

(Ludwig-Maximillians-Universität München)

Die Dissertation wurde am 01.02.2012 bei der Technischen Universität München eingereicht und durch die Fakultät Wissenschaftszentrum Weihenstephan für Ernährung, Landnutzung und Umwelt am 09.05.2012 angenommen.

Für meine Eltern, Barbara & Martin

„To move things is all mankind can do ... whether whispering or felling a forest“

-Sir Charles Scott Sherrington-
(British neurophysiologist)

CONTENTS

I SUMMARY 1

I.1 Abstract 1

I.2 Zusammenfassung 4

II INTRODUCTION 7

II.1 Spinal sensorimotor circuits controlling vertebrate locomotion 7

II.1.1 Local spinal circuits 7

II.1.2 Higher ordered circuits to initiate and modulate locomotion 9

II.2 Generation and differentiation of sensorimotor circuit components 11

II.2.1 Neurogenesis and differentiation of interneurons and motor neurons 11

II.2.2 Sensory neurogenesis 14

II.3 Axon guidance and sensorimotor circuit formation 15

II.3.1 Principles of axon guidance 15

II.3.2 Peripheral sensorimotor circuit formation in the vertebrate limb 18

II.4 Plasticity of neuronal circuits 21

II.4.1 Circuit maturation in early postnatal neuronal networks 21

II.4.2 Plasticity in adult neuronal circuits under physiological and injury conditions 22

II.5 Aim of this thesis 24

II.5.1 Characterization of sensorimotor interactions during circuit formation 25

II.5.2 Characterization of forepaw impairments in *Olig2-Cre*$^{+}$*;Npn-1*$^{cond-/-}$ mutants 25

II.5.3 Analysis of adaptive plasticity in sensorimotor circuits during postnatal development 26

III MATERIAL AND METHODS 27

III.1 Mouse husbandry 27

III.1.1 Ethic statement 27

III.1.2 Mutant mice 27
III.1.3 Genotyping 27

III.2 Mouse embryo analysis 31
III.2.1 Whole mount staining 31
III.2.2 Quantification of the fasciculation status of motor and sensory axons 33
III.2.3 Immunohistochemistry 33

III.3 Screening for bone and cartilage phenotype 35
III.3.1 Alcian blue/Alizarin red differential staining of cartilage and bone 35
III.3.2 X-ray 36

III.4 Ultrastructural analysis of forelimb nerves 36
III.4.1 Electron microscopy 36
III.4.2 EM image analysis 39

III.5 Behavioural data acquisition and analysis 39
III.5.1 Experimental design and housing 39
III.5.2 Beam walking 40
III.5.3 Catwalk 40
III.5.4 Grip strength 41
III.5.5 Grid walking 41
III.5.6 Hind limb extension reflex 42
III.5.7 Hind limb paw placement accuracy 42
III.5.8 Nociception 43
III.5.9 Open field 43
III.5.10 Rotarod 44
III.5.11 Wire climbing 44
III.5.12 Statistical analysis 44

III.6 Neuroanatomical analysis 45
III.6.1 Anesthesia 45
III.6.2 Retrograde labelling of dorsal and ventral forelimb motor pools 45
III.6.3 Reconstruction of spinal motor pool representation 46
III.6.4 Scatter index calculation for dorsal and ventral motor pool spreading 46
III.6.5 Statistical analysis 47

III.7 Electrophysiology **47**
III.7.1 Anesthesia 47
III.7.2 Nerve stimulation 48
III.7.3 EMG recordings 48

IV RESULTS **49**

IV.1 Mutual dependency of growing motor and sensory axons for correct assembly of peripheral circuitry **49**
IV.1.1 Efficient genetic ablation of sensory or motor neurons 50
IV.1.2 Impaired formation of forelimb sensory trajectories after partial ablation of motor neurons in *Olig2-Cre^{+};DT-A^{floxed}* mice 51
IV.1.3 Sensory axons influence fasciculation and timing of co-extending motor projections to the forelimb 56

IV.2 Musculoskeletal, neuromuscular and functional forelimb deficits in postnatal mice that lack *Npn-1* on motor neurons **59**
IV.2.1 Characterization of forepaw flexor posturing in *Olig2-Cre^{+};Npn-1$^{cond-/-}$* neonatal mice 60
IV.2.2 Reduced dorsal forelimb extensor muscle area and further postnatal degeneration in affected mutants 62
IV.2.3 Skilled locomotion is impaired in *Olig2-Cre^{+};Npn-1$^{cond-/-}$* mutants 64
IV.2.4 Postnatal bone malformations in the affected forepaw of *Olig2-Cre^{+}; Npn-1$^{cond-/-}$* mutants 67
IV.2.5 Alterations in the fiber composition of *N.radial* in *Olig2-Cre^{+};Npn-1$^{cond-/-}$* mutants 69

IV.3 Adaptive structural plasticity parallels motor recovery in a model of neurodevelopmental miswiring **73**
IV.3.1 Specific deficits in motor coordination in *Sema3F* mutant mice 73
IV.3.2 Loss of *Npn-2* leads to additional motor impairments 76
IV.3.3 Disturbed organisation of medial LMC neurons in *Sema3F* poor performers 78
IV.3.4 General behavioural stimulation in an enriched environment enhances recovery of motor skills in *Sema3F* mutant mice 81

IV.3.5 Aberrant activation of dorsal muscles upon stimulation of a ventral nerve in *Sema3F* mutants 83
IV.3.6 Overview of behavioural phenotyping in *Sema3F* and *Npn-2* mutants 86

V DISCUSSION 87

V.1 Coupling of sensory and motor axons during peripheral circuit assembly 88
V.1.1 Axon-axon interactions 88
V.1.2 Axon-glia interaction 92
V.1.3 Maintenance of developmental defects if Npn-1 is removed from motor or sensory neurons 93

V.2 Characteristic forelimb deficits in postnatal *Olig2-Cre^{+};Npn-1$^{cond-/-}$* mice 95
V.2.1 *Claw paw*-like forelimb phenotype observed in *Olig2-Cre^{+};Npn-1$^{cond-/-}$* mice 95
V.2.2 Putative role of Npn-1 in radial sorting 96
V.2.3 Congenital muscle atrophy and postnatal muscle degeneration in *Olig2-Cre^{+};Npn-1$^{cond-/-}$* mice 99
V.2.4 Oligodendrocyte precursors appear normal in *Olig2-Cre^{+};Npn-1$^{cond-/-}$* mutants 100

V.3 Adaptive structural plasticity parallels motor recovery after *Sema3F-Npn-2* induced embryonic circuit miswiring 102
V.3.1 Embryonic circuit miswiring in *Sema3F* and *Npn-2* mutants causes a distinct locomotor phenotype 102
V.3.2 Adaptive structural plasticity in *Sema3F* mutant mice 104
V.3.3 Role of supraspinal input in postnatal neural plasticity 105
V.3.4 Functional wiring of peripheral circuits in adult *Sema3F* mutants corroborates embryonic pathfinding deficits 106
V.3.5 Excitability of peripheral limb circuits is unchanged in *Sema3F* mutants 108
V.3.6 Enriched environment housing promotes structural plasticity paralleled by improvement of motor coordination in *Sema3F* mutants 109

V.4 Neurodevelopmental circuit miswiring and postnatal consequences 112

VI REFERENCES 114

VII APPENDIX **141**

VII.1 Abbreviations **141**

VII.2 Index of figures **145**

VII.3 Index of tables **147**

VII.4 Acknowledgements **148**

I SUMMARY

I.1 Abstract

During embryonic development neuronal circuits are wired with high precision to later on enable a wide variety of movements ranging from basic reflexes to the virtuoso body movements of professional dancers. Guidance receptors on the axonal surface direct growing fibers through interactions with environmentally-derived attractive or repellent cues in a step-wise manner to their assigned, often distant targets. Peripheral sensorimotor circuits with efferent spinal motor axons innervating target muscles and afferent sensory fibers projecting on self motor neurons provide an excellent model to study molecular mechanisms of developmental wiring and postnatal adaptive processes.

Although there is substantial knowledge on the mechanisms and cues involved in axon-environment interactions during neural circuit wiring, the role of cross-talk between homo- or heterotypic axonal projections is less well characterized. One scope of this work was to analyse the impact of trans-axonal communication between growing sensory and motor projections on correct circuit wiring. Genetic ablation of either motor or sensory neurons by cell type-specific expression of a lethal diphtheria toxin-A allowed for a critical reduction of motor or sensory neurons present in the spinal cord or DRG, respectively. Based on classical experiments involving surgical manipulation in chick embryos a dependency of sensory axons on the presence of motor axons for circuit formation was postulated. Using a genetic ablation approach, I further refined the results obtained from these elegant but coarse surgical ablation experiments. During murine sensorimotor circuit wiring, sensory axons require solely a minimal scaffold of motor projections for the formation of stereotyped nerve patterns. In addition, sensory axons mediate the fasciculation of motor projections as well as their timing of ingrowth into the developing limb. The insights from this research project thus contribute to the knowledge of mutual dependency of axonal projections for correct sensorimotor circuit formation during embryogenesis.

Selective loss of the axon guidance receptor Npn-1 on motor neurons and oligodendrocytes during development elicited extensive defasciculation of motor

projections and hindered their correct ingrowth to the limb. Postnatally, *Olig2-Cre*$^{+}$*; Npn-1*$^{cond-/-}$ mice revealed arthrogryposis-like abnormal forepaw posturing. In this project, we addressed the underlying cause for the aberrant forelimb phenotype. Using EMG recordings in forelimb extensor muscles and immunohistochemistry, we showed that the loss of active extension in the affected forepaw is permanent and associated with congenital muscle atrophy. On the ultrastructural level we found an abnormal distribution and sorting of axonal fibers in the radial nerv innervating extensor muscles but not in other nerves exclusively innervating forelimb flexors. Since we did not observe compensation for the abnormal forelimb posture in *Olig2-Cre*$^{+}$*;Npn-1*$^{cond-/-}$ mice, these mutants may serve as a model to analyse consequences and mechanisms of congenital muscle atrophy with subsequent progressive degeneration postnatally.

Early postnatal, neuronal networks are particularly sensitive to modifications in the environment or traumatic injury and react with impressive plastic adaptations to changed circumstances. Thereafter, in adult vertebrates, structural and functional plasticity after experimental injury or trauma to the CNS is limited. The molecular, anatomical and physiological characteristics of the underlying early postnatal neuroplasticity are not well understood. We focused on the characterization of postnatal functional impairments and subsequent adaptive processes in mouse models with genetically induced miswiring of neural networks. Loss of Sema3F-Npn-2 signalling results in characteristic and specific defects in dorsal-ventral limb innervation. Since *Sema3F* and *Npn-2* mutants are viable they provide excellent models to analyse postnatal adaptive plasticity after genetically-induced sensorimotor circuit miswiring. We employed a comprehensive approach of behavioural phenotyping as well as detailed neuroanatomical analysis and functional characterization of the underlying circuitry. *Sema3F* and *Npn-2* mutants segregated according to their motor capabilities into two groups of wildtype-like and poor performers, the latter with particularly poor motor coordination skills. In addition, there is a tight correlation of impaired motor coordination skills to an abnormal distribution of specific forelimb motor pools on a single animal level. Moreover, both motor coordination deficits as well as abberrant localization of distinct spinal motor pools are ameliorated by housing *Sema3F* mice in an enriched environment.

The presented mouse models of genetically-induced neuronal circuit miswiring are a suitable alternative to prevailing experimentally-induced injury models to

identify conditions that promote neuroplasticity. Thereby, extrinsic stimulation such as enriched environment housing or locomotor training can be screened for beneficial impact on plastic properties. Furthermore, the contribution of drug therapies aiming at attenuating cues inhibiting axonal regeneration in the adult CNS – applied alone or in combination with enriched environment or training – can been determined.

I.2 Zusammenfassung

Während der Embryonalentwicklung werden die neuronalen Netzwerke mit hoher Präzision verschaltet, um dem Organismus nach der Geburt eine Vielzahl an Bewegungen zu ermöglichen, von einfachsten Reflexen bis hin zu den virtuosen Körperbewegungen professioneller Tänzer. Durch die Wechselwirkung von anziehenden oder abstoßenden Wegleitungsfaktoren in der Umgebung mit Rezeptoren auf der Oberfläche der Axone werden die auswachsenden Fasern schrittweise zu ihren oft weit entfernten Zielen geführt. Periphere sensomotorische Netzwerke aus efferenten Motoneuronen, die die Zielmuskeln innervieren, und sensorischen Afferenzen, welche auf diese Motoneurone zurück projizieren, sind ein gutes Modell, um die Prozesse und Mechanismen der Netzwerkbildung und postnataler Plastizität zu untersuchen.

Obwohl die Mechanismen und Wegleitungsfaktoren für die Interaktionen zwischen Axon und Umwelt bekannt sind, ist die Bedeutung der Kommunikation zwischen hetero- oder homotypischen Axonen weniger gut charakterisiert. Ziel der vorliegenden Arbeit war es, den Einfluss der transaxonalen Kommunikation zwischen auswachsenden motorischen und sensorischen Fasern auf die neuronale Verschaltung zu untersuchen. Ablation von motorischen oder sensorischen Neuronen durch zell-spezifische Expression des tödlichen Diptheria Toxin A ermöglichte es, die Anzahl der Motoneurone im Rückenmark oder der sensorischen Neuronen in den Spinalganglien (DRG) signifikant zu reduzieren. Klassische Untersuchungen in Hühnerembryonen, bei denen die Motoneurone operativ entfernt wurden, postulieren eine Abhängigkeit der sensorischen von anwesenden motorischen Fasern während der neuronalen Verschaltung. Durch eine zelltyp-spezifische, genetisch induzierte Elimination konnte ich die Ergebnisse aus diesen frühen, eleganten, aufgrund der chirurgischen Ablation aber stark invasiven Experimenten, weiterentwickeln. Sensorische Axone benötigen während der Verschaltung der sensomotorischen Netzwerke nur ein minimales Gerüst an motorischen Projektionen zur Bildung korrekter, stereotyper Nervverzweigungen. Desweiteren zeigen meine Ergebnisse, dass sensorische Axone die Faszikulierung und das zeitliche Einwachsen der motorischen Fasern in die Gliedmaßen steuern.

Die Resultate dieses Forschungsprojekts machen deutlich, wie wichtig die Kommunikation zwischen heterotypen Fasersystemen ist und tragen daher zum

Wissen der molekularen Mechanismen bei, welche die fehlerfreie Bildung sensomotorischer Netzwerke steuern.

Der Verlust des Rezeptors Npn-1 auf Motoneuronen und Oligodendrozyten während der Embryonalentwicklung rief eine erhebliche Defaszikulierung der motorischen Projektionen hervor und beeinträchtigte deren Einwachsen in die Extremitäten. Postnatal zeigen diese *Olig2-Cre*$^{+}$*;Npn-1*$^{cond-/-}$ Mäuse eine krankhafte Beugung der Vorderextremitäten ähnlich einer angeborenen Gelenksteife (Athrogryposis). In diesem Projektteil untersuchten wir die zugrundeliegenden Ursachen für den ungewöhnlichen Phänotyp in den Vorderextremitäten. Mittels einer Kombination aus Elektromyographie (EMG) und immunhistochemischen Färbungen in den Extensormuskeln der Vorderfüße zeigten wir, dass der Verlust der aktiven Streckung in der betroffenen Vorderpfote mit angeborenem Muskelschwund einhergeht. Auf ultrastruktureller Ebene fanden wir eine Fehlverteilung der axonalen Fasern nur im Radialisnerv, welcher die Extensormuskeln innerviert, aber nicht in Nerven, die die Flexoren versorgen. Nachdem *Olig2-Cre*$^{+}$*;Npn-1*$^{cond-/-}$ Mäuse die krankhafte Beugung ihrer Vorderextremitäten nicht kompensieren, sind diese Mutanten geeignete Modelle, um die Auswirkungen und zugrundeliegenden Mechanismen des angeborenen Muskelschwunds mit fortschreitender postnataler Degeneration zu untersuchen.

Kurz nach der Geburt zeigen neuronale Netzwerke ein beeindruckendes, plastisches Anpassungsvermögen auf veränderte Umweltbedingungen oder Verletzungen. In adulten Wirbeltieren hingegen ist die strukturelle und funktionale Plastizität nach Verletzung des Zentralnervensystems eingeschränkt. Die zugrundeliegenden Merkmale molekularer, struktureller und funktioneller Neuroplastizität sind nicht umfassend bekannt. Wir konzentrierten uns auf die Beschreibung postnataler motorischer Beeinträchtigungen und anschließender adaptiver Vorgänge in Mausmodellen mit genetisch induzierter Fehlverschaltung in neuronalen Netzwerken. Verlust des Sema3F-Npn-2 Signalwegs während der Bildung der Netzwerke im Embryo führt zu charakteristischen Fehlern in der Innervation der dorsalen und ventralen Beinmuskulatur. Da *Sema3F* und *Npn-2* Mutanten lebensfähig sind, stellen sie geeignete Mausmodelle dar, um adaptive Plastizität nach genetisch induzierter Fehlverschaltung der sensomotorischen Netzwerke zu analysieren. Dazu verwendeten wir einen umfassenden Ansatz bestehend aus einer Batterie an Verhaltenstests, ausführlichen Analysen der

Neuroanatomie und funktionelle Beschreibung der zugrundeliegenden Netzwerke. *Sema3F* und *Npn-2* Mutanten teilen sich entsprechend ihren motorischen Fähigkeiten in zwei Gruppen auf: Ein Teil der Mutanten verhält sich Wildtyp-ähnlich während der andere Teil deutliche Defizite in der Motorkoordination aufweist. Zusätzlich korrelieren die koordinatorischen Fähigkeiten eines Tieres eng mit der Verteilung bestimmter Motoneuronenpools im Rückenmark, so dass Tiere mit stark beeinträchtigtem Verhalten auch weniger kompakte Motorpools aufwiesen. Interessanterweise bessert eine reizreichere *„enriched environment“* Haltung nicht nur die motorischen Defizite, sondern behebt auch die vermehrte Streuung bestimmter Motoneuronenpools im Rückenmark von *Sema3F* Mutanten.

Die vorgestellten Mausmodelle mit genetisch hervorgerufenen Fehlverschaltungen neuronaler Netzwerke sind geeignete Alternativen zu den vorherrschenden Modellen basierend auf experimenteller Verletzung des Nervensystems, um Gegebenheiten zu identifizieren, die plastische Vorgänge fördern. Extrinsische Stimulation durch eine reizreichere Umwelt oder motorisches Training kann hinsichtlich des positiven Einflusses auf das plastische Vermögen untersucht werden. Desweiteren kann der Beitrag medikamentöser Therapien bestimmt werden, die das Ziel haben, die Wirkung hemmender Faktoren auf axonale Regeneration abzuschwächen - allein oder in Kombination mit *„enriched environment“* Haltung und Training.

II INTRODUCTION

The vertebrate nervous system is designed to enable movements ranging from very basic withdrawal reflexes to complex behaviours such as the flight of birds or the skilled body movements of a professional dancer. To initiate and control these movements, higher-ordered central circuits interact with local peripheral networks. These neural circuits are wired with high accuracy during embryonic development, shaped to perfection by experience postnatally and are able to adapt to altered environmental conditions or lesions to various degrees.

II.1 Spinal sensorimotor circuits controlling vertebrate locomotion

Control of locomotion is achieved on two levels with spinal cord central pattern generator (CPG) units operating autonomously to produce basic rhythmic outputs including sensory feedback information (Grillner, 2003). The second element of locomotor control are supraspinal descending pathways essential for initiation and termination of movements, motor coordination, posture and anticipatory adjustments (Rossignol, 1996).

II.1.1 Local spinal circuits

Studies with decerebrated or spinalized animals in the late 19th and early 20th century reported that the spinal cord is still capable to elicit locomotor-like movements even if it is isolated from higher-ordered central structures (reviewed in Clarac, 2008; Guertin, 2009). After midthoracic or cervical transection in cats, “reflex stepping” on a treadmill and alternating limb movements were observed (Forssberg *et al.*, 1980a; Forssberg *et al.*, 1980b; Barbeau & Rossignol, 1987; Lovely *et al.*, 1990). This is achieved by local microcircuits in the vertebrate spinal cord: the central pattern generator. Although, CPG development and rhythm generation are independent of sensory input (Brown, 1914; Suster & Bate, 2002), sensory afferents have an essential modulatory feedback function: loss of sensory input generates robot-like

locomotion which cannot react or adapt to e.g. obstacles in the environment (Grillner, 1985; 2006; Rossignol *et al.*, 2006). Besides simple movements such as the described “reflex stepping”, CPGs generate also divergent locomotion pattern like swimming in the lamprey (reviewed in Grillner, 2003).

Another example for such a stereotyped movement is the monosynaptic reflex. In this sensorimotor circuit, motor neurons in the ventral horn of the spinal cord transmit the activation signal to the muscles via the peripheral nerves. Proprioceptive type Ia afferents provide feedback information from the muscle to the motor neurons so that the spinal reflex response is constantly controlled and modulated (Fig. 1; Lloyd, 1943b; a; Eccles *et al.*, 1957). Thus, fundamental reflexes and simple movements are autonomously controlled by CPGs in the spinal cord.

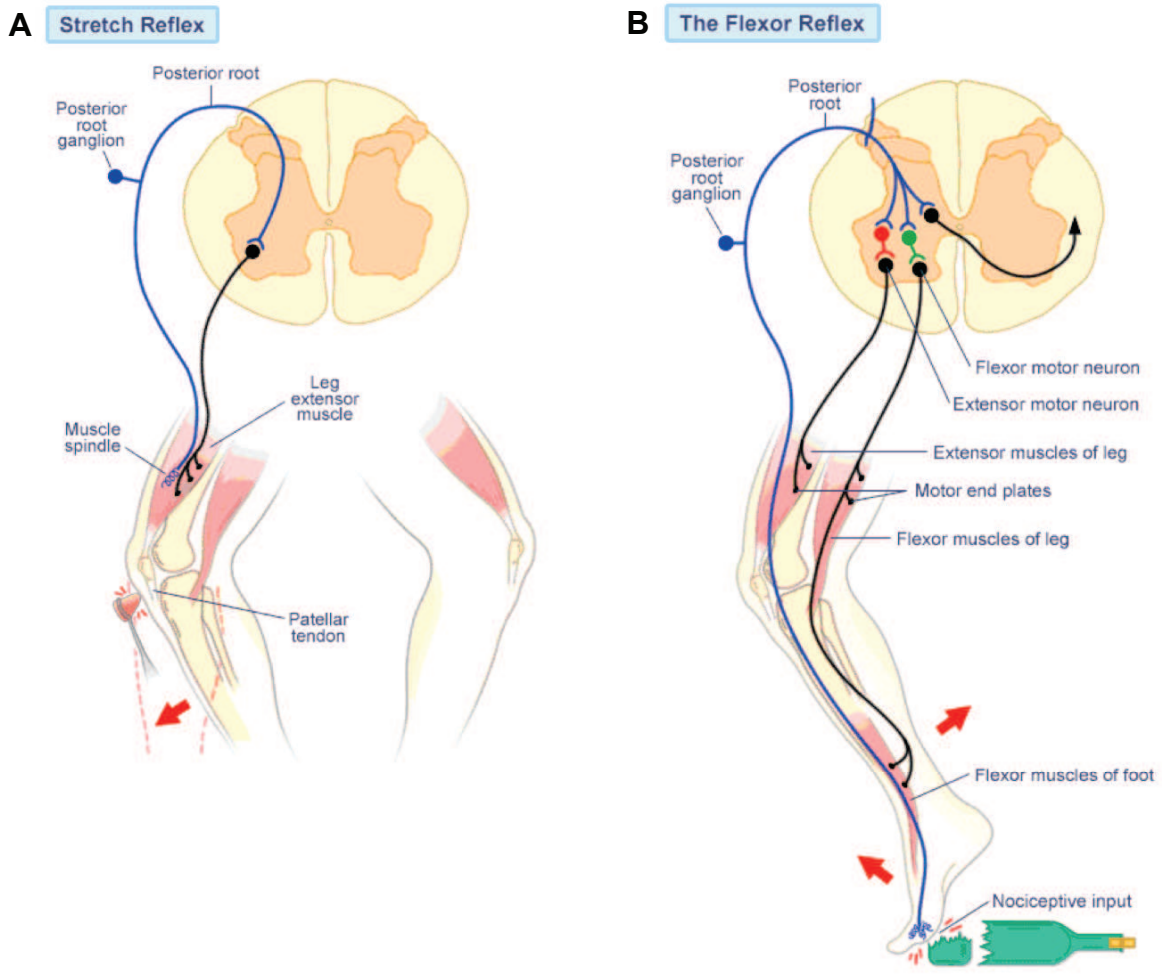


Figure 1: Components of mono- and polysynaptic reflex circuits.
Schematic illustration of spinal monosynaptic (A) and polysynaptic (B) reflex circuits. In more complex reflex circuits, this simple module is extended by interneurons which allow for inhibition of simultaneous activity of antagonistic muscles. (Pictures taken from URL on 19.12.2011: http://alexandria.healthlibrary.ca/documents/notes/bom/unit_6/lec%2025_moo_spinreflex.xml).

Pioneering studies on the coordination of more complex locomotor behaviour disproved the initial concept of simply combining reflex circuits in chains to generate intricate movements (Brown, 1911; Von Holst, 1935). Nowadays, the central pattern generator networks are regarded as the basic spinal “motor infrastructure” for precise locomotor rhythm and pattern generation both in vertebrates and invertebrates (reviewed in Grillner, 2006); however, the exact organisation of CPG networks is still obscure. Studies in lamprey identified the core of the CPG microcircuit as a pool of excitatory driven interneurons that operate in the absence of inhibitory neurons but depend on inhibitory interactions for the coordination of network activity (Cangiano & Grillner, 2003; 2005). Additional interneuron subpopulations seem to play essential roles in generating frequency, amplitude and bilateral coordination of rhythmic locomotor activity (Kullander *et al.*, 2003; Lanuza *et al.*, 2004; Gosgnach *et al.*, 2006; reviewed in Guertin, 2009).

II.1.2 Higher ordered circuits to initiate and modulate locomotion

Surprisingly, simple stepping movements can be elicited in complete absence of higher-ordered input (Bjursten *et al.*, 1976). However, these stereotyped movements are far from the coordinated and intricate patterns of skilled locomotion such as fine tuned grasping. A plethora of data from lesion studies, electrophysiological stimulation analysis and neuroimaging unraveled the role of supraspinal structures in driving and controlling the local spinal microcircuits (reviewed in Goulding, 2009).

Higher-order centers in the CNS of vertebrates serve a dual role in both initiation and modulation of voluntary locomotion. Instructive signals that initiate, terminate and modulate locomotion are either delivered directly by the corticospinal tract or indicrectly via the reticulo-, rubro- and vestibulospinal tracts in the brainstem to local spinal CPG circuits. Thereby, supraspinal control of movement is accomplished by two distinct locomotor systems: initiation/termination in the basal ganglia and fine-tuning of locomotion by motor cortex and cerebellum (Fig. 2).

The basal ganglia operate as an interface in the forebrain which filters, integrates and processes accumulating information from cortical areas, thalamic nuclei, amygdala, hippocampus and dorsal raphe (Bolam *et al.*, 2000; Yin & Knowlton, 2006; Kravitz *et al.*, 2010). Consequently, defects in structures of the basal ganglia such as loss of striatal projection neurons (Huntington’s disease) or

modulatory input from nigrostriatal neurons (Morbus Parkinson) unveiled characteristic deficits in locomotor termination and initiation, respectively (Graybiel *et al.*, 1994; Hickey *et al.*, 2008; Poewe & Mahlknecht, 2009).

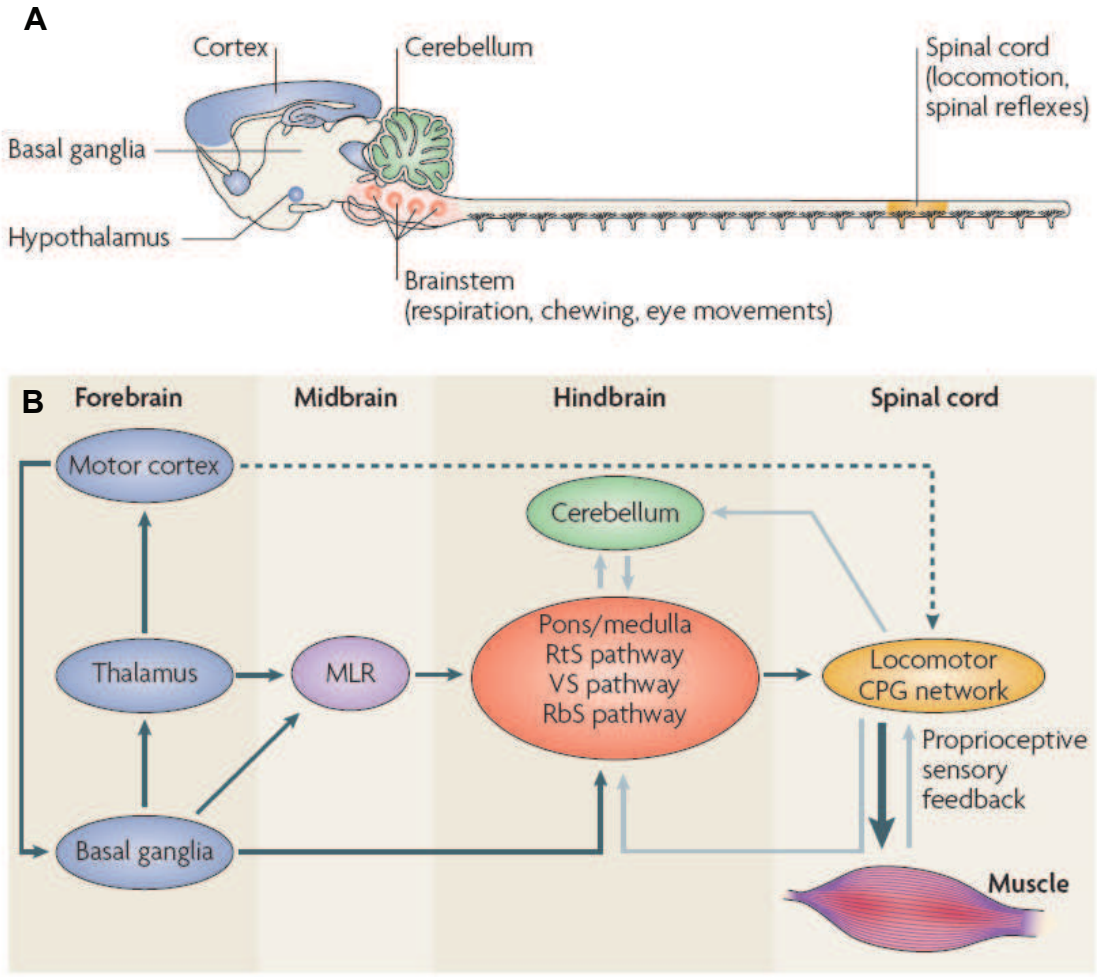


Figure 2: Supraspinal and local control of locomotion in vertebrates.
(A) Schematic illustration of CNS regions in the brain and spinal cord of rodents involved in the control and generation of locomotion. (B) Detailed scheme of interactions among supraspinal and spinal motor pathways. Black arrows indicate direct commands, grey arrows feedback loops and the dotted line represents the corticospinal tract directly projecting on spinal motor neurons for refinement of skilled movement. (Pictures taken from Goulding, 2009).

Fine-tuning of locomotor performance is achieved by two structures, the motor cortex in the forebrain and the cerebellum in the hindbrain. Pyramidotomy of the cortical spinal tract (CST) or damage to the motor cortex solely slightly affect simple, stereotyped movements but lesioned animals revealed significant deficits in posture and skilled motor tasks (Bjursten *et al.*, 1976; Grillner & Zangger, 1979; Armstrong, 1988; Drew *et al.*, 2004).

Besides the motor cortex, the cerebellum is also involved in the coordination of movements with a particular emphasis on smoothness, speed and precision of motor activity. Thereby, it processes sensory feedback from spinal circuits and transmits its modulatory commands via brainstem tracts to local circuits in the spinal cord (Grillner, 2006; Goulding, 2009). *Lurcher* mutant mice which lost their majority of cerebellar Purkinje and 90% of the granule cells by 65 days of age, show characteristic cerebellar ataxic gait signs and have deficits in rapid alternating movements (Fortier *et al.*, 1987).

In summary, the motor infrastructure to generate movement in vertebrates comprises the CPGs in the spinal cord as basic units and higher-ordered brain structures and tracts for initiation, termination and fine control of voluntary locomotion.

II.2 Generation and differentiation of sensorimotor circuit components

How are the numerous individual neuronal subtypes generated and differentiated from their common progenitors? During embryogenesis interneurons and motor neurons are generated in the ventricular zone from distinct progenitor domains along the dorsal-ventral axis of the spinal cord. Opposite gradients of two paracrine factors, Sonic hedgehog (Shh) and Bone morphogenic proteins (BMP), polarize the neural tube and instruct transcription factor cascades (reviewed in Lupo *et al.*, 2006). The precursors of sensory neurons, the neural crest cells (NCC), emerge at the dorsal boundary between the neural tube and the overlying epidermal ectoderm.

II.2.1 Neurogenesis and differentiation of interneurons and motor neurons

The key structures essential for motor and interneuron generation were identified by transplantation experiments of ventral neural tube components. Removal of the notochord or floor plate cells resulted in failure of motor neuron generation whereas conversely, supernumerary notochord or floor plate cells induced motor neurons in ectopic areas of the neural tube (Placzek *et al.*, 1991; Yamada *et al.*, 1991). Thereby, diffusible Shh secreted by the notochord and floor plate cells builds up a concentration gradient of ventral high to dorsal low (Roelink *et al.*, 1995; Ericson *et al.*, 1997a; Ericson *et al.*, 1997b).

Shh controls the expression of homeodomain (HD) transcription factors to define and maintain the five progenitor domains where interneuron subtypes and motor neurons evolve from (Fig. 3A). Graded activity of Shh represses class I (e.g. Pax6; Dbx2) and concomitantly induces class II (e.g. Nkx2.2; Nkx6.1) HD transcription factors along the dorsal-ventral axis in a concentration-dependent manner. Mutual repression between class I and II HD proteins additionally contributes to the demarcation of progenitor domains (Ericson *et al.*, 1997b; Briscoe *et al.*, 1999; Pierani *et al.*, 1999; Vallstedt *et al.*, 2001). In addition to Shh, retinoids and fibroblast-growth-factor (FGF) influence the expression profile of class I and II HD proteins for proper delineation of the pMN domain. Thereby, FGF signalling strongly supresses class I but only weakly class II HD proteins whereas retinoids (RA) enhance the expression of class I HD proteins. RA signals have additional roles in transcriptional activation of the basic helix-loop-helix transcription factor Olig2 that is essential for motor neuron and oligodendrocyte specification (Novitch *et al.*, 2003; Briscoe & Novitch, 2008). Olig2 serves a dual role in conferring motor neuron subtype identity and inducing the expression of pan-neuronal markers (Fig. 3B; Mizuguchi *et al.*, 2001; Novitch *et al.*, 2001). Within motor neuron progenitors, Olig2 in conjunction with RAs regulates subtype-specific HD protein expression of MNR2, Lim3 and postmitotically Isl1/2 and Hb9 (Pfaff *et al.*, 1996; Jurata *et al.*, 1998; Tanabe *et al.*, 1998; Briscoe *et al.*, 2000; Novitch *et al.*, 2003).

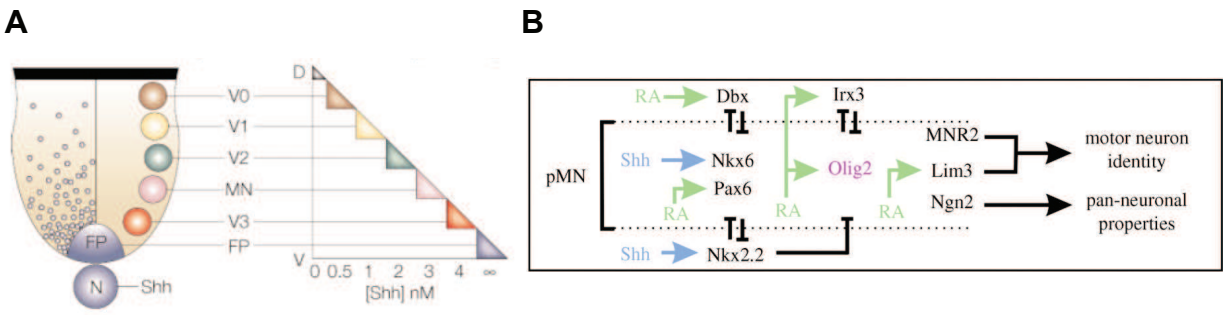


Figure 3: Induction of progenitor domains in the neural tube and subsequent generation of motor neurons.

(A) Formation of progenitor domains for generation of interneurons (V0-V3) and motor neurons (pMN) based on a Shh concentration gradient of dorsal low to ventral high. FP= floor plate; Shh= sonic hedgehog, N= notochord. (Picture taken from Jessell, 2000). (B) Scheme illustrating the combinatorial action of HD transcription factors and their downstream targets for generation of motor neurons. The combinatorial action of Pax6, Nkx6.1 and Olig2 delineates the progenitor domain pMN for oligodendrocyte and motor neuron generation and subsequently induces the genesis of $Isl2^{+}$ or $Hb9^{+}$

postmitotic motor neurons. Pan-neuronal properties are conferred by co-expression of Olig2 and Neurogenin-2 (Ngn-2). (Picture taken from Briscoe & Novitch, 2008).

All motor neurons derive from this single pMN domain in the ventral half of the developing spinal cord but each individual motor neuron has a distinct connectivity pattern. How do the newborn motor neurons acquire their unique subtype identity according to their prospective peripheral targets? Anatomical tracing studies revealed a columnar organisation of motor neurons along the rostro-caudal axis of the spinal cord and clustering of motor neurons innervating the same muscle into distinct motor pools (Romanes, 1951; Landmesser, 1978a; b; Hollyday, 1980; Gutman *et al.*, 1993). This columnar and pool specification is imposed on motor neurons by a transcriptional network of Hox genes (Fig. 4; Dasen *et al.*, 2005). Motor neurons supplying the approximately 50 different muscles of a limb (Sullivan, 1962; Romanes, 1964; Vanderhorst & Holstege, 1997) are located within the lateral motor columns (LMC) present at brachial and lumbar spinal levels (Landmesser, 1978b; Hollyday, 1980; Hollyday & Jacobson, 1990; Landmesser, 2001). Expression of Hox6 paralogs at cervical level and Hox10 proteins at lumbar level specifies brachial and lumbar LMC motor neurons, respectively (Dasen *et al.*, 2003; Shah *et al.*, 2004; Wu *et al.*, 2008). Within the LMC, motor axons innervating extensor muscles in the dorsal limb are located in the lateral subdivision whereas axons from the medial LMC (LMCm) project ventrally to flexor muscles (Landmesser, 1978a; Landmesser, 2001). At the molecular level, this divisional specification of motor neuron subclasses can be distinguished by expression of a LIM homeodomain protein code: LMCl motor neurons co-express Isl1 and Lim1 and LMCm axons are $Isl1^{+}$, $Isl2^{+}$ (Tsuchida *et al.*, 1994; Ensini *et al.*, 1998; Kania *et al.*, 2000; Sharma *et al.*, 2000).

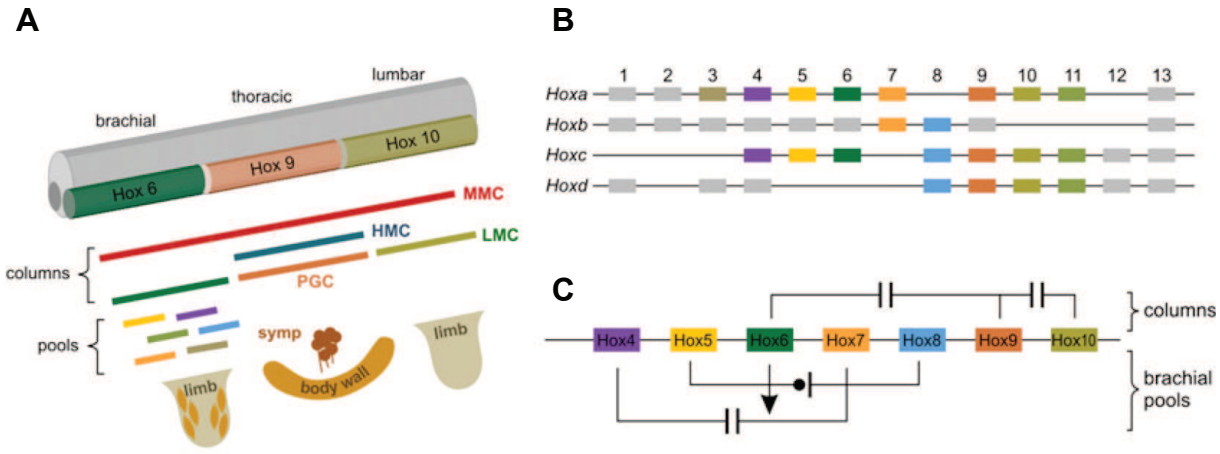


Figure 4: Transcriptional network of Hox genes for columnar and pool specification of motor neurons.

(A) Expression of Hox proteins along the rostral-caudal axis of the spinal cord and organisation of motor neurons into columns and muscle-specific pools. (B) Classification of Hox gene clusters involved in conferring spinal motor neuron identity. (C) Order of chromosomal Hox clusters and regulatory interactions for columnar and pool fate specification of motor neurons in the brachial spinal cord. MMC= medial motor column, HMC= hypaxial motor column; PGC= preganglionic motor column; LMC= lateral motor column; Symp= sympathetic chain ganglion neurons. (Pictures taken from Dasen *et al.*, 2008).

In summary, each newly generated motor neuron emerging from the pMN domain in the ventral spinal cord is impressed with a hierarchical columnar, divisional and pool specification and is already primed for its assigned peripheral target prior to its axon exiting the spinal cord (Lance-Jones & Landmesser, 1980a; b; 1981b; Ferguson, 1983; Jessell, 2000). Additionally, target-derived cues regulate the neuromuscular innervation patterns as well as the positioning and clustering of distinct motor pools by inducing the expression of pool-specific transcriptions factors such as the ETS gene Pea3 in motor neurons innervating the muscle *Cutaneous maximus* (Lin *et al.*, 1998; Livet *et al.*, 2002; Vrieseling & Arber, 2006; Ladle *et al.*, 2007).

II.2.2 Sensory neurogenesis

Trunk sensory neurons are derived from transient, migratory neural crest cells (NCC) formed between the neuronal and epidermal ectoderm at the dorsal-most region of the neural tube. The induction, specification and delamination from their site of origin as well as the terminal differentiation of NCCs are regulated by four key transcription factors. Wnts (wingless and int), BMPs (bone morphongenic proteins), Delta/Notch and FGF (fibroblast growth factor) serve as inductive signals for NCC formation and activate the expression of downstream neural crest specifier genes. Among others, SoxE transcription factors act as neural specifiers by impressing a lineage identity on pre-migratory or delaminating NCCs (reviewed in Sauka-Spengler & Bronner-Fraser, 2008). Loss of all sensory neurons in the dorsal root ganglia (DRG) in *Neurogenin-1/2* double mutant mice demonstrates the pivotal role of the proneuronal genes for the terminal specification of NCC to peripheral sensory neurons (Chen & Frank, 1999; Ma *et al.*, 1999). From their site of origin at the dorsal border of the spinal cord, trunk NCCs of prospective spinal sensory neurons migrate ventrally through the

anterior part of the sclerotome to form the DRG (Rickmann *et al.*, 1985; Loring & Erickson, 1987; Teillet *et al.*, 1987). By the time the sensory neurons accumulate and coalesce to the DRG, they co-express the POU HD transcription factor Brn3.0/3a and the LIM HD factors Isl1 and 2 (Ericson *et al.*, 1992; Tsuchida *et al.*, 1994; Xiang *et al.*, 1995). In contrast to motor neurons, postmitotic sensory neurons are not conferred with a columnar or pool identity, nor does a topographic correlation between their position in the spinal cord and DRG exist. However, three functional classes among sensory neurons can be distinguished by the expression of receptor tyrosine kinases (trk) for survival promoting neurotrophins. Nociceptors express the receptor tyrosine kinase $trkA^+$ for the nerve growth factor (NGF) and among cutaneous sensory neurons, $trkB^+$ mechanoreceptors bind brain-derived neurotrophic growth factor (BDNF) whereas $trkC^+$-NT-3 (neurotrophin-3) signalling ensures survival of proprioceptive neurons (Kaplan *et al.*, 1991; Klein *et al.*, 1991; Barbacid, 1994; Bibel & Barde, 2000).

II.3 Axon guidance and sensorimotor circuit formation

Each of the approximately 50 muscles present in a vertebrate limb is innervated by motor and sensory projections in an accurate and reliable manner. How are developing axons guided from their site of origin to their final target and eventually wire peripheral sensorimotor circuits for limb locomotion?

II.3.1 Principles of axon guidance

Neuronal circuits are established and wired with high precision during embryogenesis. For an individual axon, this requires correct navigation from the source of origin in the CNS to distant targets. Thereby, the growth cone, a highly motile structure at the axonal tip, senses the environment and reacts to extrinsic guidance cues present in the surrounding tissues *en route* (Goodman & Shatz, 1993; Tessier-Lavigne & Goodman, 1996). Four different guidance mechanisms, namely attraction and repulsion of growth cones either mediated by direct contact or long-range chemotaxis, coordinate the overall pathfinding and organisation of growing axons into nerve bundles and tracts (Fig. 5). Several phylogenetically highly conserved ligand-receptor pairs have been identified in the past years. Netrins, Slits,

Semaphorins and Ephrins constitute the four major families of guidance cues. Additionally, morphogens, growth factors as well as extracellular matrix (ECMS) and cell adhesion molecules (CAMs) are likewise involved in neuronal circuit formation (reviewed in Tessier-Lavigne & Goodman, 1996; Dickson, 2002; Kolodkin & Tessier-Lavigne, 2011).

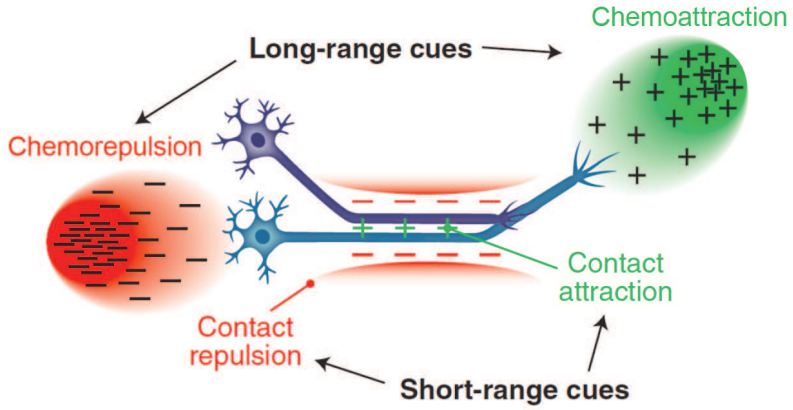


Figure 5: Functional diversity of neuronal guidance cues.
Axon guidance cues can elicit attraction or repulsion over short or long distance. (Picture modified from Kolodkin & Tessier-Lavigne, 2011).

How are the first pioneering axons guided by axon-environment interactions over long distances e.g. from their position in the spinal cord to their respective target muscle in the limb? Studies in insects proposed segmentation of the total trajectory into intermediate targets including choice points with landmark or guidepost cells located along the axonal pathway (Ho & Goodman, 1982; Klose & Bentley, 1989). Data from different vertebrate model systems suggest that axons of later-born neurons preferentially travel along pre-existing tracts laid out by preceeding pioneer axons. Thereby, follower axons contact and tightly associate with fascicles of pioneer axons using cell surface or ECM molecules (Hjorth & Key, 2002; Fekete & Campero, 2007; Pittman *et al.*, 2008; Niquille *et al.*, 2009). For example, pioneering but transient sublate neurons provide an essential substrate for thalamic lateral geniculate neurons (LGN) *en route* to their target layer 4 neurons in the cortex (Ghosh *et al.*, 1990).

Axons therefore need to distinguish among the present fascicles and selectively fasciculate upon their matching axonal bundles (Bastiani *et al.*, 1984; Raper *et al.*, 1984). Indeed, trans-axonal communication contributes significantly to

precise wiring of visual and olfactory circuitries as well as accurate organisation of motor and sensory axons into distinct bundles (Sweeney *et al.*, 2007; Gallarda *et al.*, 2008; Imai *et al.*, 2009; Huettl *et al.*, 2011; Wang *et al.*, 2011). Additionally, surround repulsion by environmental guidance cues that are expressed adjacent to the axonal bundles prevent axons from defasciculating and projecting to neighbouring, less favourable substrates and thereby channel fibers into tracts. For example, loss of Sema3A expression in the mesenchyme close to motor and sensory projections innervating the prospective forelimb results in their pronounced defasciculation and exuberant growth to areas normally devoid of axons (Huber *et al.*, 2005).

In addition to their prominent role in mediating axonal pathfinding, guidance molecules such as semaphorins and ephrins are also involved in the removal of overgrown and misguided axonal projections by selective pruning or programmed neuronal cell death (reviewed in Vanderhaeghen & Cheng, 2010). Pruning of axonal branches is mediated by repellent guidance cues such as Sema3F for visual cortical projections or Plexin-A3 and ephrin B3 for hippocampal mossy fibers (Cheng *et al.*, 2001; Low *et al.*, 2008; Xu & Henkemeyer, 2009). Programmed cell death of neurons is triggered by restricted availability of target-derived neurotrophic cues like NGF, BDNF, GDNF and NT-3/4, which are essential for neuronal survival. Additionally, the chemorepellent Sema3A in conjunction with NGF is involved in determining the final number of sensory neurons in the DRG. In absence of NGF, Sema3A induces apoptosis selectively in sensory neurons of the DRG during E12-14 (Cowan, 2001; Huang & Reichardt, 2001; Ben-Zvi *et al.*, 2006; Ben-Zvi *et al.*, 2008). Thus, axon pruning and selective neural cell death after incorrect target innervation constitute additional mechanisms to ensure precise neuronal circuit wiring.

Growing axons are constantly exposed to a plethora of guidance cues that might signal competing instructions which makes the interpretation and integration of the various inputs a complex task (Raper & Mason, 2010). Tight spatio-temporal control of the expression of guidance receptors as well as locally induced protein synthesis in the growth cone upon reaching intermediary targets are two often observed mechanisms to deal with the complexity of guidance instructions. After passing the midline in the spinal cord, EphA2 receptor expression is strongly upregulated in commissural growth cones via translational control sequences in the 3’ UTR of its mRNA in distal axon segments, thereby changing their responsiveness to midline guidance cues after crossing (Brittis *et al.*, 2002). An additional mechanism

is the modulation of the response to a given guidance cue by intracellular levels of cyclic nucleotides such as cAMP and cGMP (Song *et al.*, 1998). Dendrites and axons of rat pyramidal neurons respond differently to Sema3A: elevated cGMP levels in apical dendrites confer chemoattraction whereas the axon with lower cGMP levels is repelled by the same guidance cue Sema3A (Polleux *et al.*, 2000).

Despite the small amount of ligand-receptor pairs identified so far, it is still amazing that this limited number of cues is capable of wiring the total repertoire of the highly diverse neuronal circuits in the entire organism. The recent identification of draxin as a novel repulsive guidance cue for spinal cord and forebrain commissures indicates the existence of additional, yet unidentified, factors for axon guidance (Islam *et al.*, 2009).

II.3.2 Peripheral sensorimotor circuit formation in the vertebrate limb

Even the most simple monosynaptic reflex requires a precise interplay between the motor unit, peripheral muscles and proprioceptive sensory afferents transmitting feedback information to motor neurons. However, the complexity of the involved circuits is constantly increasing from mono- to polysynaptic reflexes to a whole neuronal network such as the spinal sensorimotor circuit.

After exiting the spinal cord through the ventral roots, growing motor axons converge with sensory projections originating from the DRG to form the spinal nerves. Thereby, intermingled sensory and motor projections sort into target-specific bundles and select a dorsal or ventral trajectory to their correct target muscle in the limb (Lance-Jones & Landmesser, 1981a). Over the past ten years several guidance cues have been identified, which regulate correct dorsal-ventral pathfinding decisions and axonal fasciculation into nerve bundles (Fig. 6, reviewed in Bonanomi & Pfaff, 2010).

Reaching the binary choice point in the limb plexus, LMCl axons encounter attractive (GDNF) and repulsive (ephrin-A) axon guidance cues expressed concomitantly by the limb mesenchyme. Thereby, EphA4 receptors on the growing LMCl axons are repelled by ephrin-A proteins in the ventral half of the limb (Helmbacher *et al.*, 2000; Kania & Jessell, 2003), simultaneously the c-Ret and GFRα1 receptor complex directs the respective axons to the attractive GDNF source in the dorsal limb (Kramer *et al.*, 2006). Additionally, “reverse” signalling among

ephrin-As on LMCl projections and EphA4 expressed in the dorsal limb area further enforces a dorsal trajectory choice (Marquardt *et al.*, 2005).

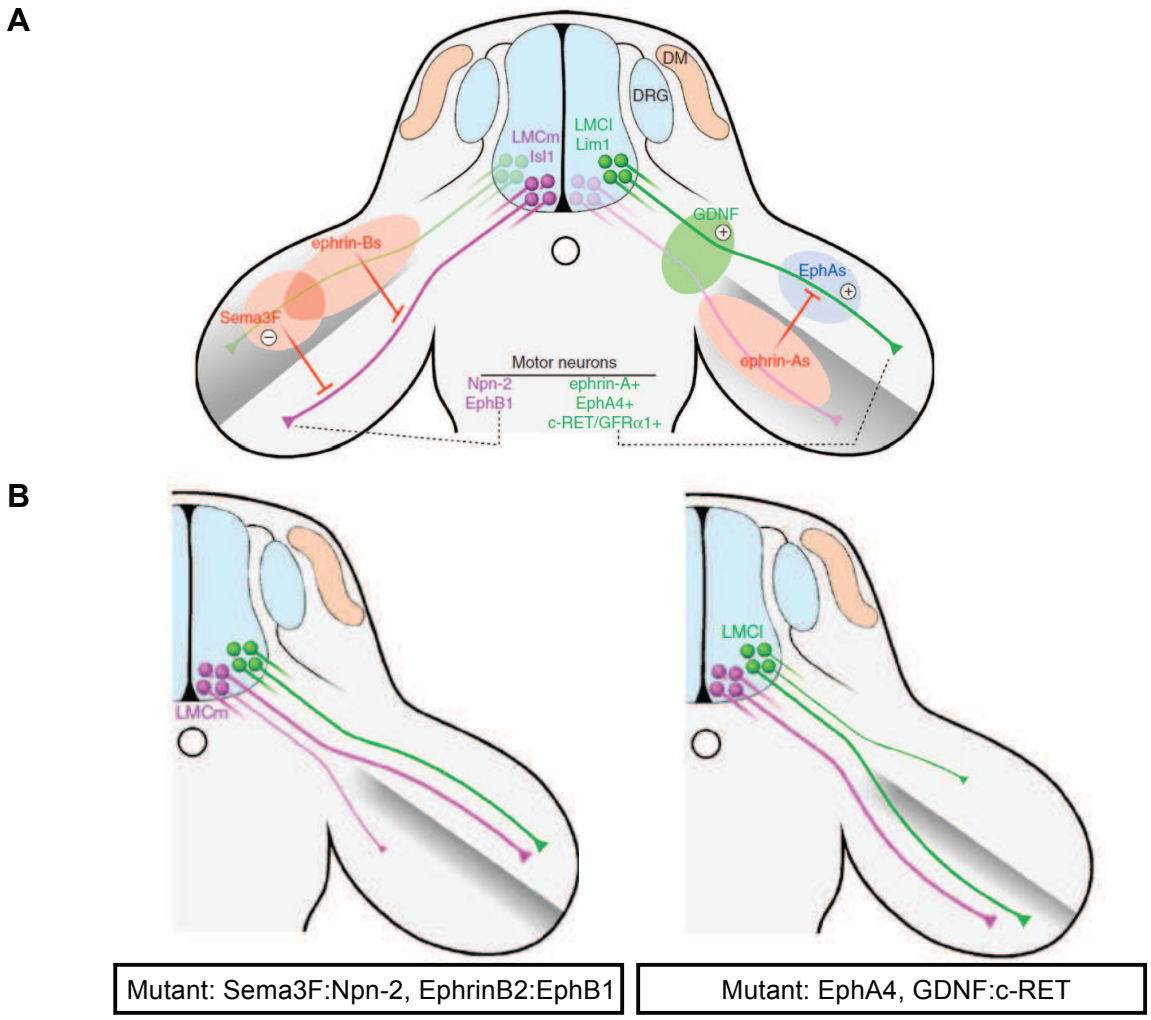


Figure 6: Guidance of motor axons to dorsal and ventral limb targets.
(A) Navigation of LMCl and LMCm motor neurons to the limb and the axon guidance ligand-receptor couples regulating the dorsal-ventral choice. (B) Left: Loss of Sema3F-Npn-2 or ephrin-B-EphB1 signalling results in misprojection of a subset LMCm neurons to the dorsal instead of ventral half of the limb. Right: Absence of EphA4 or GDNF-c-Ret causes LMCl projections to erroneously innervate the ventral limb. (Pictures modified from Bonanomi & Pfaff, 2010).

Medial LMC neurons in turn express EphB1 receptors and are repelled by ephrin-B2 positive dorsal mesenchyme to the ventral limb muscles (Luria *et al.*, 2008). In addition, repulsive interaction of Sema3F expressed in the dorsal limb with its corresponding receptor Neuropilin 2 (Npn-2) on the axonal surface diverts a subset of LMCm axons ventrally. Interestingly, timing of ingrowth and fasciculation of motor axons is completely normal in absence of either Sema3F or Npn-2. In contrary,

Sema3A-Npn-1 signalling enforces medial and lateral LMC axons to pause at the limb plexus and regulates selective fasciculation of peripheral motor and sensory projections (Huber *et al.*, 2005; Kolodkin & Tessier-Lavigne, 2011). Additionally, interaxonal signalling further contributes to sorting of axons into smaller target-specific bundles. Besides controlling fasciculation and the timing of entry into the limb, Npn-1 plays an additional role in the tight coupling of sensory and motor projections to the limb (Huettl *et al.*, 2011). Trans-axonal signalling between EphA3/A4 on motor and ephrin-As on coextending sensory axons mediates correct sorting of peripheral projections to axial muscles (Gallarda *et al.*, 2008).

Once reaching their peripheral targets, individual axons innervate specific muscle subregions. Elegant experiments characterizing muscle fiber (re-)innervation following muscle transplantation or axotomy demonstrated that muscle-specific nerve branching occurs independently of mesenchymal guidance cues but instead requires additional cues for nerve-muscle matching (reviewed in Sanes & Lichtman, 1999). Albeit the underlying molecules and mechanism are largely obscure, there is compelling evidence that ephrin-A2 and –A5 (Feng *et al.*, 2000; Lampa *et al.*, 2004) and ETS transcription factors contribute to selective innervation of muscle fibers during sensorimotor circuit wiring. Loss of the ETS transcription factor Pea3 results in aberrant intramuscular branching in *Latissimus dorsi* and *Cutaneous maximus* muscles and, consequently, in mispositioning of these motor pools in the spinal cord (Lin *et al.*, 1998; Livet *et al.*, 2002; Vrieseling & Arber, 2006; Ladle *et al.*, 2007). Another ETS transcription factor, Er81, is crucial for directly connecting a subset of proprioceptive sensory afferens to homonymous motor neurons in the spinal cord. *Er81*$^{-/-}$ mice reveal ataxia and severe coordination deficits paralleled on anatomical level by reduced group I afferent sensory input on motor neurons (Lin *et al.*, 1998; Arber *et al.*, 2000; Ladle *et al.*, 2007).

A recent publication proposed that sensory axons target specific tiers, areas arranged dorsoventrally in the spinal cord, independently of motor neuron subtype or even their presence. Thereby, motor neuron organisation into dinstinct pools and topographic positioning in the spinal cord is crucial for sensory projections to selectively innervate self motor neurons. In *FoxP1*$^{MN\Delta}$ mutants with altered dorsoventral and mediolateral positioning of motor neurons, sensory afferents consequently project on self and ectopic nonself motor neurons mispositioned in the same tier (Surmeli *et al.*, 2011).

II.4 Plasticity of neuronal circuits

From birth on, neuronal circuits that have been established during embryogenesis with astonishingly high precision, are subjected to environmental influences, learning processes and possibly injuries during the animal's life span. How do the neuronal networks of neonatals versus adults respond and adapt to environmental influences and/or disturbances in neuronal circuits?

II.4.1 Circuit maturation in early postnatal neuronal networks

In newborn vertebrates neuronal networks have been established during embryogenesis without prior interaction with the environment. During the "critical period", the first 2 to 3 postnatal weeks in mice and months in human newborns, these circuits are extremly flexible and particularly amenable to adaptive changes in response to environmental and physical conditions. The premier model for critical period plasticity showed that early postnatal monocular light deprivation by closure of one eye results in persistent loss of visual acuity in that eye and structural changes in the striate cortex (Wiesel & Hubel, 1963). Thus, ocular dominance of both eyes is dependent on the maturation of the visual sensory system triggered by the exposure of light in an early postnatal phase.

Mechanisms of circuit maturation in the motor system include competition among inputs and modulation of synaptic activity. During circuit wiring, multiple motor axons have synapsed on the same muscle fiber and excess inputs need to be diminished to a 1:1 ratio by competition (Sanes & Lichtman, 1999; Lichtman & Colman, 2000; Walsh & Lichtman, 2003). Furthermore, among the newly established neuronal circuits some will be favoured and others rather neglected, by potentiating or repressing the synapse activity, respectively (Hensch, 2004; Martin, 2005).

Interestingly, early postnatal lesions to the nervous system are met with exceptional compensatory and regenerative processes. Spinal trauma in 2 weeks old cats or peripheral forelimb amputation in neonatal rats induced extensive rearrangements of the deafferented region in the cortex (Donoghue & Sanes, 1987; McKinley *et al.*, 1987). Congenital or perinatal hemispheric brain lesions are followed by excessive branching of ipsilateral corticospinal projections from the spared to the damaged cortex area in animal models and human patients (Gomez-Pinilla *et al.*,

1986; Benecke *et al.*, 1991; Carr *et al.*, 1993). This is in contrast to permanent and substantial functional impairments after damage or injury to the CNS in adults.

II.4.2 Plasticity in adult neuronal circuits under physiological and injury conditions

Traditionally, after the postnatal critical period, neuronal networks were perceived as rather “hard-wired“, rigid structures to assure a stable, reliable network function in adults. However, accumulating evidence of spontaneous partial compensation or recovery from CNS lesions rebutted the idea of the “hard-wired“ innate nervous system (reviewed in Edgerton *et al.*, 2004; Cai *et al.*, 2006; Harel & Strittmatter, 2006; Maier & Schwab, 2006). Plastic adaptions were reported on cortical, subcortical and spinal levels and comprise anatomical, biochemical and electrophysiological changes in spared pathways (reviewed in Raineteau & Schwab, 2001). Functional motor recovery after traumatic injury in animal models and human patients is thought to arise from re-integration of damaged fibers into the original circuitry either by regeneration of the lesioned fibers or their replacement by newly sprouted uninjured intact fibers and/or from re-arrangement of existing networks (Fig.7; Raineteau & Schwab, 2001; Fridman *et al.*, 2004; Murase *et al.*, 2004; Barriere *et al.*, 2008; Courtine *et al.*, 2008; Kaas *et al.*, 2008).

Studies by Bareyre et al. demonstrated that spontaneous recovery from incomplete spinal cord injury (SCI) entails anatomical reorganisation at spinal and cortical level in adult rats. Thereby, newly sprouted CST axons from above the lesion site contacted proprioceptive sensory projections and were thus reconnected to intraspinal circuits (Bareyre *et al.*, 2004). Remodelling in the spinal cord is often paralleled by supraspinal reorganisation of the motor cortex comprising large-scale topographic as well as anatomical and synaptic changes (reviewed in Raineteau & Schwab, 2001). Intracortical microstimulation of the same area in the motor cortex of untreated rats and 4 weeks after bilateral transection of the CST at thoracic level demonstrated a shift in cortical motor representation from hind limb movement to whiskers, forelimb and trunk responses, respectively (Fouad *et al.*, 2001). Additionally, at the level of the brain stem, the intact rubrospinal tract is capable to partially take over motor functions of the lesioned CST after unilateral pyramidotomy in monkeys and rodents. Thereby, functional recovery of limb movements is

associated with profound changes in flexor and extensor activation from extensor preference in default rubrospinal tract to equal extensor/flexor facilitation after CST lesions (Lawrence & Kuypers, 1968a; b; Belhaj-Saif & Cheney, 2000; Z'Graggen *et al.*, 2000; Raineteau *et al.*, 2002).

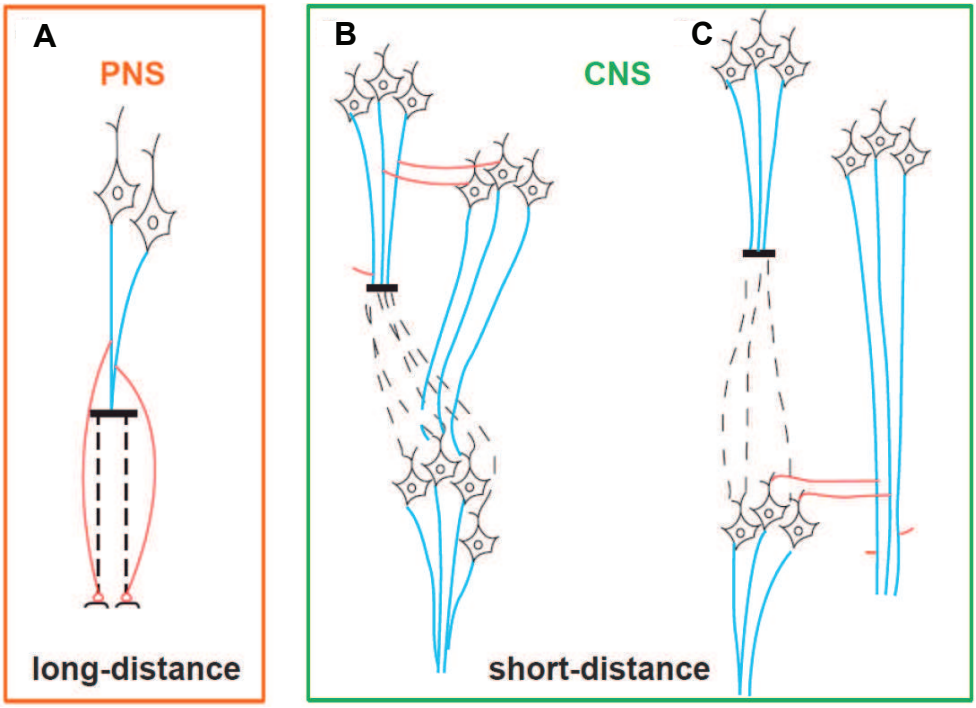


Figure 7: Spontaneous sprouting in the CNS and long-distance regeneration in the PNS. (A) Long distance regeneration of lesion axon fibers in the PNS. (B) Collateral sprouting of severed fibers over a short distance to neighbouring axons to by-pass the injury site. (C) Sprouts of spared axons to reconnect beyond the lesion site. Dotted black lines represent Wallerian degeneration of lesioned fibers. New axons sprouting from severed or spared fibers are shown in red. (Pictures modified from Giger *et al.*, 2010).

However, extrinsic factors present in the tissue surrounding the lesion such as axon guidance molecules (e.g. Sema4D, ephrinB3, netrin-1), prototypic myelin inhibitors (e.g. Nogo, myelin associated glycoprotein) and glial scar-derived chondroitin sulphate proteoglycans (CSPGs) inhibit axonal re-growth and regeneration in the adult CNS profoundly. Thus, neutralization or lowering the amount of these extrinsic growth inhibitors boosts the regenerative and plastic capacities of the CNS after injuries or diseases (reviewed in Giger *et al.*, 2010).

Besides anatomical plasticity, modulations of synaptic input in spared circuits further contribute to recovery after CNS lesions (Holtmaat & Svoboda, 2009). The predominant inhibitory GABAergic neurons in the brain maintain the somatotrophic

cortical map. Reduction of GABAergic input renders the motor cortex more amenable to cortical field reorganisation and possibly unmasks latent but previously silenced excitatory connections (Jacobs & Donoghue, 1991; Kaas, 1991).

Spontaneous functional recovery after traumatic CNS injury can be further promoted extrinsically by rehabilitative motor training in animals and human patients (Lovely *et al.*, 1990; De Leon *et al.*, 1998a; b; Edgerton *et al.*, 2004; Rossignol, 2006; Girgis *et al.*, 2007; van Hedel & Dietz, 2010). Treadmill training in human patients improves locomotion and body support after incomplete spinal cord injury and decreases spasticity in complete SCI patients (Dietz *et al.*, 1994; Dietz *et al.*, 1995; Wernig *et al.*, 1998; Field-Fote, 2001). The underlying mechanisms that contribute to the training-induced improvement in locomotor properties are not entirely clear. They might involve modulation of inhibitory input, altered firing rate in motor neurons and increased availability of neurotrophic factors (Wolpaw, 1997; Gomez-Pinilla *et al.*, 2001; Tillakaratne *et al.*, 2002).

Combination therapies aiming at promoting intrinsic plastic potential, concomitantly attenuating the unwanted extrinsic growth inhibitory cues together with rehabilitative training to strengthen functional important circuitries hold great promise for enhanced beneficial functional recovery after CNS trauma.

Contrary to recovery in the CNS, peripheral projections are capable of re-establishing functional connections to initial targets over long distances after trauma (Wigston & Sanes, 1982; Laskowski & Sanes, 1988; DeSantis *et al.*, 1992; Carlstedt, 2000). Albeit restored connections mainly innervate the correct target (DeSantis & Norman, 1993), misrouting of sensory and motor projections has also been observed (Brushart & Mesulam, 1980; Brushart *et al.*, 1981). Elegant studies by Nguyen revealed that recovering motor neurons preferentially reconstitute previous muscle innervation patterns by re-innervating the original instead of idle muscle fibers (Nguyen *et al.*, 2002).

II.5 Aim of this thesis

Hitherto there are fundamental insights on neuronal circuit assembly and the structural and functional plastic capabilities of spinal networks after traumatic injury to the nervous system. However, some aspects of neural circuit formation such as the

impact of interaxonal communication and postnatal plasticity in adult vertebrates in non-injury based paradigms are not fully elucidated and/or controversially discussed.

We chose the murine sensorimotor circuit as a model to study developmental wiring and adaptive plasticity in the nervous system. Its advantages lie in the substantial knowledge available on development, anatomy and molecular identity of its specific components as well as its accessibility for experimental manipulations. In addition, applying behavioural phenotyping provides a direct readout for the functionality of the involved circuits.

II.5.1 Characterization of sensorimotor interactions during circuit formation

While several cues mediating axon-environment interactions during embryonic circuit formation have been identified over the last years, the role of trans-axonal communication between adjacent hetero- or homotypic axonal projections for correct wiring was elusive. One of the aims of the present study therefore was to analyse the crosstalk between co-extending spinal sensory and motor projections *en route* to their peripheral targets in the developing limb. To address this question, either sensory or motor neurons were genetically ablated using cell type-specific *Cre* lines to drive the expression of lethal *diphtheria toxin-A* (Pietri, 2003; Brockschnieder *et al.*, 2006; Dessaud *et al.*, 2007). Motor or sensory projections were genetically or histologically labelled, respectively, to allow for characterization of spinal nerve projection patterns and fidelity of trajectory formation in whole mount embryo preparations.

II.5.2 Characterization of forepaw impairments in *Olig2-Cre^{+};Npn-1$^{cond-/-}$* mutants

Elimination of Npn-1 from motor neurons during embryonic development (*Olig2-Cre^{+};Npn-1$^{cond-/-}$*) revealed pronounced defasciculation and stalling of motor axons projecting to the forelimb (Huettl *et al.*, 2011). Interestingly, these mutant mice revealed congenital limb posture abnormalities: one or both forepaws are constantly flexed at the wrist and/or digits. The aim of my study was to analyse the underlying cause for the observed forelimb phenotype in postnatal *Olig2-Cre^{+};Npn-1$^{cond-/-}$* mice. This was achieved by characterizing stereotyped and skilled locomotion capabilities and analysing the musculoskeletal properties of forelimbs such as the area of

extensor and flexor muscles. Ultrastructural analysis of myelination and fiber composition in specific forelimb nerves revealed potential neurogenic causes for the observed phenotype.

II.5.3 Analysis of adaptive plasticity in sensorimotor circuits during postnatal development

Absence of the repulsive guidance cue Sema3F or its receptor Npn-2 leads to well-characterized dorsal-ventral pathfinding errors of motor axons during embryogenesis (Huber, Neuron, 2005). These embryonic wiring deficits are likely to cause motor impairments and may be corrected or compensated for postnatally. Since the mutant mice are viable, they present an excellent model to monitor postnatal motor behaviour and assess adaptive changes of miswired sensorimotor circuits. The aim of my study was to correlate the data on motor skills, spinal morphology, integrity of dorsal-ventral limb innervation and muscle recruitment patterns to determine if wiring deficits in peripheral sensorimotor circuits of *Sema3F* and *Npn-2* mutants are eliminated postnatally or rather compensated for. We used a comprehensive approach combining repetitive behavioural phenotyping of stereotyped and complex locomotor skills, neuroanatomical analysis of the motor system and electrophysiological characterization of functional peripheral limb circuit wiring.

III MATERIAL AND METHODS

III.1 Mouse husbandry

III.1.1 Ethic statement

Mice were housed in groups of 3 per cage at a 12:12 light:dark cycle with food and water available *ad libitum*. Mice were handled according to the federal guidelines for the use and care of laboratory animals, approved by the Helmholtz Zentrum München Institutional Animal Care and Use Committee. All experimental procedures were approved by and conducted in adherence to the guidelines of the Regierung von Oberbayern.

III.1.2 Mutant mice

The following mouse lines on a C57BL/6 background were used: *Hb9::GFP* (Wichterle *et al.*, 2002), *Ht-Pa-Cre* (Pietri, 2003), *Npn-1*^{cond} (Gu *et al.*, 2003), *Npn-1*$^{Sema-}$ (Gu *et al.*, 2003), *Npn-2* (Giger *et al.*, 2000), *Olig2-Cre* (Dessaud *et al.*, 2007), *R26:lacZbpA*^{flox}*DT-A* (Brockschnieder *et al.*, 2006) and *Sema3F* (Sahay *et al.*, 2003).

III.1.3 Genotyping

DNA isolation from mouse tails

Eppendorf Thermomixer 5436	(Eppendorf, Hamburg, Germany)
Eppendorf centrifuge 5417R	(Eppendorf, Hamburg, Germany)
Ethanol absolut for analysis	(Merck KGaA, Darmstadt, Germany)
Ethylendiaminintetraacetic acid (EDTA)	(Sigma-Aldrich GmbH, Steinheim, Germany)
Proteinase K (100mg)	(Invitrogen, Darmstadt, Germany)
Regular prep buffer	10mM Tris pH8.0 10mM NaCl 10mM EDTA pH8.0

	0.5% SDS filled up with MilliQ-H_2O to 50ml
Tris-Hydroxy-Methyl-Amino-Methan (Tris)	(Carl Roth, Karlsruhe, Germany)
Trizma Hydrochlorid (HCl)	(Sigma-Aldrich GmbH, Steinheim, Germany)
Sodium chloride (NaCl)	(Carl Roth, Karlsruhe, Germany)
Sodium dodecylsulfate (SDS) 10%	(Invitrogen, Darmstadt, Germany)
Sodium hydroxid (NaOH)	(Merck KGaA, Darmstadt, Germany)
1x TE buffer	10mM Tris-HCl, pH8.0 1mM EDTA

1-2mm of tail tissue was used as a source of DNA samples for mouse genotyping. Tail clips from postnatal mice and tails from mouse embryos were digested in 100µl of 50mM NaOH at 95°C in a shaker for 30min for postnatal or 20min for embryonic tissue. Afterwards 30µl of 1M Tris pH7.0 was added to stabilise isolated DNA. 1-2µl of DNA solution were directly used for polymerase chain reaction (PCR).
DNA of Sema3F mouse tails was isolated using the “Regular prep” procedure. Therefore, tail samples were incubated in 500µl Regular Prep buffer with 20µl of Proteinase K (10mg/ml) overnight in a shaker at 56°C. On the following day, the DNA was isolated and purified. After adding 250µl saturated 5M NaCl, samples were incubated with vigorous shaking (200x) for 10min, cooled down on ice for 10min and centrifuged at low speed (6000rpm) at room temperature for another 10min. 500µl of centrifuged sample were transferred to a fresh Eppendorf tube containing 1ml of 100% EtOH, mixed by inversing 4 times and centrifuged at high speed (13000rpm) at 4°C for 25min. DNA samples were purified from salt in 70% EtOH and spinned at 13000rpm at 4°C for 7min. After brief drying, the DNA pellet was resuspended in 80µl of 1x TE and subsequently used for PCR.

Polymerase chain reaction

10x CoralLoad PCR reaction buffer	(Qiagen, Hilden, Germany)
Desoxynucleotides (dNTPs)	(Fermentas, St.Leon-Rot, Germany)
25mM $MgCl_2$	(Qiagen, Hilden, Germany)
MilliQ-H_2O	(Millipore, Schwalbach, Germany)
Oligonucleotides	(Metabion, Martinsried, Germany)

5x Q-solution	(Qiagen, Hilden, Germany)
Taq DNA polymerase (5units/µl)	(Qiagen, Hilden, Germany)

Wildtype, heterozygous and homozygous mice were identified by PCR using the following primer pairs and amplification parameters in a thermocycler (Eppendorf and SensoQuest labcycler).

***Cre* allele**

Cre Forward: GTG TCC AAT TTA CTG ACC GTA CAC

Cre Reverse: GAC GAT GAA GCA TGT TTA GCT GG

Amplification parameters: Preheating: T=95°C for 5min, 30 Cycles of Denaturation: T=95°C for 1min, Annealing: T=59.5°C for 1min, Extension: T=72°C for 30sec. End: T=72°C for 15min

***GFP* allele**

872: AAG TTC ATC TGC ACC ACC G

1416: TCC TTG AAG ATG TGT CG

Amplification parameters: Preheating: T=95°C for 3min, 35 Cycles of Denaturation: T=95°C for 30sec, Annealing: T=60°C for 1min, Extension: T=72°C for 1min. End: T=72°C for 15min

***Npn-1* allele**

5'SacI Ex2: AGG CCA ATC AAA GTC CTG AAA GAC AGT CCC

3'SacI: AAA CCC CCT CAA TTG ATG TTA ACA CAG CCC

Amplification parameters: Preheating: T=95°C for 3min, 35 Cycles of Denaturation: T=95°C for 45sec, Annealing: T=63°C for 45sec, Extension: T=72°C for 45sec. End: T=72°C for 5min

***Npn-2* allele**

200bp (wt)

Exon1f: CTC TCT GTC AAA AAT GGA TAT G

Intron1b: AGA AGC CCG CTG AGA TCT

Amplification parameters 200bp: Preheating: T=94°C for 5min, 30 Cycles of Denaturation: T=94°C for 1min, Annealing: T=60°C for 1min, Extension: T=72°C for 45sec. End: T=72°C for 7min

650bp (mut)
Neo#2: TAC CTG AAA GCA CGA GGA AGC GGT
Neo#3: CTT TTT GTC AAG ACC GAC CTG TCC
Amplification parameters 650bp: Preheating: T=94°C for 5min, 30 Cycles of Denaturation: T=94°C for 1min, Annealing: T=58°C for 1min, Extension: T=72°C for 45sec. End: T=72°C for 7min

***R26:lacZbpA^{flox}DT-A* allele**
RosaFA: AAA GTC GCT CTG AGT TGT TAT
RosaRA: GGA GCG GGA GAA ATG GAT ATG
SpliceAcB: CAT CAA GGA AAC CCT GGA CTA CTG
Amplification parameters: Preheating: T=94°C for 4min, 33 Cycles of Denaturation: T= 94°C for 35sec, Annealing: T=63°C for 35sec, Extension: T=72°C for 35sec. End: T=72°C for 15min

***Sema3F* allele**
Sema3F 3-1: GAA TGC CCG GGT AAA CAC CA
Sema3F 3-2B: TCG AAG CGT ACC CTG GCT CT
Sema3F3-3A: AAG GAG CGC ACA GAG GAC CA
Amplification parameters: Preheating: T=94°C for 5min, 30 Cycles of Denaturation: T=94°C for 1min, Annealing: T=60°C for 1min, Extension: T=72°C for 1min. End: T=72°C for 10min

Agarose gel electrophoresis

Agarose	(Biozym, Oldendorf, Germany)
EDTA	(Sigma-Aldrich, Steinheim, Germany)
Ethidium bromide	(Sigma-Aldrich, Steinheim, Germany)
GeneRuler 1kB DNA ladder	(Fermentas, St.Leon-Rot, Germany)
Tris-Acetat	(Carl Roth, Karlsruhe, Germany)

TAE buffer (1x)	40mM Tris-Acetat 1mM EDTA, pH 8.0

The obtained amplification products were stored at 4°C until electrophoretic separation for size determination on a 2% agarose gel in 1x TAE buffer with 150µg/ml Ethidiumbromid.

III.2 Mouse embryo analysis

III.2.1 Whole mount staining

Aluminium block	6cm x 2,5cm, 3 holes à 1,5cm diameter (HGMU Craft services, München, Germany)
Antibodies	
Primary	
Mouse-anti neurofilament 2H3	(DSHB, Iowa,USA)
Rabbit anti-GFP	(Invitrogen, Darmstadt, Germany)
Secondary	
Goat anti-mouse Cy3	(Invitrogen, Darmstadt, Germany)
Goat anti-rabbit Cy2	(Invitrogen, Darmstadt, Germany)
BABB	Benzyl alcohol : Benzyl benzoate (1:2)
Benzyl alcohol	(Sigma-Aldrich, Steinheim, Germany)
Benzyl benzoate	(Sigma-Aldrich, Steinheim, Germany)
Blocking solution	5% normal goat serum, inactivated 75% PBS 20% DMSO
DMEM/F12	(Gibco, Darmstadt, Germany)
Dent's bleach	H_2O_2 : Dent's Fix (1:2)
Dent's Fix	DMSO : Methanol (1:4)
Dimethyl sulfoxyde (DMSO)	(Merck KGaA, Darmstadt, Germany)
Fluorescent stereo microscope	Stereo Lumar.V12 (Zeiss, Jena, Germany)

Glass cover slips	(Roth, Karlsruhe, Germany)
Hydrogen peroxide 30% H_2O_2	(Applichem, Darmstadt, Germany)
Laser scanning microscope	Zeiss LSM510 (Zeiss, Jena, Germany)
Methanol	(Merck KGaA, Darmstadt, Germany)
Normal goat serum	inactivated at 56°C for 30min (Gibco, Darmstadt, Germany)
Na_2HPO_4	(Merck KGaA, Darmstadt, Germany)
NaH_2PO_4 x H_2O	(Merck KGaA, Darmstadt, Germany)
Paraformaldehyd (PFA)	(Sigma-Aldrich, Steinheim, Germany)
PBS pH 7.5 (10x)	12.7g Na_2HPO_4 2.65g NaH_2PO_4 x H_2O 85g NaCl Add milliQ-H_2O adjust pH to 7.5 fill up to 1 litre
Rotator Mixer RM Multi-1	(Starlab, Ahrensburg, Germany)
Sylgard	(Dow Corning, Wiesbaden, Germany)

Embryo preparation:

Embryos from E10.5 to E12.5 were dissected and prepared in DMEM/F12. Hb9::GFP heterozygous embryos were identified by GFP expression and selected using a fluorescent stereomicroscope. Tails of dissected embryos were removed for subsequent genotyping as described in III.1.3. Embryos were fixed for 24h in 4% PFA rotating at 4°C. On the second day, embryos were washed 3 times in PBS to remove remaining PFA before bleaching in Dent's Fix for 24h at 4°C. On the third day, embryos were rinsed 5 times in Methanol to remove remaining Dent's Bleach and subsequently stored in Dent's Fix for at least 24h up to the date of staining.

Whole mount embryo staining procedure:

Before primary antibody incubation embryos stored in Dent's Fix were rinsed 3 times in PBS followed by 3 washing steps of 1h each in PBS. Mouse anti-neurofilament 2H3 (1:50) and rabbit anti-GFP (1:4000) primary antibodies in blocking solution were incubated at room temperature rotating for 5 days. After primary antibody incubation,

excessive washing steps, 3 times in PBS followed by 5 times for 1h each in PBS, were conducted to remove unspecific antibody binding and reduce background staining. Secondary antibodies goat anti-rabbit Cy2 (1:250) and goat-anti-mouse Cy3 (1:250) in blocking solution were added and incubated overnight rotating at room temperature.

The following day, embryos were initially rinsed in PBS 3 times and subsequently washed 5 times in PBS for 1h each prior to their evisceration. Embryo clearing was conducted in the following order: 10min incubation in PBS and methanol (1:1), washing 3 times for 20min in methanol, 10min in methanol and BABB (1:1), clearing in 100% BABB overnight and storage until analysis.

Confocal microscopy:

Embryos were imaged in BABB in a costum-made chamber of an aluminium block glued on a glass cover slip using Sylgard. Images were captured on a Zeiss LSM510 microscope using Plan-Neofluar 5x/0,15 and 10x/0,3 objectives.

III.2.2 Quantification of the fasciculation status of motor and sensory axons

Pre-plexus defasciculation in E10.5 to E12.5 embryos was determined by measuring the thickness of 6 individual spinal nerves (a_1-a_6 from anterior to posterior) converging in the forelimb plexus relative to the length of the spinal cord segment (b) these nerves occupy. In detail, the fasciculation coefficient was calculated by the ratio of $(a_1+a_2+a_3+a_4+a_5+a_6)/b$ taking into account all spinal nerves. Additionally, the fasciculation coefficient for individual nerves was determined by a_1/b, a_2/b, a_3/b, a_4/b, a_5/b and a_6/b.

III.2.3 Immunohistochemistry

Antibodies

Primary

Goat anti-FoxP1 (1:500)	(R&D Systems, Wiesbaden, Germany)
Rabbit anti-GFP (1:4000)	(Invitrogen, Darmstadt, Germany)
Mouse anti-Isl1 39.4D5 (1:50)	(DSHB, Iowa,USA)
Rabbit anti-Lim1 (1:500)	kindly provided by T.M. Jessell
Mouse anti-myosin MY32 (1:400)	(Sigma-Aldrich, Steinheim, Germany)

Mouse anti-neurofilament 2H3 (1:50)	(DSHB, Iowa,USA)
Rabbit anti-neurofilament 200 (1:1000)	(Sigma-Aldrich, Steinheim, Germany)
Rabbit anti-vGlut1 (1:1000)	(Synaptic Systems GmbH, Goettingen, Germany)
Secondary	
Goat anti-mouse Cy3 (1:250)	(Dianova GmbH, Hamburg, Germany)
Goat anti-rabbit Cy2 (1:250)	(Dianova GmbH, Hamburg, Germany)
Donkey anti-rabbit Cy5 (1:250)	(Jackson IR, Suffolk, UK)
Blocking solution	PBS-T 10% normal goat serum, inactivated
Glass cover slips	(Carl Roth, Karlsruhe, Germany)
Mowiol mounting medium	(Calbiochem, Darmstadt, Germany)
Normal goat serum	inactivated at 56°C for 30min (Gibco, Darmstadt, Germany)
PBS-T	1x PBS 0.1% TritonX-100
Slides SuperFrost Plus	(Thermo Fisher Scientific, Bonn, Germany)
Slides SuperFrost Plus Gold	(Thermo Fisher Scientific, Bonn, Germany)
TritonX-100	(Sigma-Aldrich, Steinheim, Germany)

Frozen embryo sections previously fixed in 4% PFA were thawed and dried for 30min at room temperature prior to immunohistochemistry. Sections were briefly washed in PBS for 10min at room temperature and thereafter blocked in blocking solution for 30min at room temperature. Afterwards sections were incubated in blocking solution containing the primary antibodies in a humified chamber at 4°C. On the second day, sections were washed 3 times for 5min in PBS-T to remove unspecific antibody binding and reduce background staining. Primary antibody binding was subsequently visualised by fluorescent conjugated secondary antibodies (1:250). Secondary antibodies in blocking solution were incubated for 60min on tissue sections (10-20µm) at room temperature protected from light. For coronal 40µm spinal cord sections secondary antibody incubation at room temperature was prolonged to overnight to ensure proper penetration of thicker tissue. Afterwards sections were

washed 3 times for 5min each in PBS before mounting in Mowiol. Sections were stored in the dark until miscroscopic analysis.

III.3 Screening for bone and cartilage phenotype

III.3.1 Alcian blue/Alizarin red differential staining of cartilage and bone

Aceton	(Merck KGaA, Darmstadt, Germany)
Alcian blue	(Sigma Aldrich, Steinheim, Germany)
Alizarin red	(Sigma Aldrich, Steinheim, Germany)
Alcian blue/Alizarin red staining solution	1 volume Alcian blue 1 volume Alizarin red 1 volume Glacial acetic acid 17 volumes EtOH
Ethanol (EtOH)	(Merck KGaA, Darmstadt, Germany)
Glacial acetic acid (CH_3COOH)	(Merck KGaA, Darmstadt, Germany)
Glycerol	(Sigma-Aldrich, Steinheim, Germany)
ImageJ Version 1.45	(National Institute of Health, USA)
Potassium hydrate (KOH)	(Sigma Aldrich, Steinheim, Germany)
Stereomicroscope MZ APO Light supplier KL 1500 LCD Camera DCF 320	(Leica GmbH, Wetzlar, Germany)

After preparation, P0 mice were first dehydrated in 100% EtOH for 7 days followed by fixation in 100% acetone for 3 days. After brief washing in H_2O, mice were incubated in Alcian blue/Alizarin red staining solution for 21 days with continual agitation. Thereby, alcian blue stains glycosaminoglycans in cartilage blue and calcium-containing bone structures are visualised in red by a alizarin red S-calcium chelate complex. Remaining tissue was destained and macerated in 1%KOH, 20% glycerol at 37°C for 24h and subsequently stored at room temperature until tissue is destained. Skeletons were subjected to glycerol dilution series (20%, 50%, 80% in H_2O) and stored in 100% glycerol. Alcian blue/Alizarin red stained skeletons were imaged using a MZ APO stereomicroscope. Length and width of lower forelimb bone

structures as highlighted in Fig. 19A,B were quantified in pixels as measurement by ImageJ.

III.3.2 X-ray

Faxitron X-ray Model MX-20	(Specimen Radiography Systems, Illinois, USA)
NTB Digital X-ray Scanner EZ 40	(NTB GmbH, Diepholz, Germany)
iXPect software	(NTB GmbH, Diepholz, Germany)

After fixation of the dead mouse on a plate which is permeable for X-rays, the plate with the specimen was placed in the chamber of the MX-20 cabinet X-ray system. Images were taken and the parameters bone mineral content (BMC) and bone width were analysed qualitatively using the NTB x-ray scanner and the supplied iXPect software. Settings were: Voltage 25kV, integration time 40ms.

III.4 Ultrastructural analysis of forelimb nerves

III.4.1 Electron microscopy

Dalton's chrome-osmium fixative	1 part Buffer solution 1 part Salt solution 2 parts 2% OsO_4 solution
Buffer solution (pH7.2)	5% Potassium dichromate 2.5N KOH
Salt solution	3.4% NaCl
Dodecenyl succinic anhydride (DDSA)	(Serva Electrophoresis GmBH, Heidelberg, Germany)
Epon embedding media	61.5g DDSA 81.5g MNA 130.5g Glyidether 100 (Epon 812) 3.75ml DMP-30
Formvar carbon coated copper grids with 3.05mm diameter	(Plano GmbH, Wetzlar, Germany)

Glutaraldehyde solution (25%), EM grade	(Applichem, Darmstadt, Germany)
2.5% glutaraldehyde in 0.1 M sodium cacodylate buffer	(Electron Microscopy Sciences, Hatfield, USA)
Glycerol	(Merck KGaA, Darmstadt, Germany)
Glyidether 100 (Epon 812)	(Electron Microscopy Sciences, Hatfield, USA)
Lead citrate (Ultrostain 2)	(Laurylab SARL, St Fons, France)
Methyl nadic anhydride (MNA)	(Serva Electrophoresis GmBH, Heidelberg, Germany)
NaH_2PO_4 x H_2O	(Merck KGaA, Darmstadt, Germany)
0.2M NaH_2PO_4	13,8g NaH_2PO_4 x H_2O fill up with milliQ-H_2O to 500ml
Na_2HPO_4	(Merck KGaA, Darmstadt, Germany)
0.2M Na_2HPO_4	26,81g Na_2HPO_4 fill up with milliQ-H_2O to 500ml
Osmium tetroxide (OsO_4)	(Electron Microscopy Sciences, Hatfield, USA)
0.1M PB buffer pH7.4	202,5ml 0.2M Na_2HPO_4 47,5ml 0.2M $NaH_2P\ O_4$ add milliQ-H_2O adjust pH to 7.4 fill up with milliQ-H_2O to 500ml
Potassium dichromate ($K_2Cr_2O_7$)	(Sigma-Aldrich, Steinheim, Germany)
Potassium hydrate (KOH)	(Merck KGaA, Darmstadt, Germany)
Propylene oxide (C_3H_6O)	(Serva Electrophoresis GmbH, Heidelberg, Germany)
0.2M Sodium cacodylate buffer (pH7.4)	(Electron Microscopy Sciences, Hatfield, USA)
Sodium chloride (NaCl)	(Merck KGaA, Darmstadt, Germany)
Sodium bicarbonate ($NaHCO_3$)	(Merck KGaA, Darmstadt, Germany)
Toluidine blue O	(Merck KGaA, Darmstadt, Germany)
Toluidine blue solution	1g Toluidine blue O 60ml 1% $NaHCO_3$ solution 40ml Glycerol

Transmission electron microscope (TEM) EM 10 CR	(Zeiss, Jena, Germany)
2,4,6-Tri-(dimethylaminomethyl)phenol (DMP-30)	(Serva Electrophoresis GmBH, Heidelberg, Germany)
Uranyl acetate (Ultrostain 1)	(Laurylab SARL, St Fons, France)
Ultramicrotome Ultracut E	(Leica GmbH, Wetzlar, Germany)
Washing solution	0.1M Sodium cacodylate buffer pH7.4 4% Saccharose 2mM $CaCl_2$

Animals were perfused transcardially with 1% phosphate buffered saline (PBS) for 5min followed by fixation in 4% paraformaldehyde (PFA) and 0.25% glutaraldehyde in 0.1M PB buffer for 10min. Forelimb nerves *N.radial* and *N.median* were extracted, post-fixed overnight and subsequently stored in 2.5% glutaraldehyde in 0.1M sodium cacodylate buffer (pH 7.4) for 2-5h or overnight at 4°C. Nerves were rinsed 3 times in washing solution for 20min each to remove remaining unreacted glutaraldehyde in the tissue. Post-fixation in Dalton's chrome-osmium fixative for 1-2h eliminated aldehydes left over from the primary fixation step. After extensive washing in distilled water for 3 times à 10min, samples were dehydrated in a graded series of ethanol: 50%, 70%, 90% and 96% ethanol, followed by 3 times in 100% ethanol for 15-20 min each. Subsequently, the tissue was processed for embedding by replacing the 100% ethanol with propylene oxide 2 times for 30min. Epon embedding media was prepared by thoroughly mixing the resin glyidether 100 (Epon 812) with the hardeners DDSA and MNA and the accelerator DMP-30. Tissue was first incubated in a 1:1 solution of the embedding media and propylene oxide for 1h before storing in pure epon embedding media overnight. The next day samples were transferred into molds filled with epon embedding media and the resin is subsequently polymerized at 60°C for 24-48h. Semithin transverse sections (1µm) were cut on a ultramicrotome Ultracut E and stained for examination in Toluidine blue solution. Ultrathin sections of nerve tissue (60-70nm) were mounted on Formvar carbon coated copper grids and afterwards stained for high contrast in 0.5% uranyl acetat (Ultrostain 1) followed by 3% lead citrate (Ultrostain 2). Single images were captured with a magnification of 5000x using an EM 10 CR TEM.

III.4.2 EM image analysis

Definiens
Enterprise Image Intelligence Suite software (Definiens, München, Germany)

Individual EM images were arranged by multiple image alignment (MIA) to a single image representing the whole nerve cross-sectioned. These MIAs were subsequently analysed with Definiens Enterprise Image Intelligence Suite software (Baatz *et al.*, 2006; Baatz *et al.*, 2009). The basic operation principles of the image analysis software Definiens are alogorithm-based rule sets to detect and further refine pixel clusters referred to as image objects. Thereby, single axon fibers and their surrounding myelin sheath were identified from background structures based on their staining intensity, size, shape and neighbourhood. Axons were classified into small diameter and large diameter fibers by a pixel threshold of 7000. The amount of Remak bundles and the number of axons incorporated per Remak bundle were counted in single images representing the whole nerve cross section. Additionally, the g-ratio (axon diameter/fibre diameter) was calculated for each axon.

III.5 Behavioural data acquisition and analysis

III.5.1 Experimental design and housing

Individually ventilated cages (IVC)	(Biozone Global, Kent, UK)
Mini step ladder	10cm x 5cm x 5cm, 19 rungs of 5 mm diameter each (HGMU Craft services, München Germany)
Wood-wool	(Abedd, Vienna, Austria)
Mouse Low Profile Wireless Running Wheel^{R}	(Med Associates Inc, St. Albans, USA)

Testing of the animals was performed during the light phase of the light:dark cycle. The behavioural motor tests Open field, Grip strength, Rotarod, Grid walking, Beam walking, Wire climbing and Hind limb paw placement accuracy were conducted in the indicated order over 5 consecutive days.

One group of male mice was housed under standard laboratory conditions in IVCs. The enriched environment (EE) group was housed in larger cages (37 cm x 21 cm x 18 cm) in groups of 5 animals per cage. These cages contained the following enriched environment devices: a Mouse Low Profile Wireless Running Wheel^{R}, a custom-made mini step ladder, wood-wool (5g) and metal objects for shelter. The EE objects were renewed on a weekly basis during cage cleaning.
All behaviour data were measured by experimenters blinded to the genotype of the tested male mice and littermate controls (n= 10 for each group unless indicated otherwise).

III.5.2 Beam walking

Wood beam	12mm diameter, 95cm length (Dehner GmbH&Co KG, Rain, Germany)

Mice had to traverse an elevated (75cm high) round beam. The mean time to cross the beam and the mean number of hind limb slips over 3 consecutive trials were used as a measure for balance skills.

III.5.3 Catwalk

Catwalk7.1 gait analysis system	(Noldus, Wageningen, Netherlands)

Data acquisition:
The Catwalk system is a video-based gait analysis system consisting of a walkway with a glass plate and a high speed video camera underneath to capture the run of the mouse traversing the walkway from one side to the other. The basic operating principle is based on light forced to enter the glass plate from one side which is internally reflected when there is no contact on the glass plate. As soon as parts of the animal, such as paws or tail, contact the glass plate the light is able to escape at these areas and will be taped by the high-speed video camera underneath. The following settings were used during data acquisition: Contrast (‰): 3990, Brightness x 0.001V: -420, Pixel intensity threshold: 40, Pixel number threshold: 3. Under normal data acquisition conditions, the mice traverse the walkway voluntarily except for

Olig2-Cre^{+}*,Npn-1*$^{cond-/-}$ mutants. These animals with congenital forelimb abnormalities had to be air-puffed (referred to as “forced” conditions) to ensure a straight and continuous walk. Consequently, control littermates and line *Npn-1*$^{Sema-}$ mutants and controls used for comparison were likewise subjected to these “forced” conditions.

Data analysis:

From the 6 runs videotaped during data acquisition, the 3 best were chosen based on the following criteria: comparable walking speed in the different runs, a minimum of 3 complete step cycles and a straight and continuous walk without stoppings. Runs were pre-processed with an analysis pixel threshold of 25 to differentiate unspecific background from paw prints before paw classification. The pixel areas of each paw print were classified manually as right or left fore or hind limb. The following parameters were used for analysis: Stand duration (s), Base of support (BOS), Duty cycle and Usage of 3 paws.

III.5.4 Grip strength

Grip strength meter	(Bioseb, Vitrolles Cedex, France)

The strength of the muscles in forelimb and combined fore- and hind limbs as an indicator of muscle weakness and functional neuromuscular connectivity was assessed with the grip strength meter. Mice were allowed to grasp the grid with their forelimbs only or fore- and hind limbs and were pulled backward by their tail in the horizontal plane. The force (g) applied upon release of the bar was documented. 5 consecutive trials for forelimb and combined fore- and hind limbs were averaged and normalised over the body weight of the animals to take into account the lighter mutant *Sema3F* mice.

III.5.5 Grid walking

Horziontal ladder	74cm length, 17cm high walls of Plexi glass, 146 metal rungs of 1 mm diameter (HGMU Craft services, München, Germany)

Animals were subjected to cross a costum-made horizontal ladder with irregularly spaced round metal rungs and 2 side-walls of Plexi glass. The time to cross the ladder and the number of forelimb and hind limb placement errors by either missing the rung or slipping of the rung was averaged over 3 successive trials.

III.5.6 Hind limb extension reflex

Mice were lifted by their tails for 1min and the movement of their hind limbs was observed. A negative hind limb extension reflex was noted when 1 or 2 hind limbs were retracted and dragged to the body instead of spreading them.

III.5.7 Hind limb paw placement accuracy

Catwalk7.1 gait analysis system	(Noldus, Wageningen, Netherlands)
Horziontal ladder	74cm length, 17cm high walls of Plexi glass, 146 metal rungs of 1mm diameter (HGMU Craft services, München, Germany)

The inter-limb coordination capacities of male Sema3F mice were assessed by using the ladder from the grid walk test in combination with the high-speed video camera Pulnix model TM-756/745 from the gait analysis system CatWalk. 6 mutant and wildtype littermates at 4 weeks were recorded from beneath while crossing the grid walk apparatus with irregularly spaced metal rungs. The accuracy of the ipsilateral hind limb targeting the identical rung as its corresponding forelimb was determined frame by frame over 3 successive trials. Missing the rung completely as well as placing the hind limb on a different rung than previously the ipsilateral forelimb were counted as hind limb paw placement errors. Errors were evaluated as the percentage of total hind limb paw placements.

III.5.8 Nociception

Hot plate Analgesiometer	(Accuscan Instruments, Columbus, USA)

The Hot Plate apparatus is heated to 52°C for a noxious heat stimulus to elicit nociceptive withdrawal responses in the mouse. The mouse is placed onto the surface and the latency in seconds to the following pain-reflex behaviours is measured: paw shaking, paw licking and jumping. The experiment was stopped as soon as the mouse jumps or latest at the cutoff time of 60s.

III.5.9 Open field

Open field	45.5cm x 45.5cm x 39.5cm (TSE, Bad Homburg, Germany)

4 weeks old male mice were tested for gross locomotion abnormalities in the open-field apparatus in the dark during the light phase of the light:dark cycle for 20min in total. Assessing locomotor parameters in the dark circumvents possible effects of anxiety on gross locomotor behaviour of rodents (Zadicario *et al.*, 2005). Recordings of the automated video-tracking system were analysed with regard to horizontal (distance travelled) and vertical locomotion (number of rearings) parameters as well as average locomotor speed.
An additional cohort of 4 weeks old Sema3F male mice was tested for anxiety and explorative behaviour at illumination levels of approximately 150lux in the corners and 200lux in the middle of the test arena. The following parameters were analysed individually for the 3 areas (center, periphery and total arena): resting and permanence time, distance travelled and average speed of locomotion. Additional parameters (percentage of time spend in the center, latency to first center entry and center enter frequency) focussing on anxiety related behaviour were likewise determined.

III.5.10 Rotarod

ROTA-ROD/RS	(Bioseb, Vitrolles Cedex, France)

Mice were placed on a Rotarod apparatus continuously accelerating from 4 to 40 rpm in 2min. The latency of the mice on the accelerating rod in rpm and seconds was recorded for 3 trials with 15min intertrial interval. The mice were stopped on the second passive rotation or when falling off the rod.

III.5.11 Wire climbing

Metal wire	40cm length, 2mm diameter (OBI GmbH&Co KG, Wermelskirchen, Germany)
Digital Camera Sony DCS-T100	(Sony Europe Ltd., Berlin, Germany)

We modified the SHIRPA wire manoeuvre test focussing on hind limb grip capabilities (Rogers *et al.*, 1997) to additionally evaluate the climbing performance of the mice along the wire. In order to assess the inter-limb and fore- and hind limb coordination in male mice at 4 and 8 weeks of age, they were hung by their forepaws on an elevated (52cm) metal wire (2mm diameter). 3 repetitive trials were video-taped and subjected to qualitative analysis according to the following criteria: mice had to swing their hind limbs on the wire and subsequently climb to one end of the wire. Wild-type mice revealed a stereo-typed climbing pattern with fastened hind limbs and forelimbs actively dragging the body along the wire. 3 consecutive trials were analysed according to a qualitative scale ranging from 1= precise grip on the wire with fore- and hind limbs and rhythmic climbing to 8= fore- and hind limbs clung to the wire, no rhythmic pattern or coordinated movement.

III.5.12 Statistical analysis

Graph Pad Prism 5.0	(GraphPad Software, La Jolla, USA)

All results were calculated as mean values ± SEM using Prism 5.0 software. The obtained behavioural data sets were initially checked for normal distribution with the

D'Agostino-Pearson normality test. In case the data values deviate from the Gaussian distribution, single comparisons were computed with the non-parametric unpaired Mann-Whitney test. A p-value less than 0.05 was set as statistical significance.
The percentage of improvement in motor performance from 4 to 12 weeks in wildtypes and mutants was calculated by using the mean wildtype value at 4 weeks as reference.

III.6 Neuroanatomical analysis

III.6.1 Anesthesia

Ketamine 10%	(Bela-Pharm GmbH & Co. KG, Vechta, Germany)
Xylazine 2%	(cp-pharma mbH, Burgdorf, Germany)
Meloxicam (Mobic 15mg/1.5ml)	(Boehringer Ingelheim, Biberach, Germany)

Surgical procedures were carried out under aseptic conditions using i.p. Ketamine (0.1mg/g) and Xylazine (0.01mg/g) anesthesia with Meloxicam (2µg/g) as analgesic.

III.6.2 Retrograde labelling of dorsal and ventral forelimb motor pools

Cholera toxin B subunit (CTB)	
Alexa488-conjugated	(Molecular Probes, Darmstadt, Germany)
Alexa555-conjugated	(Molecular Probes, Darmstadt, Germany)
D(+)-Saccharose	(Merck KGaA, Darmstadt, Germany)
Hamilton syringe (10ml)	(Hamilton GmbH, Höchst, Germany)
Histoacryl	(B. Braun AG, Melsungen, Germany)
Paraformaldehyd (PFA)	(Sigma-Aldrich, Steinheim, Germany)
Sliding microtome SM2000R	(Leica GmbH, Wetzlar, Germany)

Sucrose (30%)	30g D(+)-Saccharose 100ml 1x PBS

The forelimb muscles of interest were exposed for CTB injection by small incisions to the overlying skin. Alexa-conjugated Cholera toxin B subunit (CTB, 1mg/ml in neutral phosphate buffer) was unilaterally pressure-injected using a 10µl Hamilton syringe in either the dorsal (CTB-Alexa555) or ventral (CTB-Alexa488) distal forelimb muscles or in the biceps (CTB-Alexa488) or triceps (CTB-Alexa555) muscles in the upper arm. After injection the skin was sutured with the tissue adhesive Histoacryl. 2-3 days post injection animals were perfused transcardially with 1% phosphate buffered saline (PBS) for 5min followed by the ice-cold fixative (4% PFA in PBS) for 10min. The spinal cervical vertebra C2 was used as a reference point. Tissue was post-fixed for 4h in 4% PFA, incubated in 30% sucrose and sectioned with a sliding microtome in 40µm thick slices.

III.6.3 Reconstruction of spinal motor pool representation

Fluorescent microscope	Axiovert 200
Camera	AxioCam HR
Image capturing software	AxiovisionX.X (Zeiss, Jena, Germany)
Reconstruct™ software	(http://synapses.clm.utexas.edu)

2 of the 4 consecutive series of coronal 40µm spinal cord sections were used for quantification and reconstruction of labelled forelimb motor pools. CTB-Alexa labelled motor neurons were captured on a fluorescent microscope. Serial section images were aligned by means of 4 optical reference points and individual motor neurons were traced using the Reconstruct™ software (Fiala and Harris, 2001b; Fiala, 2005).

III.6.4 Scatter index calculation for dorsal and ventral motor pool spreading

The physiologically increased diameter of spinal sections at the level of the cervical enlargement was corrected for by post-section alignment. A reference curve was defined for all sections using 5 points on the lateral edge of the spinal cord grey matter. For each individual section the intercept point between the reference curve

and the perpendicular to the main (mid-sagittal) symmetry axis through the central canal was calculated. Each section was then separately readjusted after spline interpolation of these intersection points.

A scatter index (SI) as the quantitative readout for the spreading of medial and lateral motor pools was calculated by determining the area of an ellipse fitted to the samples using a method similar to Principal Component Analysis: The covariance matrix of the X- and Y-Coordinates of the motor neuron traces was computed for both motor pools. Its 2 eigenvectors are perpendicular and represent the major and minor axes of an ellipse centered at the data mean, with width adjusted to the directional standard deviations (in other words the optimal fit of a bivariate correlated Gaussian distribution). By multiplying the product of the 2 eigenvalues with π, we determined the area of the ellipse and thus a single, comparable value: the scatter index [$SI = \pi \cdot \prod_{i=1,2} eig_i(\mathrm{cov}([x;y]))$] which is obtained for each motor pool.

III.6.5 Statistical analysis

Graph Pad Prism 5.0 (GraphPad Software, La Jolla,USA)

All results were calculated as mean values ± SEM using Prism 5.0 software. Unpaired 2-tailed Student's t test was used for single comparisons. A p-value less than 0.05 was set as statistical significance.

III.7 Electrophysiology

III.7.1 Anesthesia

Ketamine 10%	(Bela-Pharm GmbH & Co. KG, Vechta, Germany)
Xylazine 2%	(cp-pharma mbH, Burgdorf, Germany)

Electrophysiological experiments were carried out under aseptic conditions with Ketamine (0.1mg/g) and Xylazine (0.01mg/g) anesthesia administered i.p. Ketamin was previously reported to have negligible side-effects on reflex excitability during

electrophysiological recordings (Ho & Waite, 2002). An additional dose of anesthesia was given if required during the experiment. After the experiment mice were euthanized without regaining consciousness.

III.7.2 Nerve stimulation

Amplifier P511 DC	(Astromed GmbH, Rodgau, Germany)
Digidata 1440A Digitizer	(Molecular devices, Sunnyvale, USA)
Isoflex- Flexible stimulus isolator	(A.M.P.I, Jerusalem, Israel)
Master-8 pulse generator	(A.M.P.I, Jerusalem, Israel)

The nerves of interest were stimulated with single trains of bipolar electric pulses (single pulse: 100µs duration, 3.3ms interval,) using custom-made stimulation electrodes with 2 hooks (stainless steel, 0,2mm in diameter with 1mm spacer inbetween them). Stimulation intensity was increased in 0.5 intervalls from 0-10 x 0.01mA. The elicited movement in the limb was described in terms of direction and body parts involved and afterwards compared between wildtype and mutant animals.

III.7.3 EMG recordings

AxoScope software	(Molecular devices, Sunnyvale, USA)
Teflon insulated multi-stranded fine wire	(A-M Systems Inc., Sequim, USA)

Bipolar EMGs were fabricated from Teflon-insulated multi-stranded fine wire as previously described (Pearson *et al.*, 2005). A small incision was made above the brachial plexus area to gain access to the forelimb nerves and muscles. Electrodes were inserted unilaterally into the forelimb muscles Triceps brachii (TB; dorsal extensor) and antagonistic Biceps brachii (BB; ventral flexor) using the needles at their distal ends. An additional needle electrode was inserted into the animal's body for grounding. EMG activity was recorded in parallel from TB and BB by stimulating the corresponding *N. musculocutaneous* for BB or the *N.radial* for TB activity. Muscle activity was taped and analysed using the AxoScope software.

IV RESULTS

IV.1 Mutual dependency of growing motor and sensory axons for correct assembly of peripheral circuitry

How are outgrowing motor and sensory axons guided to their correct targets and interconnected in complex neuronal networks? This question has been puzzling neurobiologists for decades. So far, substantial knowledge is available on the mechanisms and molecules mediating motor neuron connectivity. Depending on their assigned subtype, e.g. medial or lateral LMC, growing motor axons are responsive to different environmentally- or target-derived guidance cues (reviewed in Bonanomi & Pfaff, 2010). These data suggest an independency of motor axons from co-extending sensory projections regarding correct target innervation. The published data on the pathfinding capabilities of sensory axons in chick limbs deprived of motor innervation on the other hand are rather controversial and sensitive to the time point of motor neuron depletion. Sensory projections fail to innervate target muscles when spinal motor neurons in the chick ventral neural tube were removed prior to DRG formation (HH stage 17-18; Landmesser & Honig, 1986; Swanson & Lewis, 1986) whereas later depletion of motor neurons (HH stage 21) has a less profound effect on sensory trajectory formation (Wang & Scott, 1999). Additionally, a major drawback lies in the applied methods: surgical removal or UV irradation of the ventral neural tube are invasive approches (Landmesser & Honig, 1986; Swanson & Lewis, 1986; Wang & Scott, 1999). Destruction and possibly alteration of the tissue surrounding the lesion site may also influence axonal outgrowth, fasciculation and guidance and eventually confound the observed results.

To circumvent these caveats, we chose a genetic approach for selective and early removal of either sensory or motor neuron precursors. We then assessed the consequences on axonal outgrowth and trajectory fidelity during limb innervation.

IV.1.1 Efficient genetic ablation of sensory or motor neurons

Recent publications presented the conditional *R26:lacZbpA^{flox}DT-A* mouse line (abbreviated *DT-A^{floxed}*) for *in vivo* cell depletion following Cre-mediated activation of a silenced diphteria toxin fragment A (DT-A) transgene inserted into the ROSA26 locus for ubiquitous expression in all somatic cells (Brockschnieder *et al.*, 2004; Brockschnieder *et al.*, 2006). The time frame from the onset of DT-A transgene activation upon Cre-mediated recombination till death of targeted Cre$^+$ cells was approximately 2 days for adult mice but is more variable during embryogenesis depending on tissue and cell types (Brockschnieder *et al.*, 2004).

We made use of the conditional *DT-A^{floxed}* mouse line to selectively activate lethal toxin expression in Ht-PA-Cre$^+$ sensory or Olig2-Cre$^+$ motor neurons (Pietri, 2003; Dessaud *et al.*, 2007). The *Olig2-Cre* line expresses the Cre recombinase under the control of the promoter for the basic helix-loop-helix (bHLH) transcription factor Olig2 essential for motor neuron and oligodendrocyte precursor cell formation during development (Rowitch *et al.*, 2002). To assess the efficiency of motor neuron depletion in *Olig2-Cre$^+$;DT-A^{floxed}* mice, we immunohistochemically quantified the number of medial and lateral LMC neurons present in the spinal cord at E11.5 in comparison to control mice without DT-A activation (Fig. 8A,B). Both FoxP1$^+$ lateral LMC and FoxP1$^+$, Isl1$^+$ medial LMC spinal motor neuron numbers were dramatically reduced in *Olig2-Cre$^+$;DT-A^{floxed}* mice albeit not completely ablated (Fig. 8C).

Sensory neurons of the DRG were targeted by Cre-expression from the *human tissue plasminogen activator* promoter (*Ht-PA-Cre*) specifically in peripheral neural crest cell (NCC) derivatives (Pietri, 2003). Sensory neurons per DRG were significantly reduced about 11 times from 181.69 ± 25.71 to 16.64 ± 4.45 in *Ht-PA-Cre$^+$;DT-A^{floxed}* mice. Similarly to the incomplete ablation of motor neurons in *Olig2-Cre$^+$;DT-A^{floxed}* embryos, some residual Isl1$^+$ sensory neurons remained at E11.5 (Fig. 8D-F).

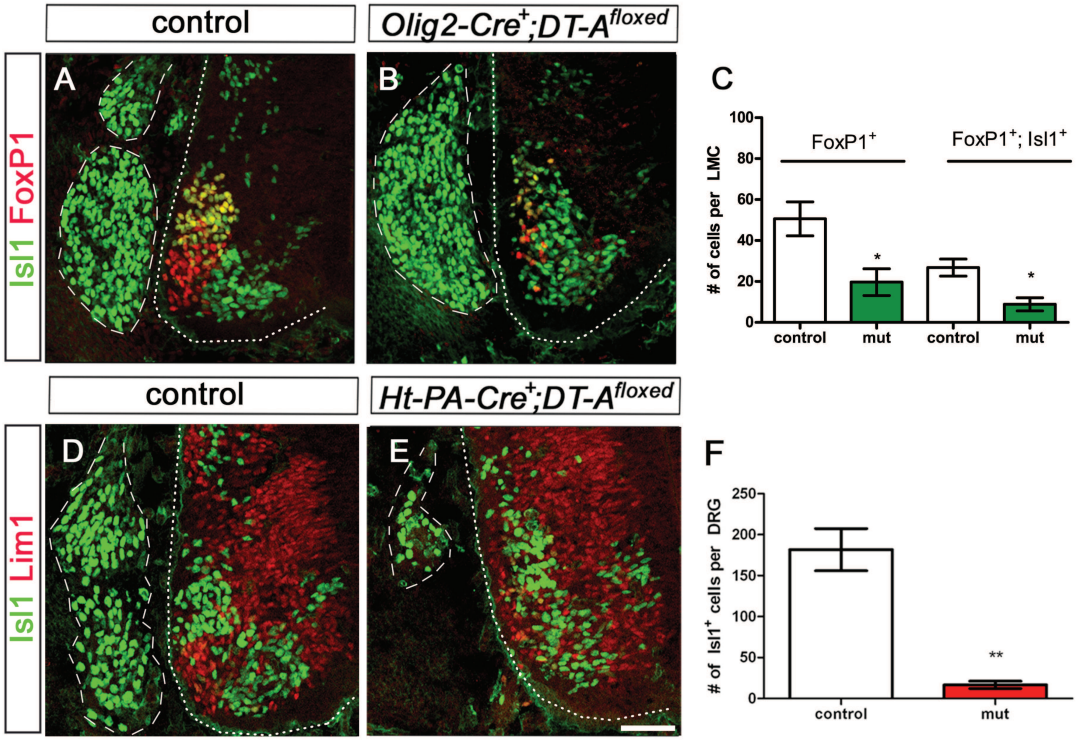


Figure 8: Partial genetic ablation of *Olig2-Cre*$^{+}$ motor or *Ht-PA-Cre*$^{+}$ sensory neurons upon tissue-specific DT-A^{floxed} activation.

(A-C) Dramatic loss of medial (FoxP1^{+}; Isl1^{+}) and lateral (FoxP1^{+}) LMC neurons in the spinal cord of *Olig2-Cre*$^{+}$*;DT-A*^{floxed} (B) versus controls (A) at developmental stage E11.5. (D-F) 10.92 fold decrease in the number of Isl1^{+} sensory neurons per DRG (F) in *Ht-PA-Cre*$^{+}$*; DT-A*^{floxed} (E) mutants relative to controls (D). DRG are outlined with white dashed line, spinal cord is outlined with white punctate line. Scale bar equals 50µm in A-E. Data were analysed with the two-tailed, unpaired Student's t-test; asterisks indicate significance *p<0.05, **p<0.01.

Together, our data demonstrate the partial ablation of sensory or motor neurons by a conditional *DT-A*^{floxed} based approach using either *Ht-PA-Cre* or *Olig2-Cre* to induce elimination of sensory or motor neurons, respectively.

IV.1.2 Impaired formation of forelimb sensory trajectories after partial ablation of motor neurons in *Olig2-Cre*$^{+}$*;DT-A*^{floxed} mice

We analysed the pathfinding and formation of sensory trajectories in *Olig2-Cre*$^{+}$*; DT-A*^{floxed} embryos with substantially reduced number of motor neurons at developmental time points when sensory and motor axons converge in the plexus region (E10.5) and one day later when the projections have navigated the dorsal-ventral choice point and started to invade the limb (E11.5). In order to label motor axons selectively, *Olig2-Cre*$^{+}$*;DT-A*^{floxed} mice were crossed to the transgenic mouse

line *Hb9::GFP*, expressing enhanced green fluorescent protein (eGFP) under the control of the mouse motor neuron promoter Hb9 (Wichterle *et al.*, 2002). Furthermore, sensory and motor axons were visualised by anti-neurofilament staining (Dodd *et al.*, 1988). Therefore, in whole mount embryo preparations motor axons double stained from *Hb9::GFP* transgene expression (Wichterle *et al.*, 2002) and anti-neurofilament were differentiated from sensory projections stained only by anti-neurofilament in absence of eGFP. Thereby neurofilament positive motor and sensory neurons are eventually visualised in red and *Hb9::GFP* expressing motor projections are additionally overlayed in green, resulting in a yellow appearance. However, since the readout of the DT-A mediated ablation of motor axons depends on resolution of very fine axonal branches, we optimized confocal microscope settings as previously described (Wichterle *et al.*, 2002; Harper *et al.*, 2004; Corti *et al.*, 2008). By reducing the saturation in the red channel to avoid unintenteded masking of fine motor projections, sensory projections are represented in red and motor axons in green.

In control embryos at E10.5, motor and sensory projections have converged into the plexus and started fasciculating into distinct spinal nerves (Fig. 9A-A''). Activation of the toxin in *Olig2-Cre*$^{+}$;*DT-A*^{floxed} embryos resulted in a visible reduction of spinal motor neuron numbers and hardly any motor projections exciting the spinal cord (Fig. 9B' inlay and arrows). Despite the severe reduction in motor axons, sensory axons from the 6 DRG contributing to the forelimb plexus, correctly navigated towards the plexus region. However, their projections seem thinned and delayed as the individual nerves have not joined for plexus formation by E10.5 (Fig.9B'',D).

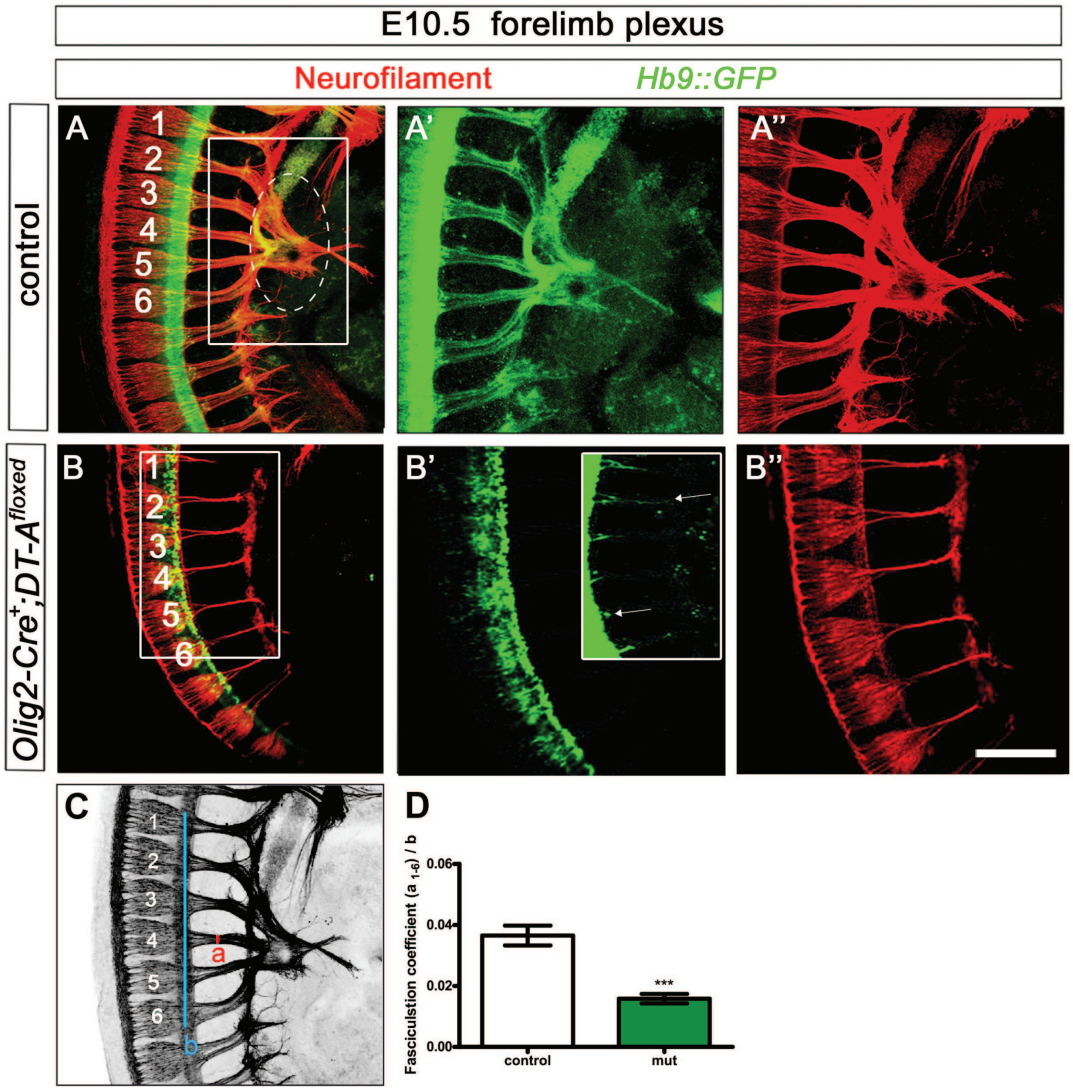


Figure 9: **Loss of motor neurons in *Olig2-Cre*$^{+}$;DT-A^{floxed} mice delays plexus formation of outgrowing sensory projections.**

Whole mount antibody staining of E10.5 embryos to differentially visualise motor axons (anti-GFP, green) and motor and sensory nerves (anti-neurofilament, red). Motor projections (A') and sensory axons from 6 spinal DRG project and converge to form the limb plexus (circled) in control embryos. In contrast, partial ablation of motor neurons in *Olig2-Cre*$^{+}$*; DT-A*^{floxed} mutants (B' and inlay) delayed the formation of the forelimb plexus but did not influence sensory axon guidance to the plexus (B,B''). Arrows in the inlay in B' point to thin motor projections. Scheme (C) and quantification (D) of axonal defasciculation and thinning before the projections reach the plexus: the sum of the six spinal nerves (a_1-a_6) normalised over the area (b) occupied by them. Scale bar equals 500µm in all panels. Data were analysed with the two-tailed, unpaired Student's t-test; asterisks indicate significance ***p<0.001.

By E11.5, few substantially thinned motor projections were present in *Olig2-Cre*$^{+}$*;DT-A*^{floxed} embryos (Fig. 10B',C' asterisks) but co-extending sensory axons nevertheless reached and converged in the plexus region. Interestingly, we observed an abormal variability in the number of DRG contributing to sensory projections to the

plexus and in the number of peripheral nerve branches formed after the plexus in *Olig2-Cre^{+};DT-A^{floxed}* embryos. In control embryos, sensory projections from 6 DRG converged to the plexus region and are sorted into the 4 distinct major spinal forelimb nerves. The number of sensory DRG projections converging into the plexus ranges between 3 and 4 forming either supernumerary or reduced spinal nerves in embryos with partially ablated motor neurons (Fig. 10A''- C'').

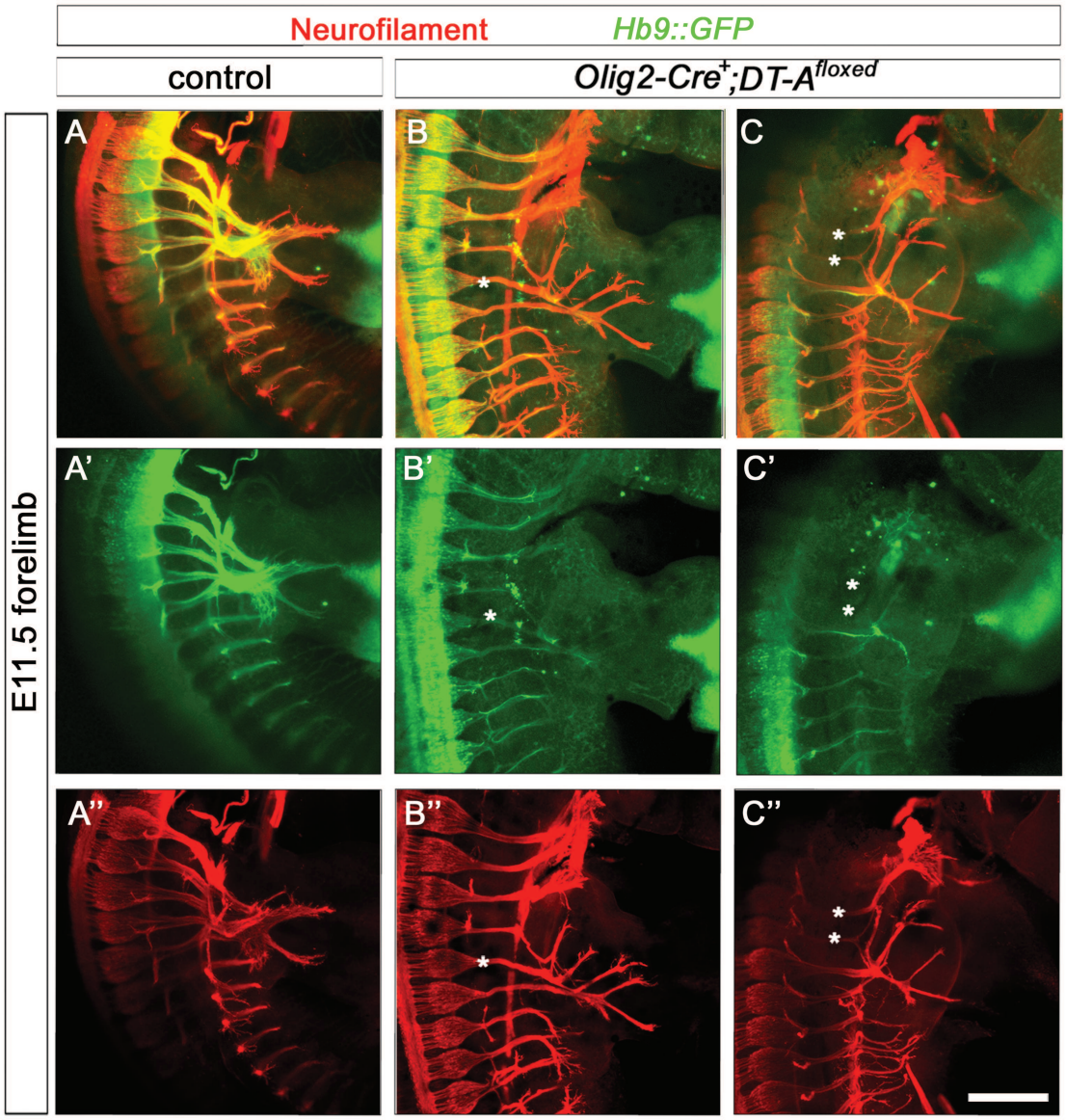


Figure 10: Increased variability in the formation of the plexus und spinal nerves in *Olig2-Cre^{+};DT-A^{floxed}* mice.

Whole mount antibody staining in E11.5 embryos with motor axons visualised by anti-GFP (green) and motor and sensory nerves by anti-neurofilament staining (red). Individual motor (A') or sensory (A'') projections and merged image (A) in controls. (B-C'') Despite complete absence of motor axons (B', C' asterisks), sensory projections from 3-4 DRG converged to the plexus. Subsequent branching resulted

either into supernumerary (B'') or reduced (C'') spinal nerves in *Olig2-Cre*$^{+}$*; DT-A*^{floxed} mutants. Scale bar equals 400µm in all panels.

At E12.5 in the fore- and hind limb of control embryos, motor and sensory axons have navigated the plexus and sorted into individual nerve branches (Fig. 11A,C). Fore- and hind limbs in *Olig2-Cre*$^{+}$*; DT-A*^{floxed} mutants display thinning of sensory nerves, delayed ingrowth to the limb and at times missing nerve branches (Fig. 11B,D; arrows). The data from E12.5 embryos mirror the delay of sensory axon growth and abnormal spinal nerve projection patterns observed at earlier embryonical stages.

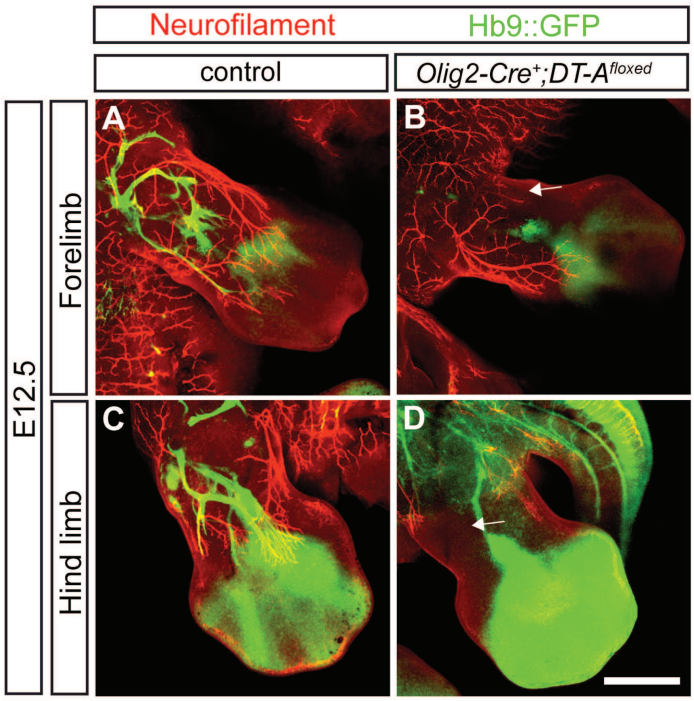


Figure 11: Effects of early motor neuron ablation on sensory projections are maintained at E12.5.

Whole mount antibody staining of fore- (A,B) and hind limbs (C,D) in control (A,C) and *Olig2-Cre*$^{+}$*; DT-A*^{floxed} mutants at E12.5 (B,D). The phenotype of significantly reduced motor projections in *Olig2-Cre*$^{+}$*; DT-A*^{floxed} mutants is associated with thinned and missing sensory nerves (B,D; arrows) in fore- and hind limbs. (A-D) Motor axons are visualised in green (anti-GFP) and motor and sensory projections in red (anti-neurofilament staining). Scale bar equals 500µm in all panels.

Our data suggest that a minimum of outgrowing motor projections is sufficient for correct navigation of sensory axons to the forelimb plexus region. Reduction of motor neuron numbers seems to influence the timing of sensory outgrowth by E10.5 and later on the formation and number of spinal forelimb nerves.

IV.1.3 Sensory axons influence fasciculation and timing of co-extending motor projections to the forelimb

As previously shown, tissue-specific expression of DT-A in peripheral neural crest cells significantly reduced the amount of sensory neurons present in the DRG and thereby enables us to analyse the dependency of outgrowing motor axons on adjacent sensory projections (Fig. 8D-F).

Whole mount embryo preparations at E10.5 showed that the effect of sensory ablation on spinal nerves is determined by their anterior-posterior position in *Ht-PA-Cre*$^{+}$*;DT-A*^{floxed} embryos: nerves 1 and 2 were thinned or absent whereas nerves 3 to 6 appeared defasciculated (Fig. 12B,C). Interestingly, both sensory and motor projections of nerves 3 to 5 were defasciculated (Fig. 12B',B'', arrows) without visible deficits in pathfinding or timing of plexus formation when compared to control animals (Fig. 12A-A'').

Similarly to E10.5, absence of some anterior nerves and branches as well as defasciculation of remaining motor and sensory axons were also observed at E11.5 (Fig. 13D-F'). Additionally, the ingrowth of motor projections into the limb seemed less far advanced than in adjacent sensory axons in *Ht-PA-Cre*$^{+}$*;DT-A*^{floxed} embryos (Fig. 13E',F', arrowhead). Interestingly, pathfinding of motor axons was not hampered in mutant embryos which fits with previous results on target pre-specification of spinal motor projections prior to their outgrowth of the spinal cord (Lance-Jones & Landmesser, 1981a; Landmesser, 2001). Together, the presence of co-extending sensory projections influences the fasciculation status and distal advancement of nearby growing motor axons.

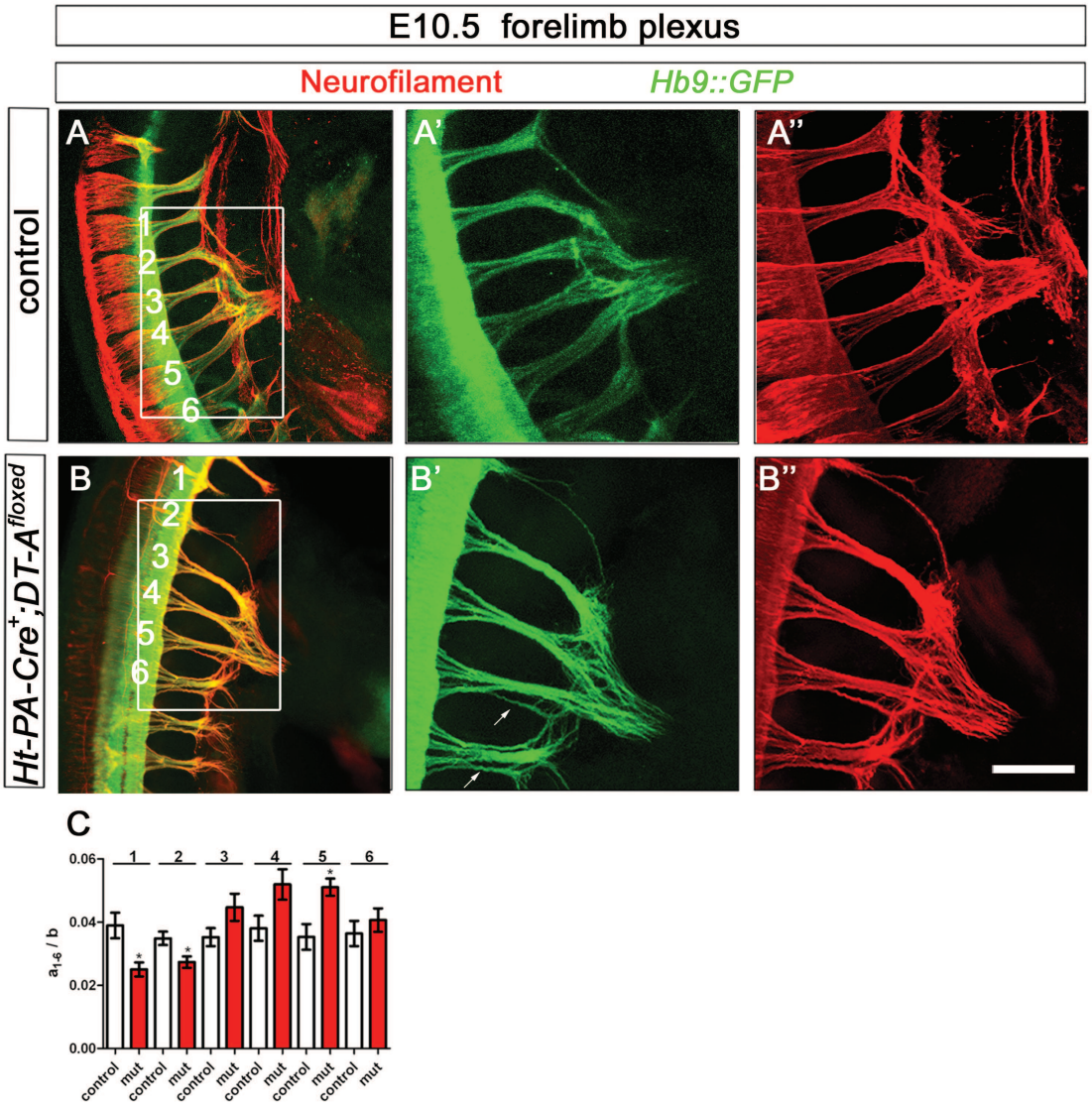


Figure 12: Impaired fasciculation of motor projections in *Ht-PA-Cre*$^{+}$;DT-A^{floxed} mice.
Whole mount E10.5 embryos stained with anti-GFP (motor axons, green) and anti-neurofilament antibody (motor and sensory nerves, red). Significant reduction of sensory neurons in *Ht-PA-Cre*$^{+}$*;DT-A*^{floxed} mutants elicits absent or thinning of anterior spinal nerves 1 and 2 and defasciculation of more posterior motor and sensory projections (B-B''; arrows) relative to control embryos (A-A''). Inlays represent the area of spinal nerves 1-6 (A'-A'') or 2-5 (B'-B'') converging to the plexus. (C) Quantification of the pre-plexus fasciculation of individual spinal nerves a_1-a_6 corroborate the previous observations. Scale bar equals 500µm in all panels. Data were analysed with the two-tailed, unpaired Student's t-test; asterisks indicate significance *p<0.05.

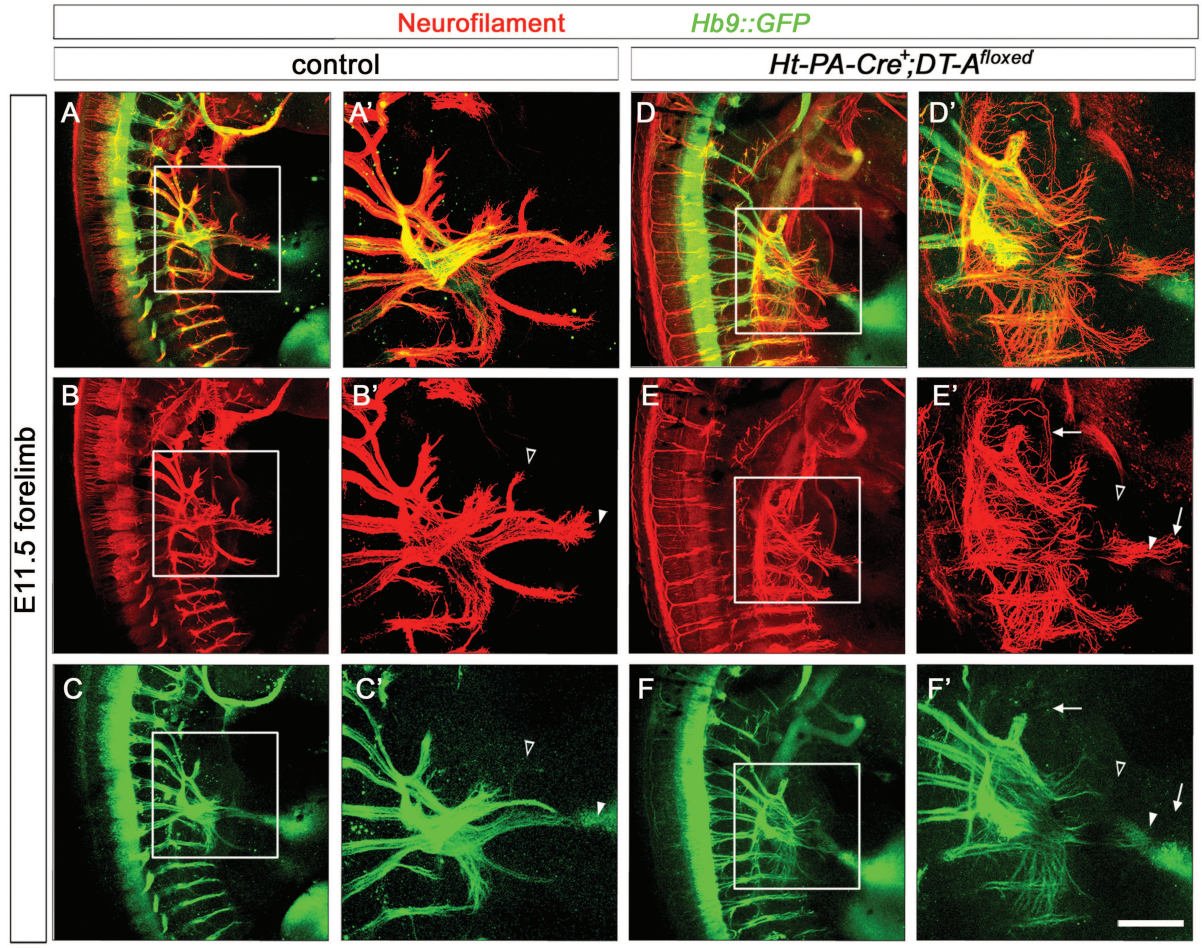


Figure 13: Elimination of sensory neurons impairs the correct formation of motor projections.

Whole mount antibody staining with motor axons shown in green (anti-GFP) and motor and sensory projections in red (anti-neurofilament staining). Control embryos at E11.5 (A-C) and higher magnification of the plexus area (A'-C'). *Ht-PA-Cre*$^{+}$*;DT-A*^{floxed} mutants (D-F') reveal absence of anterior spinal nerve branches (B' compared to E', open arrowhead), severe defasciculation in motor and sensory projections (E-F', arrows) and delay of motor axon ingrowth (E',F', arrowhead). Scale bar equals 400µm in (A-F) and 200µm in (A'-F').

In summary, our data gained from analysis of partial genetic ablation of motor or sensory neurons support previous results that outgrowing spinal sensory and motor axons mutually influence each other *en route* to their limb targets (Lance-Jones & Landmesser, 1981a; Landmesser & Honig, 1986; Swanson & Lewis, 1986; Landmesser, 2001). On the one hand, co-extending motor projections ensure correct timing of sensory axons growth to the plexus as well as formation of stereotypical spinal nerve projection patterns. On the other hand, the presence of sensory neurons contributes to the fasciculation status of motor projections and their timing of limb ingrowth but does not affect the choice of trajectory.

IV.2 Musculoskeletal, neuromuscular and functional forelimb deficits in postnatal mice that lack *Npn-1* on motor neurons

Results from the previous chapter propose a dependency of co-extending sensory and motor axons on their mutual presence for correct wiring of spinal sensorimotor circuitry. However, the underlying mechanisms and molecular cues involved in reciprocal axon-axon interactions are only partially unraveled so far. Evidence is accumulating that axon guidance cues and receptors also serve additional roles in interaxonal communication. Trans-axonal ephrinA-EphA3/A4 signalling is crucial for adjacent axial sensory and motor projections to preserve their separation and prevent inappropriate intermingling of heterotypic axons (Gallarda *et al.*, 2008). Additionally, pre-target sensory axon sorting and olfactory map topography are sensitive to Npn-1 and Sema3A expression levels on olfactory sensory neurons (Imai *et al.*, 2009).

Recent studies in the laboratory used a conditional approach to assess the role of Neuropilin-1 on motor and sensory projections in axon bundling and interaxonal communication *en route* to peripheral limb targets (Huettl *et al.*, 2011). Deletion of Npn-1 from sensory neurons affected the fasciculation but not trajectory fidelity of sensory and motor axons. Loss of Npn-1 in Olig2-Cre expressing motor neurons, however, induces strong defasciculation of motor but not sensory projections to the limb. Additionally, motor axons revealed dorsal-ventral pathfinding defects. Interestingly, in *Olig2-Cre*$^{+}$*;Npn-1*$^{cond-/-}$ mice the distal advancement of defasciculated motor projections was strongly reduced with hardly any motor fibers present in the distal forelimb at E12.5. This finding was corroborated by the inability to retrogradely trace motor projections at E12.5. It was therefore of interest to determine if these defects in embryonic miswiring of motor axons have any impact on postnatal development and behaviour in *Olig2-Cre*$^{+}$*;Npn-1*$^{cond-/-}$ mice. I compared the effect of absence of the entire Npn-1 receptor in motor neurons (*Olig2-Cre*$^{+}$*; Npn-1*$^{cond-/-}$) to loss of Sema-Npn-1-signalling in the entire organisms. *Npn-1*$^{Sema-}$ knockin mice harbour a 7 amino acids substitution in the Sema binding domain of Npn-1 (Gu *et al.*, 2003). In addition to defasciculation and dorsal-ventral pathfinding deficits of motor projections that were likewise observed in *Olig2-Cre*$^{+}$*;Npn-1*$^{cond-/-}$

mice, *Npn-1*$^{Sema-}$ embryos also showed defasciculation of sensory axons and a premature ingrowth to the developing limb (Huber *et al.*, 2005).

IV.2.1 Characterization of forepaw flexor posturing in *Olig2-Cre*$^{+}$*;Npn-1*$^{cond-/-}$ neonatal mice

At birth, *Olig2-Cre*$^{+}$*;Npn-1*$^{cond-/-}$ mutant mice reveal constant flexor posturing by abnormal flexion in one or both paws or forelimbs, which is reminiscent of the defining arthrogryposis phenotype described in the *claw paw* mutant (Bermingham *et al.*, 2006). The phenotype is completely penetrant in *Olig2-Cre*$^{+}$*;Npn-1*$^{cond-/-}$ mutants albeit with variable expressivity affecting one or both paws with differing severity of flexor posturing. These posture abnormalities in the forepaws persist throughout postnatal development without visible amelioration or aggravation. Impairments in hind limbs have never been observed (Fig. 14A-D). No such postnatal fore- or hind limb abnormalities were observed in *Npn-1*$^{Sema-}$ mutants. Additionally, affected *Olig2-Cre*$^{+}$*;Npn-1*$^{cond-/-}$ mutants are retarded in growth, which is manifested by a decreased weight from P4 on when compared to littermate controls (Fig. 14F,G). The reduced number of mutants weaned (16% for females and 18% for males instead of the 25% expected) point to increased prenatal or early neonatal death in these mice (Fig. 14E).



E

Olig2-Cre^{+}; Npn1cond $^{+/-}$	*Olig2Cre^{+}; Npn1cond $^{-/-}$*	*Olig2-Cre^{wt}; Npn1cond$^{+/-}$*	*Olig2-Cre^{wt}; Npn1cond$^{-/-}$*	Total	
25	16	44	15	100	♀
28	18	40	14	100	♂
25	**25**	**25**	**25**	**100**	expected

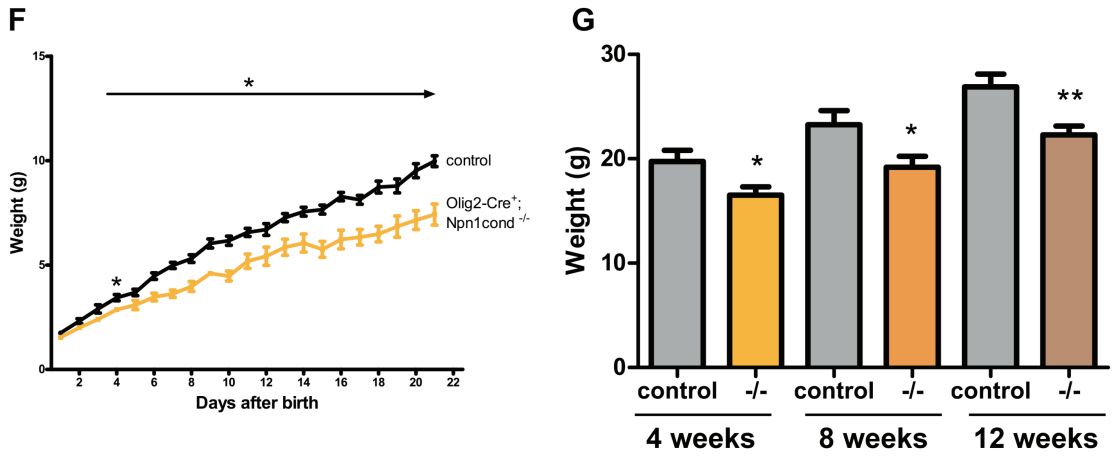


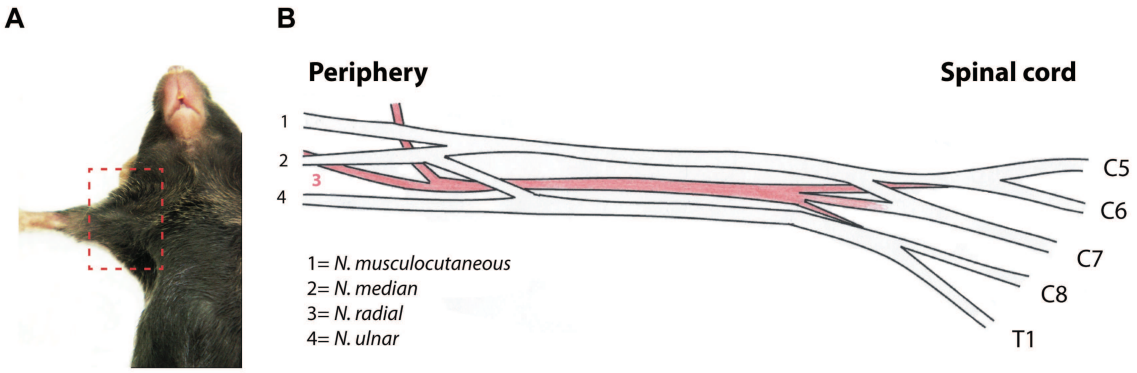
Figure 14: ***Olig2-Cre^{+};Npn-1$^{cond-/-}$* mutants reveal forepaw posture abnormalities and reduced body weight.**

(A-D) Forepaw flexor posturing in mutants (P0 in B, adult in D) compared to controls (P0 in A, adult in C). (E) Genotypes and numbers of female and male mice weaned from *Olig2-Cre^{+};Npn-1$^{cond+/-}$ x Npn-1$^{cond-/-}$* backcrosses relative to expected proportions of genotypes from Mendelian inheritance. (F,G) The weight gain (in g) in *Olig2-Cre^{+}; Npn-1$^{cond-/-}$* from P0 to P22 (F) and at 4, 8 and 12 weeks (G). P0: $n_{control}$= 6; n_{mut}= 6; 4 weeks: $n_{control}$= 10; n_{mut}= 10. Data were analysed with the two-tailed, unpaired Student's t-test; asterisks indicate significance *p<0.05, **p<0.01.

To test wether the peripheral neural circuits activating distal forelimb extensor muscles are functional and thus enable active extension in the wrist, we characterized the movement of the forepaw upon stimulation of the *N.radial* that innervates exclusively extensor muscles (Fig. 15A,B).

Single train stimulation of the *N.radial* distal to the brachial plexus in control mice older than 12 weeks resulted in extension of the digits and wrist of the forelimb. In the affected paws in all *Olig2-Cre^{+};Npn-1$^{cond-/-}$* mice analysed, we could never elicit extensor-like movements in any forelimb parts distal to the elbow. Instead flexion movements of the elbow were observed. If only one paw showed loss of active extension, extension could be elicited by stimulation of the *N.radial* in the unaffected forelimb. Stimulation of the other major forelimb nerves, *N.median* and *N.ulnar,* that innervate distal antagonistic flexor muscles caused flexion of elbow, wrist and digits in control animals and in *Olig2-Cre^{+};Npn-1$^{cond-/-}$* mutants. Innervation of muscles like

Biceps brachii located proximal of the elbow joint by *N.musculocutaneous* was also indistinguishable from control animals (Fig. 15C).



C

	Nerve	Control		Olig-2Cre^{+};Npn-1$^{cond-/-}$	
1	*N. musculocutaneous*	Flexion	Elbow	Flexion	Elbow
2	*N. median*	Flexion	Wrist	Flexion	Wrist
3	*N. radial*	Extension	Wrist / Digits	**No extension** Flexion	Elbow
4	*N. ulnar*	Flexion	Elbow	Flexion	Elbow

Figure 15: Loss of active extension in the distal forelimb of *Olig2-Cre^{+};Npn-1$^{cond-/-}$* mutants upon stimulation of *N.radial.*

(A,B) Illustration of the brachial plexus area (red dashed line) and the 4 major nerves innervating extensor and flexor muscles in the forelimb (B). (C) Forelimb flexor or extensor movements elicited by single nerve stimulation in control or mutant mice. $n_{control}$= 3; n_{mut}= 3.

Together, the absence of extension in affected distal forepaws in *Olig2-Cre^{+};Npn-1$^{cond-/-}$* mutants might be explained by defects in neuronal circuit wiring and forepaw muscle innervation. However, other factors might likewise contribute to this phenotype, alone or in combination. We therefore investigated the peripheral musculoskeletal and neuromuscular system.

IV.2.2 Reduced dorsal forelimb extensor muscle area and further postnatal degeneration in affected mutants

Paralysis of peripheral nerves or degeneration of forelimb extensor muscles results in wrist-drop of the paw and appears very similar to the phenotype we have observed in *Olig2-Cre^{+};Npn-1$^{cond-/-}$* mutants (reviewed in Darbas *et al.*, 2004). Visual inspection of

the forelimb in 4 weeks old mice revealed a reduction in dorsal extensor muscles exposing tendons located beneath in *Olig2-Cre*$^{+}$*;Npn-1*$^{cond-/-}$ mutants compared to the volume of extensor muscles and localization of tendons in control mice (Fig. 16F,G). To quantitify their size, we determined the area that forelimb extensor *Carpi Radialis longus* and *brevis* and control wrist flexor muscle *Carpi ulnaris* occupy in cross sections of both affected and unaffected limbs of *Olig2-Cre*$^{+}$*;Npn-1*$^{cond-/-}$ mice at P0. The position of the specified muscles was identified according to previously published anatomical data and visualised by immunohistochemistry using anti-myosin for musculature and anti-neurofilament for peripheral nerves (Fig. 16A; Watson *et al.*, 2009). This was done as a part of the bachelor thesis of Julia Sundermeier whom I supervised (Sundermeier, 2009).

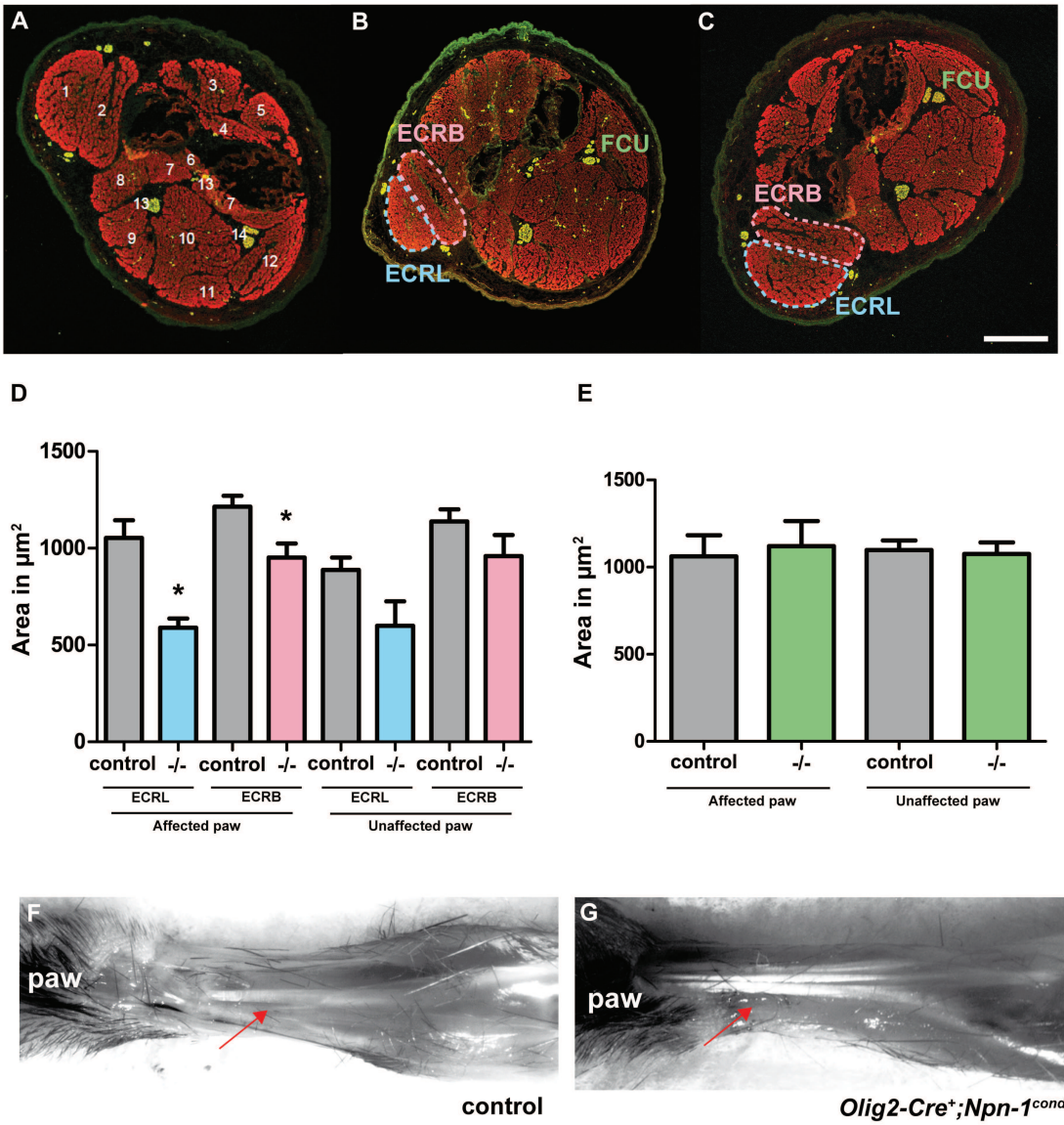


Figure 16: Reduced forelimb extensor muscle area in newborn *Olig2-Cre^{+};Npn-1$^{cond-/-}$* mutants.

(A) Immunohistochemistry with anti-myosin (muscles, red) and anti-neurofilament (nerves, green) antibodies in cross sections of the distal forelimb of P0 mice (*1= Extensor Carpi Radialis Longus, 2= Extensor Carpi Radialis Brevis, 3= Extensor Digitorum Communis, 4= Extensor Pollicis, 5= Extensor Indicis Proprius, 6= Pronator Quadratus, 7= Flexor Digitorum Profundus, 8= Supinator, 9= Flexor Carpi Radialis, 10= Flexor Digitorum Sublimis, 11= Extensor Digiti Quarti, 12= Flexor Carpi Ulnaris, 13= Nervus medianus, 14= Nervus ulnaris*). Localization of the 2 extensor muscles *Extensor carpi radialis longus (ECRL*, blue*)* and *Extensor carpi radialis brevis (ECRB*, pink*)* and antagonistic *Flexor carpi ulnaris (FCU*, green*)* in control (B) and newborn *Olig2-Cre^{+};Npn-1$^{cond-/-}$* mutants (C). Area in µm^2 of ECRL and ECRB (D) and FCU (E) in forelimbs affected by posture abnormalities and unaffected paws in mutant and control animals. Dorsal extensor muscles in the distal forelimb of 4 weeks old control (F) and *Olig2-Cre^{+};Npn-1$^{cond-/-}$* mutants (G). Red arrow indicates the area where the tendons are covered by dorsal muscles in control but not mutant mice. Scale bar equals 500µm in A-C. $n_{control}$= 3; n_{mut}= 3. Data were analysed with the two-tailed, unpaired Student's t-test; asterisks indicate significance *p<0.05. (Experiments A-E performed by Julia Sundermeier).

Interestingly, the mean area of both distal forelimb extensors *Carpi Radialis longus* (ECRL) and *brevi*s (ECRB) were signifcantly reduced in the affected paw of P0 mutants and tend to be decreased in unaffected paws relative to control littermates (Fig. 16B-D). In contrast, ventral flexor *Carpi ulnaris* (FCU) muscles size both in wrist-drop affected and functional forelimb is indistinguishable from wildtype values (Fig. 16E).

Our data demonstrate that the observed *claw paw*-like forelimb posture abnormalties in *Olig2-Cre^{+};Npn-1$^{cond-/-}$* mutants are accompanied by a reduction in the size of dorsal extensor but not antagonistic flexor muscles already at birth. During subsequent postnatal development the extensor muscles atrophy even further.

IV.2.3 Skilled locomotion is impaired in *Olig2-Cre^{+};Npn-1$^{cond-/-}$* mutants

Sensorimotor wiring deficits in the forelimbs of *Olig2-Cre^{+};Npn-1$^{cond-/-}$* mice during embryogenesis predict impairments in motor innervation but not in the formation of sensory projections (Huettl *et al.*, 2011). In order to ensure that sensory function is not affected if Npn-1 is removed from motor neurons, the response to heat as a noxious stimulus was measured on the Hot Plate. We found no significant difference in the latency of forepaw shaking or licking in mutant animals relative to control littermates ($p_{shaking}$= 0.40, $p_{licking}$= 0.89; $n_{control}$= 9, n_{mut}= 9; non-parametric Mann-Whitney test). Similarly, *Npn-1^{Sema-}* mutants did not reveal deficits in noxious sensory

functions ($p_{shaking}$= 0.22, $p_{licking}$= 1.00; $n_{control}$= 6, n_{mut}= 6; non-parametric Mann-Whitney test).

The loss of active extension in affected forelimbs of *Olig2-Cre^{+};Npn-1$^{cond-/-}$* mice predicts functional deficits in stereotyped overground locomotion. In order to assess gross motor capabilities, control and mutant animals were tested for voluntary movement in the open field apparatus. Interestingly, mutant *Olig2-Cre^{+};Npn-1$^{cond-/-}$* mice move with a comparable velocity to control mice and reveal no deficits in horizontal or vertical locomotion (rearings). All three parameters are slightly reduced in mutants but not significantly different from control mice (Fig. 17A-C). Similar, loss of Semaphorin-Npn-1 signalling in *Npn-1^{Sema-}* mice does not affect their gross locomotor capabilities represented by the total distance travelled (horizontal locomotion; p= 0.19), number of rearings (vertical locomotion; p= 0.37) or locomotor speed (p= 0.23).

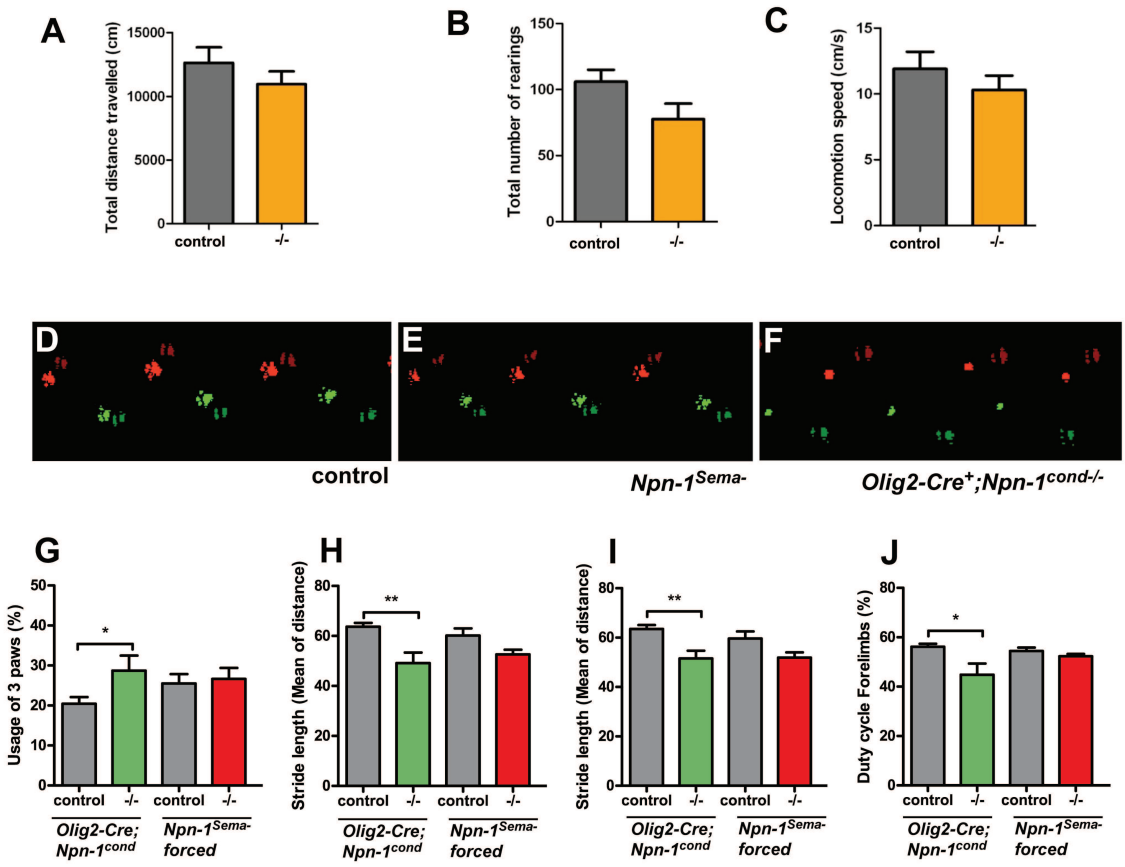


Figure 17: Gait irregularities in *Olig2-Cre^{+};Npn-1$^{cond-/-}$* mutants.
(A-C) Gross locomotion parameters such as horizontal (A) or vertical locomotion (B) and velocity of voluntary movement (C) tested in the open field of 4 weeks old *Olig2-Cre^{+};Npn-1$^{cond-/-}$* mutants and controls. (D-J) Catwalk derived gait analysis parameters such as paw prints of fore- and hind limbs in control (D), *Npn-1^{Sema-}* mutants (E) and *Olig2-Cre^{+};Npn-1$^{cond-/-}$* affected in both forelimbs (F), the usage

of 3 paws in % (G), stride length of fore- (H) or hind paws (I) and the duty cycle in forelimbs in % (J). *Olig2-Cre;Npn-1*^{cond}: $n_{control}$= 9; n_{mut}= 8; *Npn-1*$^{Sema-}$: $n_{control}$= 5; n_{mut}= 9. Data were analysed with the non-parametric Mann-Whitney test; asterisks indicate significance *p<0.05, **p<0.01.

Next, we analysed dynamic gait parameters in detail to reveal subtle changes. Regularity of walking was lost in *Olig2-Cre*$^{+}$*;Npn-1*$^{cond-/-}$ mutants: we detected disturbances in parameters like usage of 3 paws (Fig. 17G) as an indicator of balance problems and specifically in the stride length of fore- and hind limbs (Fig. 17H,I). Additionally, the loss of extension in forepaws accounts for the characteristic paw prints in the affected forelimbs of mutant mice resembling walking on fists (Fig. 17D,F) and the reduced stance duration of forepaws repesented in the duty cycle (Fig. 17J). We then assessed more complex motor skills such as performance on the accelerating rotarod and motor coordination on the grid walk.

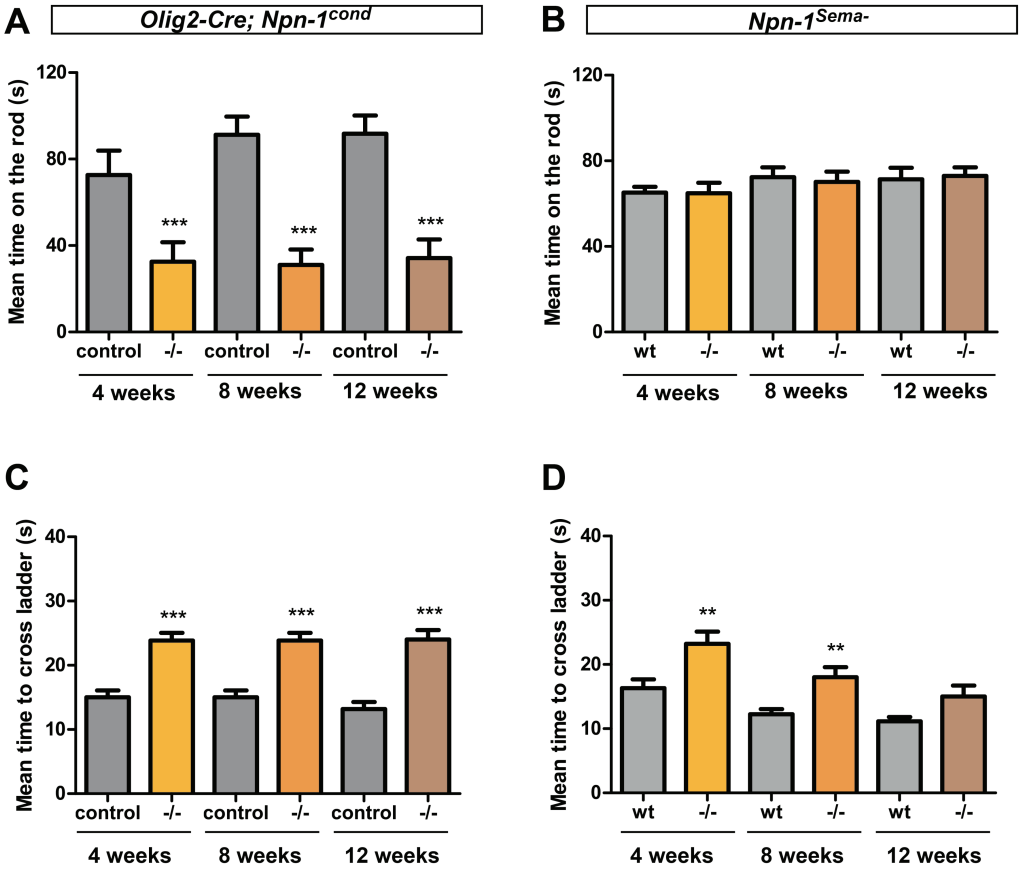


Figure 18: Persistent deficits in skilled locomotion in *Olig2-Cre*$^{+}$*;Npn-1*$^{cond-/-}$ mutants.
(A,B) Mean time that the mice spent on the accelerating rotarod as an indicator of balance and motor coordination in *Olig2-Cre*$^{+}$*;Npn-1*$^{cond-/-}$ mutants and controls (A) and in *Npn-1*$^{Sema-}$ mice (B). (C,D) Motor coordination capabillities tested in the grid walk: mean time to cross the horizontal ladder in *Olig2-Cre*$^{+}$*;Npn-1*$^{cond-/-}$ (C) as well as *Npn-1*$^{Sema-}$ mice (D). *Olig2-Cre;Npn-1*^{cond}: $n_{control}$= 10; n_{mut}= 10;

Npn-1^{Sema-}: $n_{control}$= 12; n_{mut}= 12. Data were analysed with the non-parametric Mann-Whitney test; asterisks indicate significance **p<0.01, ***p<0.001.

Olig2-Cre^{+}*;Npn-1*$^{cond-/-}$ mutants were able to stay on the accelerating rod approximately half the time than control animals and were unable to improve their performance from 4 to 12 weeks (Fig. 18A). Interestingly, *Npn-1*$^{Sema-}$ animals performed at wildtype-level on the rotarod (Fig. 18B). To investigate whether forelimb-hind limb coordination capabilties were impaired, mice were assessed in the grid walk test: the time it takes the mouse to cross a horizontal ladder with irregularly spaced bars is measured. *Olig2-Cre*$^{+}$*;Npn-1*$^{cond-/-}$ mutants performed significantly worse than their control littermates and did not improve their performance up to 12 weeks of age (Fig. 18C; improvement in mutants from 4 to 12 weeks: -2,90%). *Npn-1*$^{Sema-}$ mutants also performed significantly worse than their wildtype littermates at 4 weeks. However, over the course of the next 8 weeks these mutants improved their motor coordination skills (Fig. 18D; improvements in mutants from 4 to 12 weeks: +33.85%) suggesting functional or anatomical compensation in *Npn-1*$^{Sema-}$ mice.

Together, forelimb abnormalities in *Olig2-Cre*$^{+}$*;Npn-1*$^{cond-/-}$ mutants do not interfere with gross locomotion but cause specific irregularities in walking patterns and deficits in skilled motor performance. These deficits are unchanged during further postnatal improvement. In contrast, *Npn-1*$^{Sema-}$ mutants also showed severe impairments in motor coordination at 4 weeks but improved locomotor performance from 4 to 12 weeks.

IV.2.4 Postnatal bone malformations in the affected forepaw of *Olig2-Cre*$^{+}$*; Npn-1*$^{cond-/-}$ mutants

The majority of vertebrate bones are generated postnatally by secondary endochondral ossification of cartilaginous templates into bones (Hartmann, 2009). Based on the biomechanical link of bone and muscles, there is a direct correlation of neuromuscular function to bone properties and remodelling throughout skeletal growth (Gross *et al.*, 2010). Murine models of muscle pathologies e.g. spinal muscular atrophy or traumatic injury to the CNS or PNS with focal paralysis of muscles revealed a significant influence of muscle and nerve dysfunction on bone homeostasis, morphology and skeletal degradation (Kingery *et al.*, 2003; Warner *et al.*, 2006; Morse *et al.*, 2008; Shanmugarajan *et al.*, 2009). Since *Olig2-Cre*$^{+}$*;*

Npn-1$^{cond-/-}$ mice showed loss of active functional extension of the paws and muscular atrophy in the respective forelimb extensor muscles, we analysed putative effects on bone structural properties. Differential staining of P0 skeleton of control and mutant mice with Alizarin Red S and Alcian blue for fetal bone and cartilage, respectively, as well as radiographic analysis in 40 weeks old adult mice were conducted in cooperation with Christian Cohrs (Institute of Experimental Genetics, HGMU).

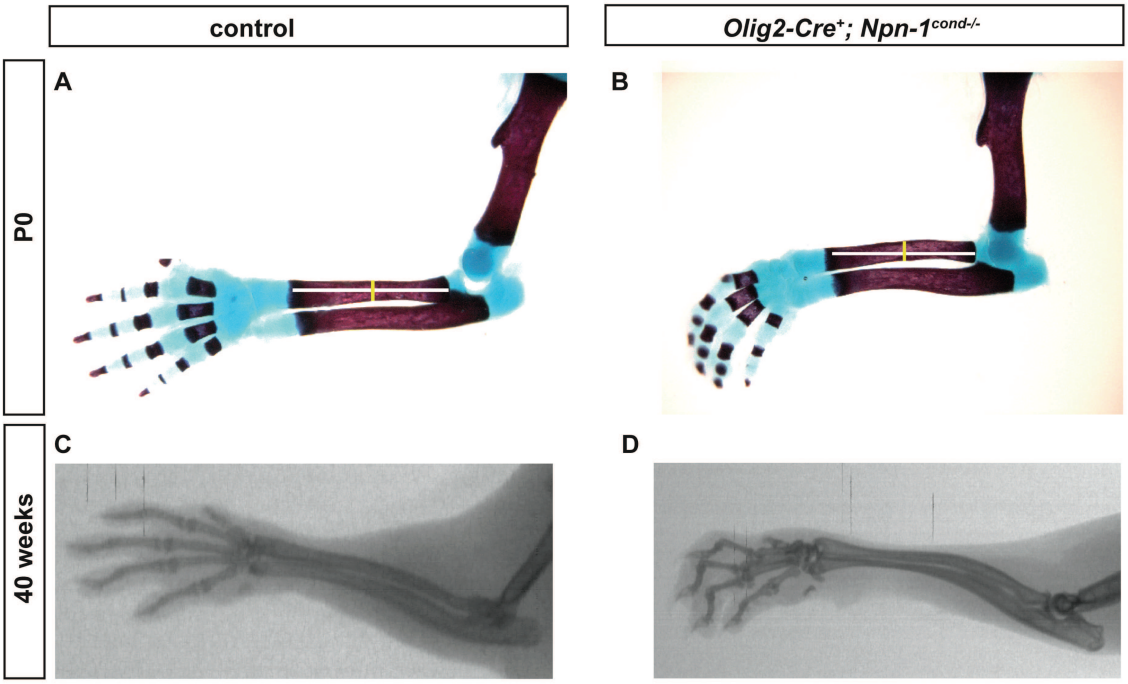


Figure 19: Distal forelimb bone malformations in *Olig2-Cre*$^{+}$*;Npn-1*$^{cond-/-}$ mutants.
(A,B) Skeletal preparations of control (A) and affected forelimbs of *Olig2-Cre*$^{+}$*;Npn-1*$^{cond-/-}$ (B) stained with Alizarin Red and Alcian Blue to visualise the bone-cartilage structure at P0. (C,D) X-ray images of forelimb bone morphology in 40 weeks old control (C) and *Olig2-Cre*$^{+}$*;Npn-1*$^{cond-/-}$ (D) mice. *Olig2-Cre;Npn-1*^{cond} P0: $n_{control}$= 2; n_{mut}= 3; 40 weeks: $n_{control}$= 2; n_{mut}= 2.

The morphological pattern of skeletal elements in forelimbs at birth did not reveal abnormalties in generation or distribution of cartilage and bone nor in bone thickness or length in mutants relative to controls (Fig. 19A,B; p_{length}= 0.20; $p_{thickness}$= 0.12). In order to address secondary endochondral ossification deficits due to mechanical disuse in affected forepaws, we assessed the bone morphology by X-ray in 40 weeks old *Olig2-Cre*$^{+}$*;Npn-1*$^{cond-/-}$ mice. The bone digits of affected paws exhibit severe deformity and ulna and radius bones seem to be reduced in thickness compared to *Olig2-Cre*$^{+}$*;Npn-1*^{cond} controls (Fig. 19C, D). Indeed, quantification of bone width (p= 0.003) revealed a significant reduction in mutant mice.

In summary, forelimb neuromuscular dysfunction in *Olig2-Cre^{+};Npn-1$^{cond-/-}$* mutants promotes bone deformity in the distal forelimb during postnatal secondary endochondral ossification.

IV.2.5 Alterations in the fiber composition of *N.radial* in *Olig2-Cre^{+};Npn-1$^{cond-/-}$* mutants

During embryogenesis, peripheral axons are sorted into prospective nerves while they are growing towards their respective targets. Axons tightly associate with Schwann cells that myelinate single large diameter axons or ensheath numerous small unmyelinated fibers into Remak bundles (Jessen & Mirsky, 2005).

To determine whether Npn-1 plays a role in axon sorting and/or axon-Schwann cell interaction, we assessed the myelination status and composition of defined nerves mediating forelimb extension or flexion. The *N.radial* innervating extensor muscles and *N.median* representing a nerve projecting to flexor muscles were ultrastructurally analysed in mice older than 12 weeks. The Institute of Pathology (HGMU) helped in preparing the tissues for EM analysis and quantified the nerve pictures with the Definiens image analysis software (see Material and Methods III.4). For a reliable readout of correct myelination, the g-ratio as a quantitative index of the thickness of myelin sheath with respect to the total axon diameter was used (Fig. 20A). Myelination in *N.radial* and *N.median* in affected paws of *Olig2-Cre^{+}; Npn-1$^{cond-/-}$* mice did not differ from control animals. Similarly, inactivation of the semaphorin binding site in *Npn-1^{Sema-}* mutants did not seem to interfere with proper myelination of *N.radial* (Fig. 20B).

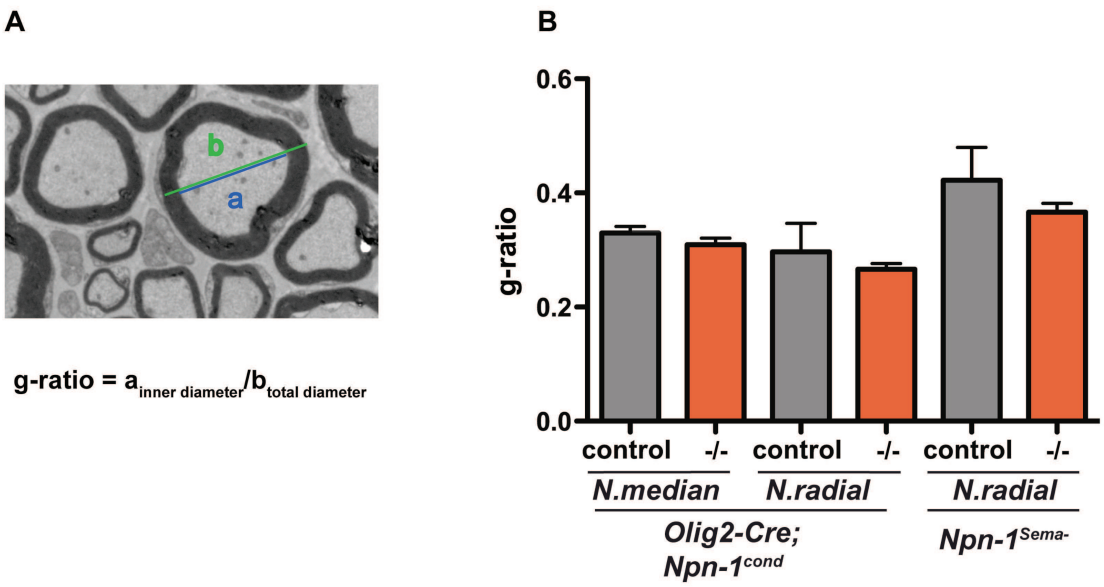


Figure 20: Normal myelination of PNS forelimb nerves in *Olig2-Cre^{+};Npn-1$^{cond-/-}$* and *Npn-1^{Sema-}* mutants.

(A) Determination of the g-ratio as the quotient of inner (a) to total axon diameter (b). (B) g-ratio of *N.median* and *N.radial* nerve in *Olig2-Cre^{+};Npn-1$^{cond-/-}$* and *Npn-1^{Sema-}* mutants and controls. *Olig2-Cre;Npn-1^{cond}*: $n_{control}$= 3; n_{mut}= 3; *Npn-1^{Sema-}*: $n_{control}$= 1; n_{mut}= 1. Data were analysed with the two-tailed, unpaired Student's t-test.

Loss of active extension in the forepaw of *Olig2-Cre^{+};Npn-1$^{cond-/-}$* mutants might be associated with changes in the *N.radial* innervating the extensor muscles. Thus, the composition of *N.radial* and a nerve innervating flexor muscles, *N.median* as control, was analysed with regard to the amount of large and small diameter axons and Remak bundles. Indeed, the composition of *N.radial* in *Olig2-Cre^{+}; Npn-1$^{cond-/-}$* mutants appeared changed with an increase in the size of Remak bundles and amount of small diameter axons relative to control animals (Fig. 21A,B). Interestingly, no changes in the relation of small and large axons or Remak bundles were apparent in *N.median* projecting to antagonistic flexor muscles (Fig. 21C,D). Again, distribution of axons versus Remak bundles in *N.radial* of *Npn-1^{Sema-}* mutants appeared comparable in mutant and wildtype controls (Fig. 21E,F).

The observations were quantified with the help of the Institute of Pathology (HGMU) using the Definiens image analysis software by setting a pixel threshold to distinguish between large and small diameter axons (Fig. 21G). Quantification data corroborated the previous observations that in the *N.radial* of *Olig2-Cre^{+};Npn-1$^{cond-/-}$* mutants a significant reallocation from large diameter axons to predominantly small diameter axons occured (Fig. 21H). Quantification of *N.median* in the affected

forelimb revealed increased numbers of Remak bundles whereas the number of axonal subtypes was not altered compared to age-matched control mice (data not shown, p_{AxonsL}= 0.94; p_{AxonsS}= 0.64; $p_{Remak\ bundles}$<0.05; unpaired, two-tailed Student's t-test).

Additionally, the number of Remak structures and fibers per bundle were counted. The number of axon fibers ensheathed per Remak bundle in *Olig2-Cre*$^{+}$*; Npn-1*$^{cond-/-}$ mutants relative to control mice was increased by roughly 2,38 times. In contrast, the number of fibers incorporated per Remak bundle (Fig. 21I) were not altered in *N.median* of *Olig2-Cre*$^{+}$*;Npn-1*$^{cond-/-}$ animals.

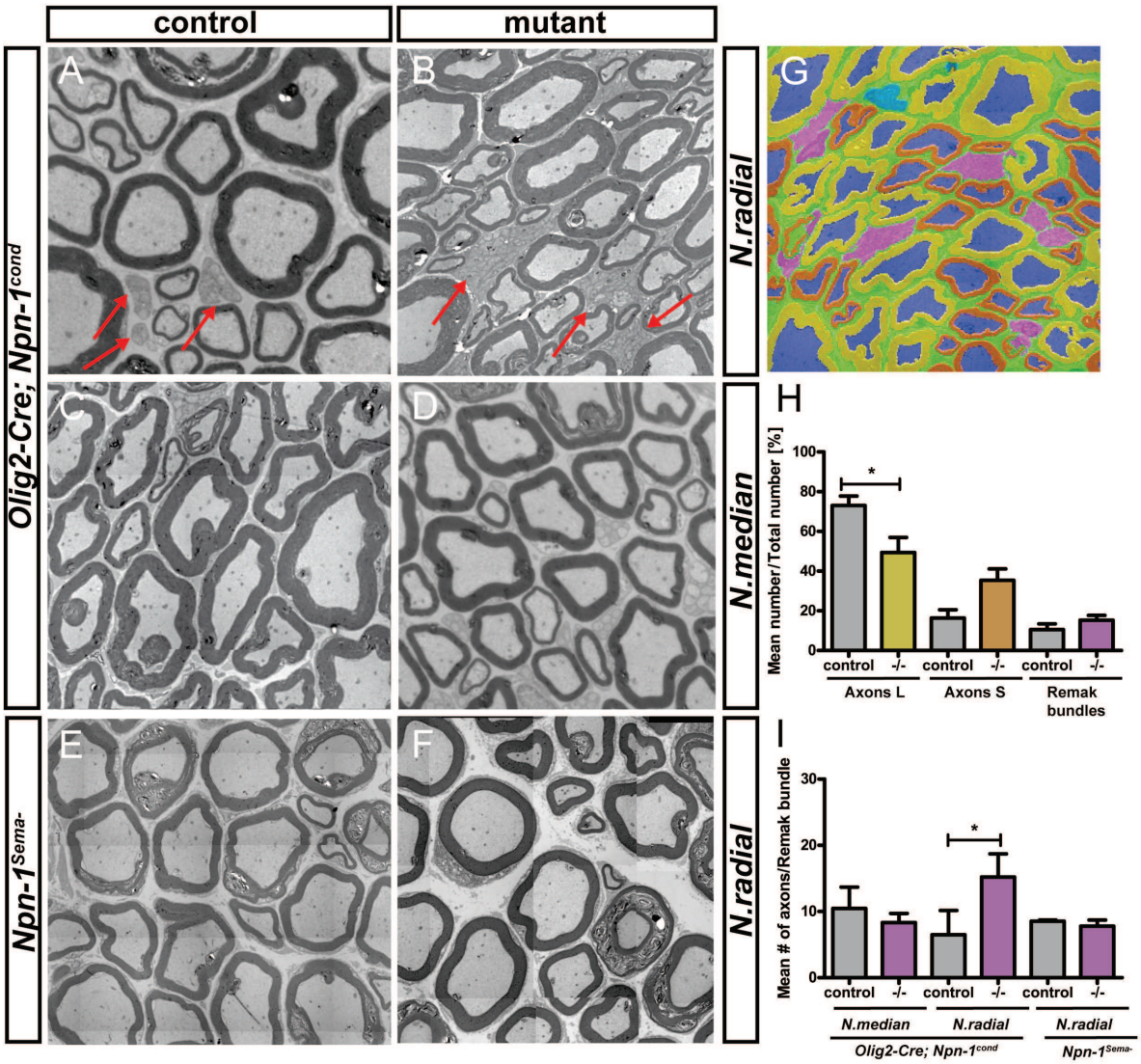


Figure 21: Significant changes in axon size and number of fibers in *N.radial* of *Olig2-Cre*$^{+}$*; Npn-1*$^{cond-/-}$ mutants.

(A-F) Electron microscopy images (magnification: 5000x) of *N.radial* (A,B) and *N.median* (C,D) in control and *Olig2-Cre*$^{+}$*;Npn-1*$^{cond-/-}$ mutants and *Npn-1*$^{Sema-}$ (E,F) mice. Remak bundles in A,B are marked by red arrows. (G) Scheme for axon classification by size into small (brown) or large diameter

(yellow) axons and unmyelinated Remak bundles (purple) using Definiens image analysis software. (H) Mean number of large diameter axons (Axons L), small diameter axons (Axons S) and unmyelinated Remak bundles as percentage of total axon numbers. (I) Mean number of axons incorporated per Remak bundle in *N.median* or *N.radial* of control and *Olig2-Cre*$^{+}$*;Npn-1*$^{cond-/-}$ and *Npn-1*$^{Sema-}$ mutants. *Olig2-Cre; Npn-1*^{cond}*:* $n_{control}$= 3; n_{mut}= 3; *Npn-1*$^{Sema-}$: $n_{control}$= 1; n_{mut}= 1. Data were analysed with the two-tailed, unpaired Student's t-test; asterisks indicate significance *p<0.05.

Preliminary results indicate that the semaphorin binding domain in the Npn-1 receptor is not required for proper myelination of peripheral *N.radial* nor for the correct ratio of small and large diameter axons to unmyelinated Remak bundles (data not shown) or fibers ensheathed per Remak bundle (Fig. 21I) as no differences were found in *Npn-1*$^{Sema-}$ mutants.

Our data suggest a reallocation in the ratio of large to predominantly smaller myelinated axons and an approximately twofold increase of fibers incorporated per Remak bundle in the *N.radial* of affected *Olig2-Cre*$^{+}$*;Npn-1*$^{cond-/-}$ mutants.

IV.3 Adaptive structural plasticity parallels motor recovery in a model of neurodevelopmental miswiring

During nervous system development, growing axons need to interconnect and wire the entire neuronal circuits of the organism. At spinal level, interaction of the chemorepellent Sema3F with its receptor Npn-2 is crucial for correct wiring of sensorimotor networks. Thus, loss of Sema3F-Npn-2 signalling results in aberrant pathfinding of medial motor projections of the lateral motor column (LMC) to dorsal limb targets (Huber *et al.*, 2005). This pronounced genetically-induced wiring defect of peripheral sensorimotor circuitry proposes defined postnatal deficits in motor and/or sensory function. Since *Sema3F* and *Npn-2* mutants are viable, we assessed their locomotor abilities as well as potential mechanisms to compensate for or adapt to the miswired peripheral circuitry by combining behavioural phenotyping with neuroanatomical and functional analyses of spinal neural networks.

IV.3.1 Specific deficits in motor coordination in *Sema3F* mutant mice

Sema3F and *Npn-2* mutant mice displayed no deficits when we tested them for sensory functions such as the optokinetic reflex, somatosensory whisker representation or nociception (data not shown). The proper connection of motor axon terminals with the target muscles via neuromuscular junctions was analysed by the grip strength test. The neuromuscular strength of forelimbs ($p= 0.41$) or the combined fore- and hind limb strength ($p= 0.08$) was not significantly altered in *Sema3F* mutants at 4 weeks.

Embryonic dorsal-ventral motor axon pathfinding defects suggest functional deficits in motor behaviour. Indeed, the majority of adult *Sema3F* mutant mice flex one or both hind limbs when lifted by their tail instead of extending them as observed in wildtype littermates. This change in the hind limb extension reflex test suggests a motor phenotype in *Sema3F* mutants (Barneoud *et al.*, 1997). Mice were subjected to a battery of behavioural test at 4, 8 and 12 weeks of age to thoroughly assess locomotor skills and reveal potential impairments and subsequent changes in motor performance during postnatal development. The locomotor performance of the tested *Sema3F* and *Npn-2* mice in the behaviour test battery is summarized in Table 1 in

IV.3.6. We first tested general locomotor behaviour in the open field, where horizontal and vertical locomotion, locomotor speed and anxiety-related behaviours were recorded. We found no significant differences in any of these parameters in *Sema3F* mutants when compared to wildtype littermates ($p_{Total\ distance}$= 0.48; $p_{Rearings}$= 0.35; $p_{Locomotor\ speed}$= 0.86; $p_{Distance\ travelled\ in\ the\ center}$= 0.91). Additionally, we assessed more complex and precise motor skills such as balance on an elevated narrow beam and performance on the rotarod, under accelerating velocity conditions. 4 weeks old *Sema3F* mutants crossed the elevated beam significantly slower ($p<0.05$) than control littermates. The rotarod tests revealed no impairments in *Sema3F* mutant mice (p= 0.85). Thus, *Sema3F* mutants have no obvious deficits in overground and gross locomotion but slight impairments in balance at 4 weeks only.

We addressed skilled locomotor capabilities further by testing the forelimb-hind limb coordination during walking on a horizontal ladder with irregularly spaced bars. *Sema3F* mutants required significantly more time to cross the ladder and showed an increased number of paw slips (Fig. 22A,C). Additionally, they displayed deficits in fine motor control of hindpaw placement at 4 weeks of age (Fig. 22D). During postnatal development, *Sema3F* mutants gradually improved their performance from 4 to 12 weeks, however, without attaining wildtype performance levels (Fig. 22A). When the performance on the grid walk of individual mutant animals was analysed, a significant segregation of the population became obvious. One group behaved close to wildtype levels (wildtype-like performers) and another group of mutant animals performed at least 2 standard deviations worse than the wildtype mean (poor performers, Fig. 22B; highlighted in blue and orange, respectively). This segregation of *Sema3F* mutants into two groups was less prominent at 12 weeks. Separate quantification of motor improvements for the two mutant populations revealed that recovery rates over 8 weeks of poorly performing mutants surpassed those of wildtype-like performers (Fig. 22E; $improvement_{Grid\ walk}$ from 4 to 12 weeks in time= 47,75% and slips= 62,22%).

These findings were corroborated in a wire climbing test where mice are hung on a thin horizontal wire by their forepaws and have to lift their hind limbs up to the wire and pull themselves forward. We modified the SHIRPA wire manoeuvre test focussing on hind limb grip capabilities (Rogers *et al.*, 1997) to additionally evaluate the climbing performance of the mice along the wire. Apart from muscular strength, this requires precise inter-limb coordination.

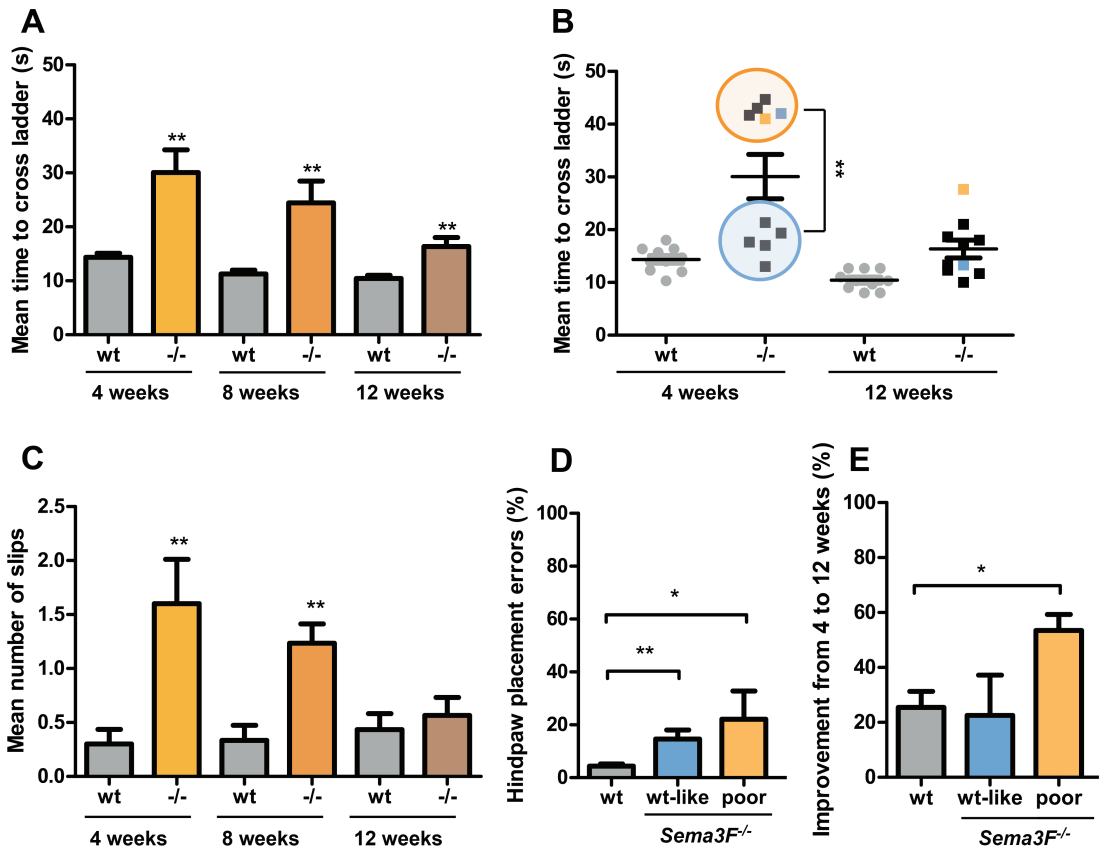


Figure 22: Motor coordination deficits improve during postnatal development in *Sema3F* mutants.

(A,C) Grid walk: mean time to cross the horizontal ladder (A) and mean number of paw slips (C) at 4, 8 and 12 weeks. (B) Segregation of *Sema3F* mutants into wildtype-like (blue circle) and poor performers (orange circle) at 4 and 12 weeks. Individual poor performers either improve their coordination skills from 4 to 12 weeks to wildtype level (blue rectangle) or still show significant motor deficits (orange rectangle). (D) Errors in precise hindpaw placement as % of total paw placements at 4 weeks (n= 3 for all groups). (E) Improvement of motor coordination from 4 to 12 weeks with respect to mean time for crossing the ladder. Data were analysed with the nonparametric Mann-Whitney test; asterisks indicate significance *p<0.05, **p<0.01.

The wire climbing strategies of the mice were rated according to a qualitative scale. The scores ranged from 1 for coordinated, rhythmic climbing with both fore- and hind limbs to 8 corresponding to uncoordinated climbing lacking any rhythmic movements. *Sema3F* mutants showed signifcant difficulties in pulling themselves up to the wire, coordinating fore- and hind limbs while climbing along and displayed clasp-like hind limb movements at 4 weeks of age (Fig. 23C). The wire climbing test cannot be done at 12 weeks as the mice are unable to lift themselves up to the wire due to the physiological increase in body weight from 8 to 12 weeks.

Together, embryonic loss of Sema3F-Npn-2 signalling results in postnatal motor coordination deficits whereas stereotyped overground locomotion is unaffected. *Sema3F* mutants segregate into wildtype-like performers with coordination skills comparable to wildtype littermates and poor performers with severe deficits in motor coordination. The significant, subsequent improvement in behavioural performance of *Sema3F* mutants over the course of 8 weeks is a strong indication that adaptive changes occured in these mutant animals.

IV.3.2 Loss of *Npn-2* leads to additional motor impairments

Neuropilin-2 is the only known receptor for Sema3F and essential for the chemorepulsive action of this ligand on LMCm motor projections. The locomotor performance of mice lacking Npn-2 was assessed in the same battery of behavioural tests as previously described for *Sema3F* mice. The observed motor deficits in *Npn-2* mutants were very similar to the motor phenotype in *Sema3F* mutants (Fig. 23A,B,D-F). In addition, *Npn-2* mutant mice also revealed deficits in parameters assigned to gross locomotion like vertical locomotion by decreased amount of rearings in the open field ($p<0.05$) as well as in tests examining a combination of balance and coordination skills: the time that 4 weeks old *Npn-2* mutants spent on the rotarod was decreased under accelerating velocity conditions (Fig. 23F). Similar to *Sema3F* mice, *Npn-2* mutants required significantly longer to traverse an elevated narrow beam relative to their wildtype littermates (Fig. 23E). Coordination skills on the horizontal ladder also segregated *Npn-2* mutants into wildtype-like and poor performers (Fig. 23B). Improvement of locomotor performance in *Npn-2* mutants during postnatal development from 4 to 12 weeks of age mirrored the results we had already obtained for *Sema3F* mutants (Fig. 23A).

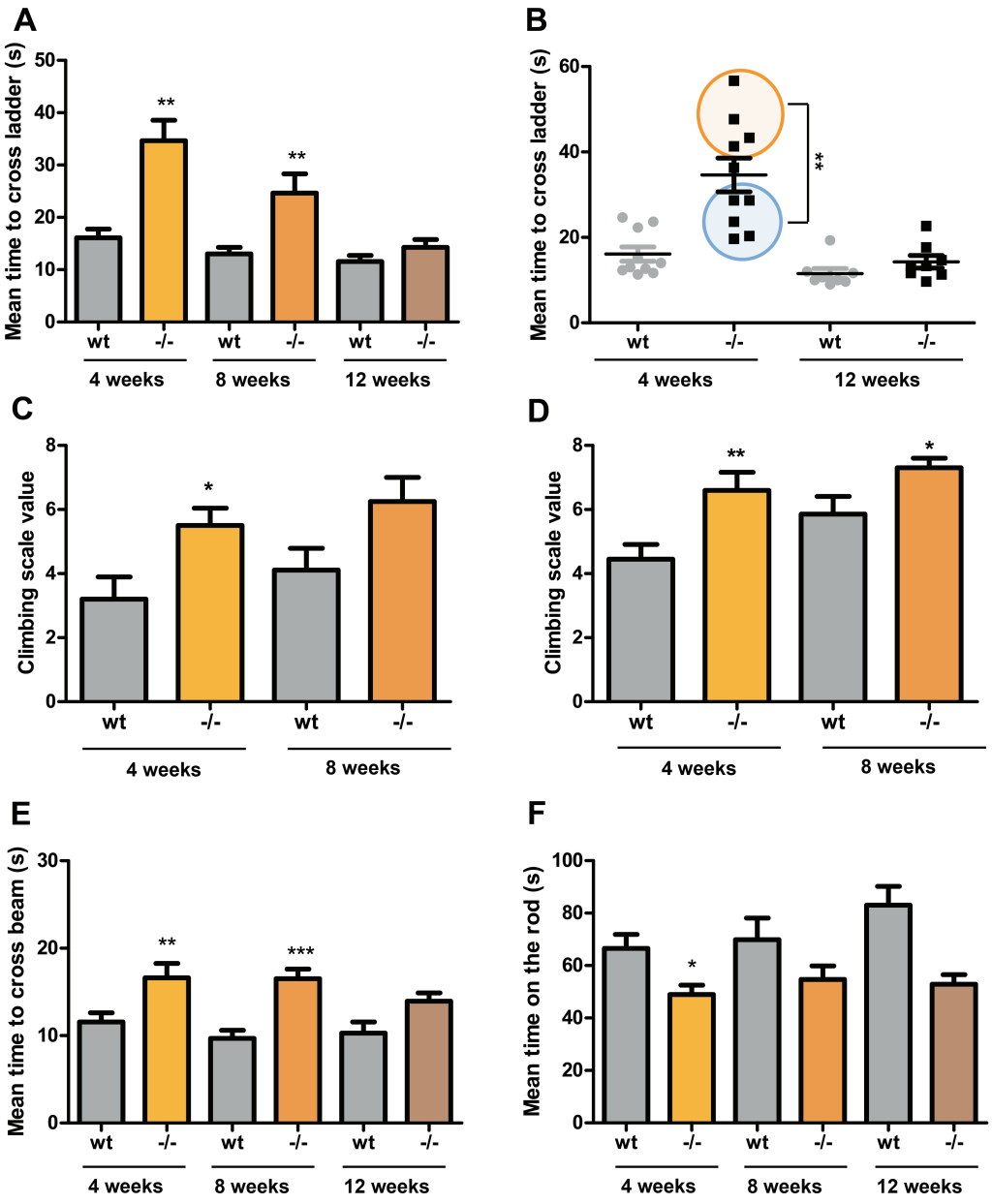


Figure 23: Locomotor deficits in *Npn-2* mutants.
(A) Mean time to cross the horizontal ladder at 4, 8 and 12 weeks. (B) Segregation of *Npn-2* mutants into wildtype-like (blue circle) and poor performers (orange circle) at 4 and 12 weeks. The wire climbing performance of *Sema3F* (C) and *Npn-2* (D) mice at 4 and 8 weeks was evaluated using a qualitative scale ranging from 1= precise grip onto the wire with fore- and hind limbs, rhythmic climbing to 8= fore- and hind limbs clung to the wire, no coordinated movements, no rhythmic pattern. (E) Mean time to cross the narrow beam at 4, 8 and 12 weeks is shown. (F) Mean time on the rotarod at 4, 8 and 12 weeks. Data were analysed with the nonparametric Mann Whitney test; asterisks indicate significance *p<0.05, **p<0.01, ***p<0.001.

Our data show that *Sema3F* and *Npn-2* mutant mice revealed very similar motor coordination deficits. Both, *Npn-2* and *Sema3F* mutants segregate into groups that display wildtype-like or severely impaired motor performance. Poor motor

coordination capabilities in mutants recovered spontaneously, albeit only partially, from 4 to 12 weeks of age. Loss of the receptor *Npn-2* revealed additional impairments in general locomotion, pointing towards a slightly more severe motor phenotype. Moreover, our data suggest that adaptive processes lead to a spontaneous recovery from genetically induced motor impairments in both *Npn-2* or *Sema3F* mice.

IV.3.3 Disturbed organisation of medial LMC neurons in *Sema3F* poor performers

At E13.5, the dorsal-ventral pathfinding choice of peripheral motor axons to the limb is compromised in absence of Sema3F-Npn-2 signalling: roughly 30% of medial LMC neurons misproject to dorsal instead of ventral muscles (Huber *et al.*, 2005). It is still elusive whether this embryonic miswiring in the sensorimotor circuitry is corrected later during development. Thus, we investigated the underlying neuroanatomy of peripheral forelimb circuitry in *Sema3F* mutants at different postnatal time points. Molecular markers that are commonly used to assign motor neurons to the medial or lateral LMC divisions during embryonic development, Isl1 and Lim1, respectively, are no longer expressed in the postnatal spinal cord. We therefore retrogradely traced motor projections from dorsal and ventral muscles of the distal forelimb by injecting different fluorescent conjugates of the neuronal tracer cholera toxin subunit B (CTB): CTB-Alexa555 and CTB-Alexa488, respectively. 48 hours after tracer application, spinal cords were processed for histological analysis and motor neurons were marked on each spinal cord section for subsequent reconstruction of their location along the spinal cord. To validate the tracing method and detect potential changes in the number of motor neurons in *Sema3F* mutants, we counted the numbers of retrogradely labelled motor neurons after CTB injection in dorsal and ventral forelimb muscles. No differences in numbers of traced motor neurons were found in wildtypes or *Sema3F* mutants at 4 (p_{dorsal}= 0.16, $p_{ventral}$= 0.36) or 12 weeks (p_{dorsal}= 0.76, $p_{ventral}$= 0.19).

For further analysis of the localization and organisation as well as dorsal-ventral and mediolateral distribution of motor pools at 12 weeks, the positions of all labelled motor neurons were collapsed into a single transverse plane using Reconstruct™ software (Fig. 24A-C). In *Sema3F* wildtype littermates and wildtype-

like performing mutants, ventrally and dorsally projecting motor neurons were located in two distinct and compact motor pools in the spinal cord (Fig. 24B,C). In contrast, ventrally projecting motor neurons of poorly performing *Sema3F* mutants spread into and mixed with dorsally projecting motor pools (Fig. 24C). Moreover, the localization and distribution of individual motor pools was quantified by calculating their scatter index (SI): the geometric center of each individual pool in the transverse plane. The SI measures its extent by the area of a fitted ellipse spanning all medial or all lateral motor neurons, respectively (for a detailed description see Material and Methods III.6.4). The scatter index analysis confirmed the previous observation: increased spreading of exclusively ventrally projecting motor neurons in poorly performing *Sema3F* mutants but no difference in the SI of wildtype-like performers and wildtype littermates (Fig. 24F).

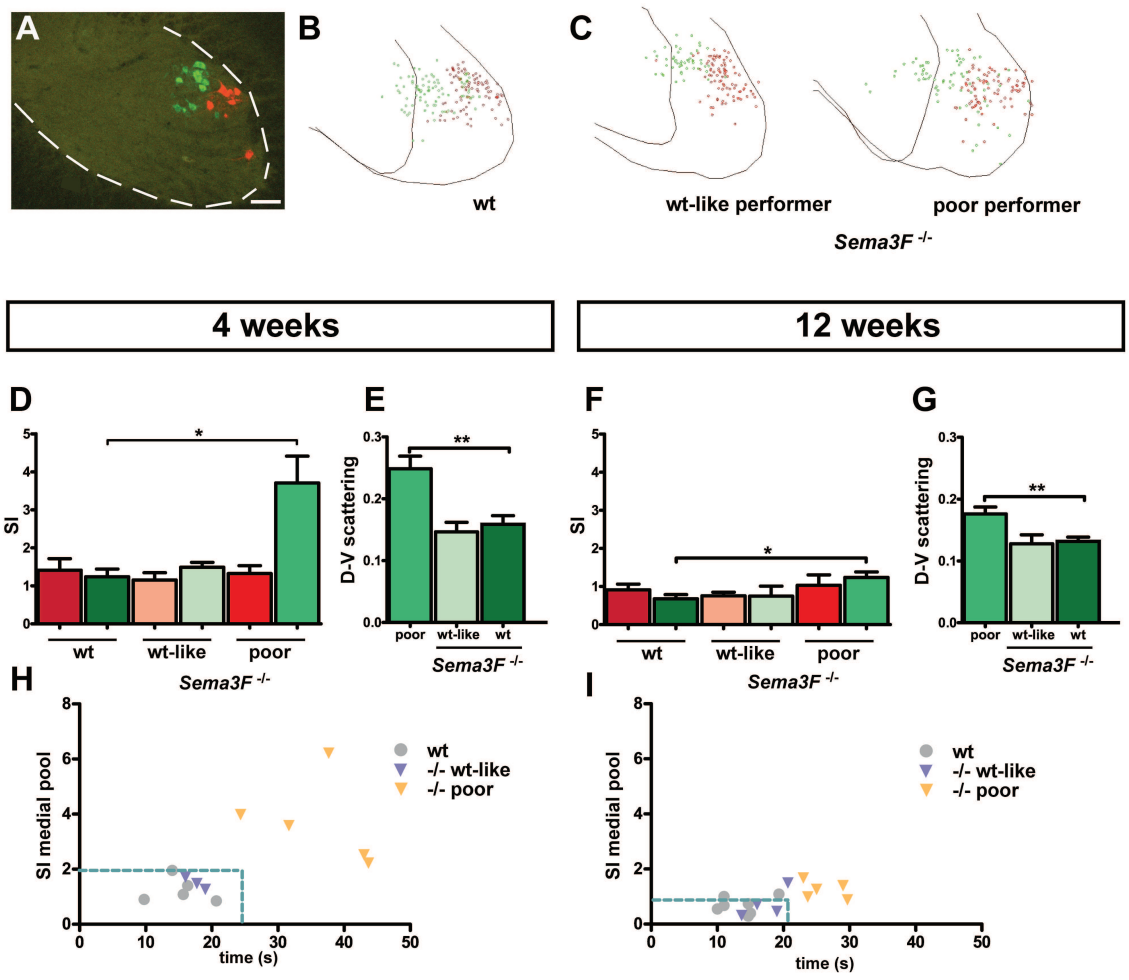


Figure 24: Anatomical analysis of distal forelimb motor pools representation in the spinal cord.

(A) Spinal cord section with retrogradely traced motor neurons from dorsal (CTB-Alexa555, red) and ventral (CTB-Alexa488, green) forelimb muscles. Scale bar represents 100µm. Reconstruction of the

total number of dorsally (red) and ventrally (green) projecting motor neurons collapsed onto a single plain in control (B) or *Sema3F* mutants (C). Scatter index (SI) for distal forelimb motor pool distribution at 4 (D) and 12 weeks (F). The medial motor pool shows increased spreading in the dorsal-ventral direction at 4 (E) and 12 weeks (G). Correlation of motor coordination (time to cross the horizontal ladder) with the scatter index of the medial motor pool at 4 (H) and 12 weeks (I). Dashed blue lines represent 2 standard deviations from the mean. Data were analysed with the two-tailed, unpaired Student's t-test; asterisks indicate significance *p<0.05, **p<0.01.

During postnatal development, embryonically established neuronal networks are subject to structural refinements (Goodman & Shatz, 1993). Therefore, we assessed if the distribution and organisation of defined motor pools changed postnatally from 4 to 12 weeks. Similar to the motor pool localization in *Sema3F* mutants at 12 weeks, exclusively medial motor pools of poor performers were already significantly more scattered at 4 weeks (Fig. 24D). Next, we determined the spreading direction of ventrally projecting motor neurons in the spinal cord. Interestingly, medial motor pools preferentially scattered in the dorsal-ventral orientation of the spinal cord (Fig. 24E,G) but revealed no aberrant changes in the mediolateral distribution (data not shown).

To determine whether a relationship exists between behavioural deficits and abnormal anatomy, both parameters were correlated on a single animal level. Interestingly, *Sema3F* mutants with particularly poor locomotor performance on the grid walk also exhibited strong neuroanatomical defects in terms of motor pool spreading. These animals make up a population outside the dashed box demarcating 2 standard deviations from the mean of their grid walk performance and scatter index of ventrally projecting motor neurons. Similarly, genetically mutant animals with no or only minor locomotor impediment, wildtype-like performers, also showed no detectable anatomical defects and are mainly located within the dashed lines (Fig. 24H,I).

In summary, our data correlated motor coordination deficits with an aberrant, increased dorsal-ventral scattering of ventrally projecting motor neurons in *Sema3F* mutant poor performers. These data match with embryonic pathfinding errors of medial LMC neurons previously described for *Sema3F* and *Npn-2* mutants (Huber *et al.*, 2005). The reconstruction of spinal motor pool localization and quantification of the scatter index was done with the help of a practical student, Stefan Winzeck, whom I supervised (Winzeck, 2011).

IV.3.4 General behavioural stimulation in an enriched environment enhances recovery of motor skills in *Sema3F* mutant mice

There is substantial evidence reporting pronounced beneficial effects of physical enrichment on functional recovery after spinal cord injury, stroke or age-related neurodegeneration in the hippocampus (Johansson & Ohlsson, 1996; Nithianantharajah & Hannan, 2006; Fischer & Peduzzi, 2007; O'Callaghan *et al.*, 2009). Especially, increased voluntary physical activity using running wheel devices is associated with improvement in motor coordination skills on the rotarod (Madronal *et al.*, 2010). Hence, we determined the influence of enriched environment housing combining social interaction and voluntary physical activity on the motor coordination deficits of *Sema3F* mutants. Therefore, *Sema3F* mice were born and housed in groups of 5 in larger cages (vs. 3 mice in regular cages) containing nesting material, running wheels and mini horizontal ladders to stimulate motor behaviour. Motor skills were assessed at 4, 8 and 12 weeks through the same behavioural test battery used for standard housed *Sema3F* mice. Similar to regularly housed animals, 4-weeks old *Sema3F* mutants experiencing environmental enrichment required significantly more time to traverse the horizontal ladder and showed increased number of paw slips relative to wildtype littermates (Fig. 25A,C). However, *Sema3F* mutants did not segregate into two distinct groups of mutant and wildtype-like performers (Fig. 25B). Moreover, improvement of motor coordination skills in *Sema3F* mutants raised in an enriched environment occurred more rapidly and to a level comparable to wildtype littermates (Compare Fig. 25A,C and Fig. 22A,C; $improvement_{Grid\ walk}$ from 4 to 12 weeks in time= 15,99% and slips= 19,35%). Interestingly, inter-limb coordination skills as measured in the wire climbing test did not differ significantly among mutant and wildtype *Sema3F* littermates under enriched conditions (Fig. 25D).

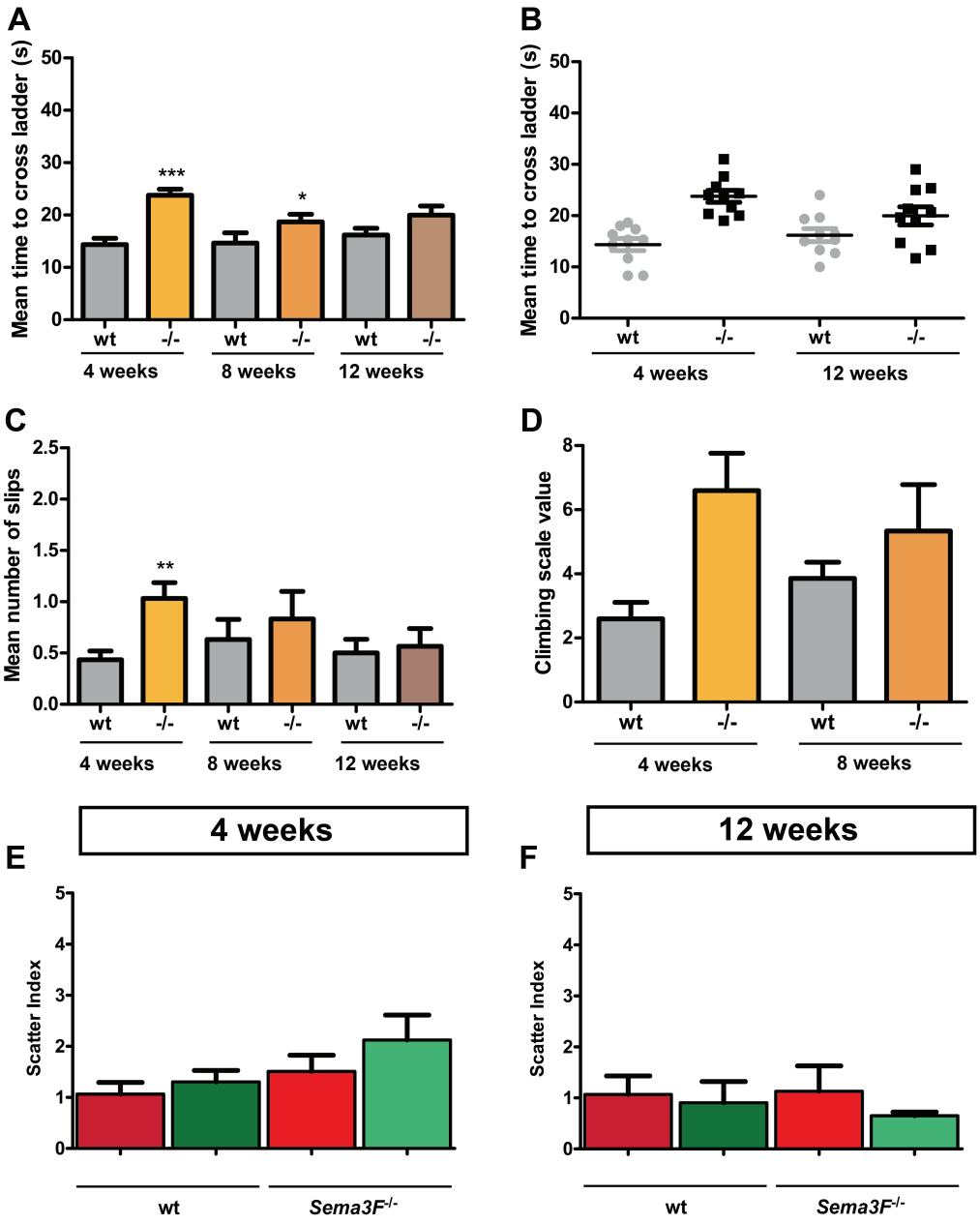


Figure 25: Housing in enriched environments induces recovery of behavioural and anatomical deficits in *Sema3F* mutants.

(A,C) Grid walk: mean time to cross the ladder (A) and mean number of slips (C) at 4, 8 and 12 weeks. (B) Mean values of the time to cross the ladder for individual *Sema3F* mice and wildtype littermates at 4 and 12 weeks. (D) Wire climbing performance at 4 and 8 weeks. Scatter index for the distribution of distal forelimb motor pools at 4 (E) and 12 weeks (F). Data were analysed with the nonparametric Mann-Whitney test (A-D) or the two-tailed, unpaired Student's t-test (E-F); asterisks indicate significance *p<0.05, **p<0.01, ***p<0.001.

Previously we have reported a tight link between motor coordination deficits and neuroanatomical aberrations in *Sema3F* mice. Hence, we addressed the question whether the rapid improvement in motor performance under physical enrichment is paralleled by a re-organisation of spinal motor pools. Therefore, ventral

and dorsal distal forelimb projections were labelled by intramuscular injection of fluorescently conjugated CTB, the position of dorsally and ventrally projecting motor pools was reconstructed and the scatter index calculated. Indeed, the organisation and localization of medial motor pools in enriched environment housed *Sema3F* mutants was indistinguishable from wildtype littermates at 4 and 12 weeks of age (Fig. 25E,F).

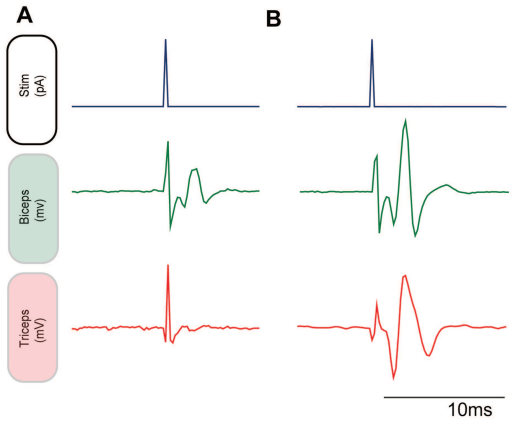
Our data indicate that enhanced physical activity in an enriched environment significantly improves motor skills of *Sema3F* mutants which is paralleled by wildtype-like organisation of forelimb motor pools in the spinal cord of all *Sema3F* mutants.

IV.3.5 Aberrant activation of dorsal muscles upon stimulation of a ventral nerve in *Sema3F* mutants

Motor neurons innervating the same peripheral target muscles are clustered into distinct pools in the spinal cord. In the limb sensorimotor circuitry, axons from the lateral subdivision of the LMC innervate dorsal extensor muscles whereas medial LMC motor projections target antagonistic ventral flexors (Landmesser, 1978b; Hollyday, 1980; Gutman *et al.*, 1993; Landmesser, 2001). Hence, we investigated the muscle innervation pattern in the limb of *Sema3F* mutants. The recruitment of antagonistic forelimb muscles was characterized using simultaneous EMG recordings from flexor and extensor muscles. However, muscles in the distal mouse forearm are small in size and located in close physical proximity rendering EMG recordings of an individual muscle without perturbing signals from adjacent muscles technically not feasible. Instead, the more voluminous and spatially separated biceps and triceps muscles in the upper forelimb were selected as ventral and dorsal antagonists.

In wildtype *Sema3F* animals older than 12 weeks, the *N.musculocutaneous* supplying ventral muscles was stimulated by single trains (n= 1 pulse) with increasing intensity. Bursts of EMG activity were recorded in the innervated flexor muscle, *Biceps brachii,* but not the antagonistic dorsal extensor muscle, *Triceps brachii* (Fig. 26A). Interestingly, stimulating the same ventrally projecting nerve in *Sema3F* mutants elicits synchronous EMG signals in both flexor and extensor muscles

regardless of their behavioural performance, wildtype-like or poor, on the grid walk (Fig. 26B,C).



C

Sema3F		EMG	
	n	Biceps	Triceps
wt	6	6	0
-/- wt-like	3	3	3
-/- poor	3	3	3
Sema3F EE			
wt	5	5	0
-/-	6	6	6

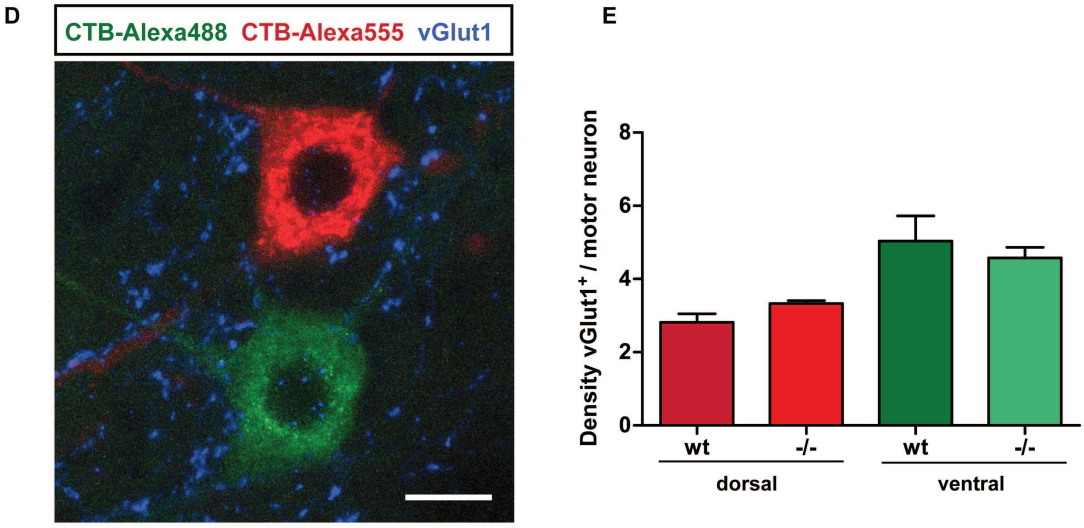


Figure 26: Synchronous activation of antagonistic forelimb muscles in *Sema3F* mutants. EMG recordings in controls (A) and *Sema3F* mutants (B) after 12 weeks of age display stimulus (upper lane, blue), *Biceps brachii* activity (middle lane, green) and *Triceps brachii* (lower lane, red); scale bar equals 10ms. (C) Table summarizing the EMG activity in *Biceps brachii* and *Triceps brachii* muscle upon stimulation of *N.musculocutaneous*. EE= enriched environment. (D) Image of retrogradely labelled ventral (CTB-Alexa488, green) and dorsal (CTB-Alexa555, red) motor neurons in a 4 weeks old *Sema3F* mutant stained for excitatory synapses with anti-vGlut1 antibodies (Cy5, blue). Scale bar represents 20µm. (E) Quantification of mean density of vGlut1$^+$ synapses per labelled motor neuron. Data were analysed with the two-tailed, unpaired Student's t-test. (Experiments in D, E performed by Stefan Winzeck).

We further investigated whether the physiological abnormalities in the activation pattern of dorsal muscles is also reflected in the localization and organisation of motor neurons in the spinal cord. Motor neurons innervating the

biceps or triceps muscles were retrogradely labelled and the SI was determined. The mediolateral (M-L) and dorsal-ventral (D-V) distribution of the corresponding motor pools in the spinal cord in mutants did not differ from wildtype littermates (data not shown). The localization and mean number of labelled motor neurons in the respective forelimb pool was very similar to previous reports (Tada *et al.*, 1979; Crews & Wigston, 1990).

We next assessed EMG signals in *Sema3F* mutant animals housed in enriched environment cages to determine if increased motor stimulation influences the flexor-extensor muscle recruitment patterns in the forelimb. Similar to mice housed under normal conditions, we also found simultaneous EMG activity in biceps and triceps muscles upon stimulation of the ventral musculocutaneous nerve in enriched environment housed *Sema3F* animals (Fig. 26C).

In addition to structural changes on the anatomical level and functional alterations in the recruitment patterns of muscles in sensorimotor circuits, adaptive mechanisms may also occur on a synaptic level by modulating excitatory and inhibitory input for the fine tuning of neuronal circuits (Sanes & Yamagata, 2009). To address this possibility, the density of excitatory glutamatergic synapses on lateral and medial motor neurons retrogradely labelled from distal forelimb muscles, respectively, was assessed. Mean vGlut1^{+} excitatory input on labelled lateral or medial motor neurons was not altered in 4 weeks old *Sema3F* mutants compared to control animals (Fig. 26E).

In summary, we demonstrate aberrant EMG activity in dorsal upper arm muscles in *Sema3F* mutants upon stimulating a nerve normally supplying exclusively ventral muscles. This physiological abnormality is not paralleled by anatomical mislocalizations of *Biceps brachii* and *Triceps brachii* motor pools in the spinal cord. Even though increased behavioural stimulation through enriched environmental conditions improved motor coordination impairments and anatomical localization of forearm motor pools in *Sema3F* mutants, abnormal synchronous activity of dorsal and ventral antagonistic upper arm muscles persist in *Sema3F* mutants that were housed in an enriched environment.

IV.3.6 Overview of behavioural phenotyping in *Sema3F* and *Npn-2* mutants

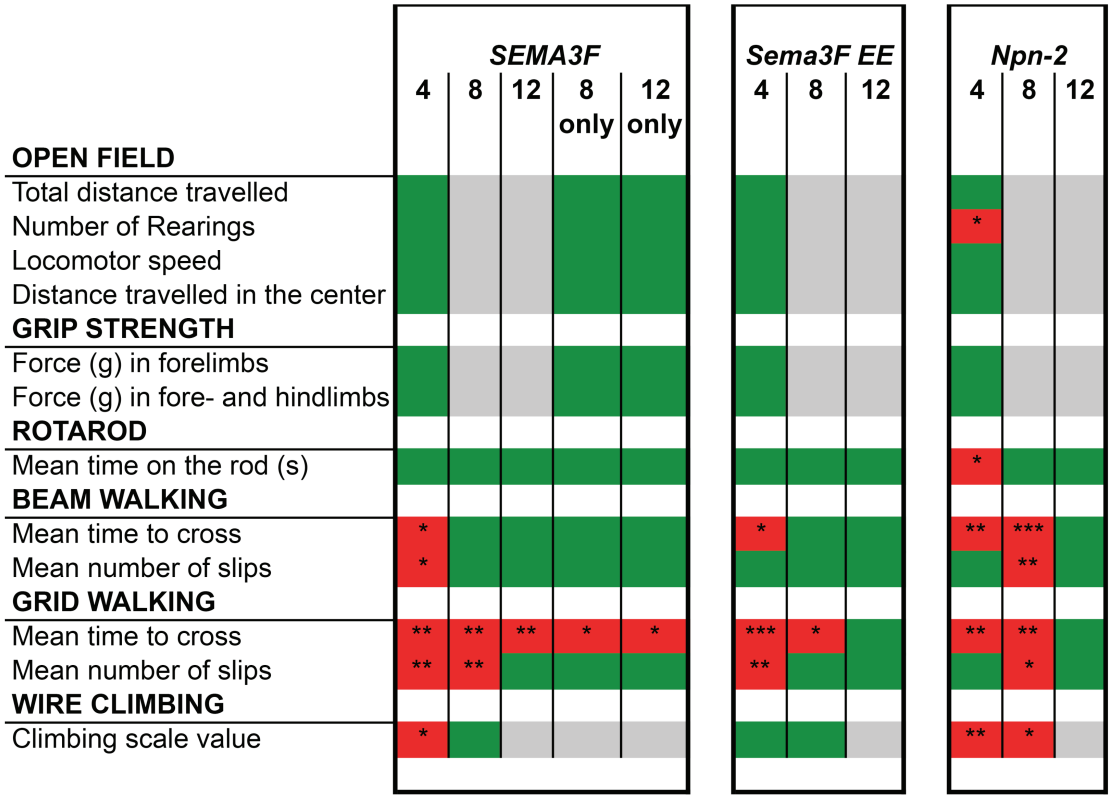


Table 1: Summary of motor skills in *Sema3F* and *Npn-2* mutants tested at 4, 8 and 12 weeks.

Overview of the behavioural performance of *Sema3F* housed under normal and enriched environment conditions (*Sema3F EE*) as well as *Npn-2* mutants and wildtypes in locomotor tests of the designed behavioural test battery. Red visualises a significant difference of performance between mutants and wildtypes in the indicated test, green encodes comparable behaviour test outcome among the different genotypes. In case animals were not repetitively tested at 4, 8 and 12 weeks, missing time points are marked grey. 8 only and 12 only refers to animals solely tested at 8 or 12 weeks, respectively. Data were analysed with the nonparametric Mann-Whitney test; asterisks indicate significance *p<0.05, **p<0.01, ***p<0.001.

V DISCUSSION

Locomotion in vertebrates relies on correctly laid-out spinal circuitries with efferent motor axons innervating their assigned target muscles and afferent sensory projections providing feeback information. Although several axon guidance ligand-receptor pairs mediating neural circuit wiring have been characterized (Tessier-Lavigne & Goodman, 1996; Dickson, 2002), less is known about the impact of trans-axonal communication among co-extending projections and the mechanisms and molecules involved therein. In this context my thesis focuses on the formation of sensorimotor projections and adaptive plasticity of locomotor circuitry in the postnatal animal.

Using genetic ablation of motor or sensory neurons in mouse, I showed that co-extending spinal motor and sensory axons are interdependent for correct establishment of the limb circuitry. So far, data on the dependency of growing sensory on motor axons is available in the chick based on surgical removal of motor neurons as well as in the mouse by genetic ablation of EphA3/4 receptors in motor neurons (Landmesser & Honig, 1986; Wang *et al.*, 2011). I refined previous results by showing that a minimal substrate of either projection is sufficient for correct timing, axonal fasciculation and the formation of stereotyped and precise trajectories.

Embryonic loss of Npn-1 on motor projections of *Olig2-Cre*$^{+}$*;Npn-1*$^{cond-/-}$ mice caused pronounced congenital forelimb posture abnormalities. This arthrogryposis-like phenotype is associated with permanent deficits in functional forepaw extension and skilled locomotion, muscle atrophy and ultrastructural changes in extensor nerve composition, which are not susceptible to adaptive compensation.

Newly established neuronal networks are flexible and amenable to adaptive changes. In adults, however, spontaneous functional and structural compensation is limited and was mainly studied in traumatic experimental CNS injury models so far. This work investigated the postnatal effects of genetically-induced embryonic miswiring of limb circuits and the competences for re-shaping these neural networks at structural and functional levels. We found that lack of Sema3F-Npn-2 signalling caused pronounced deficits in motor coordination, which tightly correlate with aberrant neuroanatomy. These parameters are accessible for compensatory

plasticity associated with functional motor improvement by housing in an enriched environment.

In the following, I will discuss the obtained results in the context of published literature and give suggestions for possible directions of future research on the formation and plasticity of sensorimotor circuits.

V.1 Coupling of sensory and motor axons during peripheral circuit assembly

The question of mutual dependency of co-extending sensory and motor projections for correct target innervation and circuit wiring was addressed using a genetic approach. The cell-type specific activation of lethal DT-A expression specifically in motor or sensory neurons resulted in ablation of the majority of the targeted neuronal subtype albeit not in their complete removal. Temporal control of sensory projection growth and spinal nerve formation is sensitive to the presence of a minimum of motor axons. Sensory axons in turn influence tight bundling of motor fascicles and their timing of ingrowth to the limb. In summary, these data suggest reciprocal dependency of spinal motor and sensory axons to establish a stereotyped neural circuitry.

V.1.1 Axon-axon interactions

Seminal studies based on manipulations in chick embryos proposed that sensory axons depend on pre-established motor projections as an aligned substrate for the formation of their peripheral nerve patterns (Taylor, 1944; Landmesser *et al.*, 1983; Honig *et al.*, 1986; Landmesser & Honig, 1986; Swanson & Lewis, 1986; Tosney & Hageman, 1989). After early ablation of motor neurons prior to axonal outgrowth in chick embryos (HH17-18), the main nerve trunks and cutaneous nerves formed similar to controls whereas afferent muscle innervation in the wing or limb was either completely absent or critically reduced (Taylor, 1944; Landmesser & Honig, 1986; Swanson & Lewis, 1986). To completely remove motor neurons, rather large interventions like surgical ablation, UV irradation or ectopic transplantations of the ventral neural tube segments were necessary. These manipulations may lead to

disturbances in neighbouring tissues either through developmental scars or absence of required secreted signals after removal of the entire ventral spinal cord.

Genetic ablation of motor neurons

We therefore chose a genetic elimination strategy based on lethal DT-A expression to target early precursors of motor neurons and oligodendrocytes emerging from the pMN domain. Thereby the number of spinal motor neurons present at E11.5 in *Olig2-Cre^{+};DT-A^{floxed}* mice was significantly reduced by approximately 2.6 fold for LMCl and 3 fold for LMCm relative to controls whereas the assembly of sensory neurons in the DRG was not affected (Fig. 8). Compared to previously performed mechanical ablation of motor neurons in chick and frog, the advantages of our strategy based on genetic ablation lies in the highly selective elimination of Cre-expressing cells only. Thereby, the tissues where axons have to grow through remain untouched. Furthermore, combining the conditional *DT-A* line with Cre-lines targeting different neuronal subtypes allows to address the role of virtually any cell type a Cre-line is available for.

In *Olig2-Cre^{+};DT-A^{floxed}* mice sensory projections were thinned and delayed but capable of correctly converging to the limb plexus and subsequently forming spinal nerves (Fig. 9,10). Compared to previous experiments using early surgical elimination of motor neurons in chick embryos (HH17-18), we report less profound impairments in sensory afferent formation and guidance. The underlying reasons may lie in the different experimental procedures and the consequential efficiency of motor neuron ablation. Surgical ablation is accompanied by removal or destruction of surrounding tissues to various extents. At HH17-18 the sensory precursors, NCC, are still migrating and have not yet coalesced into the dorsal root ganglia. Thus, focal UV irradiation or surgical removal of the ventral two thirds of the spinal cord to eliminate motor neurons (Landmesser & Honig, 1986; Swanson & Lewis, 1986) may also destroy spinal cord derived signals essential for NCC migration or differentiation (Kalcheim & Le Douarin, 1986; Le Douarin, 1986). The environmental-derived cues essential for NCC migration and pathfinding comprise ECM proteins, T-cadherin, PNA-glycoproteins and repulsive ephrin-B2 as murine NCC express the coressponding EphB receptor (reviewed in Krull, 2001). Supporting this notion, elimination of motor neurons after DRG formation (HH21) by removal of two thirds of

the ventral spinal cord did not influence the correct targeting or muscle innervation pattern of sensory axons in the chick hind limb (Wang & Scott, 1999).

Furthermore, the extent of motor neuron ablation likely determines the severity of the impact on sensory projections. Early surgical removal of ventral spinal cord parts completely ablated motor neuron precursors whereas the *Cre-loxP* based genetic approach achieved a critical reduction of motor neurons with a few surviving neurons that are still extending projections (Fig. 9). A recent study reported that the generation of spinal vAChT^{+} motor neurons and later on formation of projections were completely blocked when *Olig2-Cre*$^{+}$ mice were crossed to the *Rosa26-eGFP-DT-A* mouse line (Wang *et al.*, 2011). Apparently, the time lapse of 16 to 20h between onset of DT-A activation and cell ablation is shorter in the *Rosa26-eGFP-DT-A* mouse line (Ivanova *et al.*, 2005) compared to 36 to 48h in the conditional *R26:lacZbpA*^{flox}*DT-A* mice we have used (Brockschnieder *et al.*, 2004; Brockschnieder *et al.*, 2006). Consequently, an earlier activation of DT-A may lead to a more complete removal of motor neurons and allow for analysis of sensory trajectory formation in complete absence of motor neurons.

The few residual motor projections in *Olig2-Cre*$^{+}$*;DT-A*^{floxed} embryos possibly laid out the motor tracts and thereby provided sufficient substrate for sensory axons to track along. The concept of transient or permanent pioneer axons establishing the initial axonal tract where axons of later born neurons migrate along has been described in grasshopper for axons crossing the ganglionic midline and reverse projection of sensory axons from the limb to the CNS (Raper *et al.*, 1984; Klose & Bentley, 1989), DL-1 interneuron pathfinding and formation of the ventral nerve innervating the trunk in fish as well as for establishing thalamocortical connections in the cat (Kuwada, 1986; Ghosh *et al.*, 1990; Pike *et al.*, 1992). Interestingly, loss of pioneering axons significantly delays outgrowth of follower axons in grasshopper and fish (Raper *et al.*, 1984; Kuwada, 1986; Pike *et al.*, 1992). Along this line, we also reported a delay in axonal growth after partial ablation of motor precursors suggesting that the absence or reduction of pre-extended pioneer axons interferes with the timing of sensory afferent growth to the plexus (Fig. 9).

Genetic ablation of sensory neurons

Previous studies analysing the dependency of co-extending sensory and motor axons for proper spinal sensorimotor circuit formation in chick focused on the

influence of motor on sensory projections but not vice versa (Honig *et al.*, 1986; Landmesser & Honig, 1986; Swanson & Lewis, 1986; Tosney & Hageman, 1989; Wang & Scott, 1999). Thus, so far no data on the impact of sensory on adjacent motor axons during embryonic neural circuit formation is available. However, data on motor neuron pre-specification with respect to peripheral targets together with smaller growth cone morphology and reduced expression of cell adhesion molecules, e.g. NCAM, in sensory axons suggest that motor axons are in the lead and sensory axons rather rely on motor neurons for selection of their pathways to the limb (Duband *et al.*, 1985; Tosney & Landmesser, 1985b; a; Landmesser & Honig, 1986).

We addressed the role of sensory axons for correct limb circuit formation in mouse embryos where DRG neurons were significantly reduced by expression of lethal DT-A in neural crest cell lineage derivatives (*Ht-PA-Cre;Dt-A*^{floxed}). Indeed, critically reduced numbers of sensory axons projecting to the limb did not interfere with motor axon pathfinding. Instead, co-extending sensory projections influence correct fasciculation of spinal motor nerves and their timing of ingrowth to the limb (Fig. 12,13).

In conclusion, we could corroborate previous data from chick embryos on the dependency of sensory on motor axons for correct wiring of limb circuitry in mammals using a *Cre-loxP* based genetic approach instead of surgical ablation techniques. However, I unraveled that for the formation of stereotyped nerve pattern, sensory axons rely on only a minimal scaffold of motor projections. Additionally, the fasciculation and timing of co-extending motor projections during limb circuit establishment is mediated by sensory axons - an issue that has not been addressed previously. Furthermore, we could confirm the previous hypothesis of independency of motor from sensory axons in terms of trajectory fidelity, possibly due to motor axon pre-specification with regard to peripheral targets prior to spinal cord exit.

Molecular cues mediating trans-axonal interaction

Having shown the mutual influence of sensory and motor axons on fasciculation, timing of ingrowth to the limb and formation of stereotyped nerve projection pattern during spinal sensorimotor circuit wiring, the question arises which cues are mediating this interaxonal communication. Recently, evidence accumulated that the same axon guidance molecules and their cognate receptors mediating axon-environment attraction or repulsion are also involved in the direct communication

between axons. Trans-axonal interactions have been implicated in the assembly of visual and olfactory circuitries, segregation of axial projections into discrete motor and sensory pathways and in mediating fasciculation and target specificity of projections to the developing mouse limb (Sweeney *et al.*, 2007; Gallarda *et al.*, 2008; Imai *et al.*, 2009; Huettl *et al.*, 2011; Wang *et al.*, 2011). For example, the correct sorting of axial motor and sensory projections into target-specific nerve bundles depends on interaction of EphA3/A4 receptors on motor axons and corresponding ephrins on sensory fibers (Gallarda *et al.*, 2008). In the olfactory system, pre-target axonal sorting of olfactory sensory neurons (OSN) is based on trans-axonal interactions of Npn-1 and Sema3A expressed on their surface. Thereby, pre-target sorting determines the targeting of OSN in the olfactory bulb and, hence, the topography of the glomerular map (Imai *et al.*, 2009).

During sensorimotor limb circuit wiring co-extending motor and adjacent sensory projections are in the spatial positions for homo- or heterotypic axon-axon interactions. Partial ablation of sensory neuron precursors triggered defasciculation in specific spinal nerves (Fig. 12,13). This observation is consistent with previous data on genetic ablation of Npn-1 in sensory neurons (*Ht-PA-Cre*$^{+}$*;Npn-1*$^{cond-/-}$). Absence of Npn-1 on outgrowing sensory projections results in their exuberant growth as well as defasciculation of both sensory and motor trajectories with sensory growing ahead of motor projections (Huettl *et al.*, 2011). Thus, the phenotypes described after removal of motor or sensory neurons might derive from blocking trans-axonal interactions by removal or significant reduction of the corresponding interaction partner, e.g. the Npn-1 receptor.

V.1.2 Axon-glia interaction

Over the last 30 years, the role of CNS glia cells at choice points or as intermediate targets influencing axon guidance, axonal sorting and targeting was characterized. Additionally, these reciprocal axon-glia interactions also regulate migration and survival of glia cells (reviewed in Learte & Hidalgo, 2007). In contrast, PNS glia mostly travel along laid-out axonal tracts and thus play a minor role in guidance of peripheral axons (Giangrande, 1994; Gilmour *et al.*, 2002; Aigouy *et al.*, 2004). However in terms of sensory axons, axon-glia interaction in the PNS of *Drosophila* contribute to correct timing and target fidelity of peripheral sensory axons and

formation of olfactory glomeruli (Bailey *et al.*, 1999; Sepp & Auld, 2003). Loss of PNS glia early in embryogenesis causes stalling and misrouting of sensory axons (Sepp *et al.*, 2001). Thus, the remarkable pathfinding capabilities of sensory projections after massive ablation of motor neurons and their projections (*Olig2-Cre*$^{+}$*;DT-A*^{floxed}) might be due to peripheral glia that guide these sensory axons.

To address this issue further, the effect of peripheral glia ablation on sensory and motor trajectory formation should be assessed by analysing embryos lacking Schwann cells and glial precursors. The receptor tyrosine kinase erbB2 on Schwann cells is required for their neuregulin-mediated survival and migration (Dong *et al.*, 1995; Mahanthappa *et al.*, 1996). Thus, the impact of peripheral glia on growing sensory and motor axons can be addressed in *erbB2*$^{-/-}$ mice lacking Schwann cells. So far phenotyping of *erbB2*$^{-/-}$ mutants described axonal defasciculation of the phrenic nerve at E12.5. However, fasciculation status and pathfinding of sensory or motor projections to the developing limbs were not analysed (Lin *et al.*, 2000). Alternatively, peripheral glia can be targeted by crossing available *P0-Cre* lines to a conditional *DT-A* mouse line for selective expression of lethal DT-A in Schwann cells. Thereby, the P0 promoter directs Cre-mediated recombination particularly to peripheral Schwann cells leaving other NCC derived cell populations such as DRG neurons unaffected (Feltri *et al.*, 1999; Giovannini *et al.*, 2000).

V.1.3 Maintenance of developmental defects if Npn-1 is removed from motor or sensory neurons

The data presented for the mutual dependency of motor and sensory axons covered the embryonic stages E10.5 to E12.5. Notwithstanding, the question arises if the observed impairments such as axonal fasciculation and timing of growth are maintained or corrected for at later embryonic stages or after birth.

Neurons are generated in excess during early embryogenesis, however, by E15.5 massive neuronal cell death reduces neuronal numbers to physiological levels (Oppenheim, 1991; Oppenheim *et al.*, 1991). For *Sema3A* mutants, it was previously reported that abnormal peripheral projection patterns were largely correct by E15.5 and thus undetectable in the postnatal PNS (Behar *et al.*, 1996; White & Behar, 2000). In contrast, Haupt et al. recently showed that after embryonic loss of Sema3A-Npn-1 signalling the defasciculation of limb motor and sensory projections is retained

beyond the wave of neuronal cell death and in terms of the sciatic nerve even in the postnatal animal (Haupt *et al.*, 2010).

Unfortunately, whole mount staining becomes technically less feasible with increasing embryonic age due to the reduced penetrance of the applied reagents and increasing background in the utilised *Hb9::GFP* line to visualise motor projections. Although successfull whole mount stainings of mouse limbs have been reported until stage E15.5 (Haupt *et al.*, 2010), it was not possible to visualise motor or sensory projections in *Ht-PA-Cre*$^{+}$ or *Olig2-Cre*$^{+}$*;DT-A*^{floxed} mice at E15.5. This might be due to lethal DT-A expression that significantly diminishes the amount of sensory or motor projections for staining and concomitantly increases the number of dying axons and their cell debris which produce unspecific background signals (Fig. 11C,D).

The dramatic reduction of spinal motor neurons present in *Olig2-Cre*$^{+}$*; DT-A*^{floxed} mice at E11.5 by roughly 3 fold relative to controls suggests that these mice are not viable and, indeed, we never found this genotype at weaning age (P21). Therefore, we cannot specify if increased death either occurs during embryogenesis or early postnatally. In addition to sensory neurons, activation of DT-A expression in the pan-NCCs line *Ht-PA-Cre*$^{+}$ also targets craniofacial structures, endocrine, enterice and cardiac derivatives as well as melanocytes. However, we would expect *Ht-PA-Cre*$^{+}$*;DT-A*^{floxed} mutants to be viable as no vital organs are affected as a whole. Especially the cardiac derivatives are mainly restricted to the endoderm of the aortic sac and do not target the entire heart tissue (Pietri, 2003). In fact, recombined *Ht-PA-Cre*$^{+}$*;DT-A*^{floxed} mice are viable and do not exhibit an overt phenotype postnatally although they were born at fewer (1:13) than predicted Mendelian frequencies (1:4). Thus, the morphology of the neuromuscular system and the functionality of the wired limb circuitry could be characterized postnatally in *Ht-PA-Cre*$^{+}$*;DT-A*^{floxed} mice. Stimulation of different nerves innervating the forelimb with simultaneous recordings in antagonistic flexor and extensor muscles would provide data on the integrity of sensorimotor limb innervation and antagonistic muscle recruitment pattern. Thereby, dorsal-ventral misprojections, denervation due to stalling of nerve branches or mismatches between sensory afferents and motor projections might be unravelled.

V.2 Characteristic forelimb deficits in postnatal *Olig2-Cre^{+};Npn-1$^{cond-/-}$* mice

Selective ablation of the axon guidance receptor Npn-1 from motor neurons during embryogenesis revealed its crucial role in the proper fasciculation and distal advancement of axonal projections innervating the limb. Postnatally, these *Olig2-Cre^{+};Npn-1$^{cond-/-}$* mice are characterized by forepaw posture abnormalities, congenital muscle dystrophy and altered extensor nerve composition on the ultractructural level. Hitherto, mutants with similar postnatal arthrogryposis-like forelimb deficits have been associated with defects in radial sorting or progressive motor neuropathy. In the following the phenotypes of these available mouse models and *Olig2-Cre^{+}; Npn-1$^{cond-/-}$* mice are compared and underlying molecular causes for the congenital muscle dystrophy as well as a potential role for Npn-1 in mediating axon-glia communication are discussed.

V.2.1 *Claw paw*-like forelimb phenotype observed in *Olig2-Cre^{+};Npn-1$^{cond-/-}$* mice

The abnormal forepaw posturing that was observed in *Olig2-Cre^{+};Npn-1$^{cond-/-}$* mutants at P0 strongly resembles the early-onset and morphology of limb posture abnormalities in mice homozygous for the autosomal recessive mutation *claw paw* (Henry *et al.*, 1991). Positional cloning identified an insertion in exon 4 of the *Lgi4* gene as the underlying molecular basis for the observed *claw paw (clp)* phenotype (Bermingham *et al.*, 2006). Affected forelimbs are flexed towards the body at one or more joints: the wrist and/or digits. Even though there is no active extension movement in mutants, the abnormal posture is not fixed as the digits and paw can be extended passively. Similar to *clp* mutants, we observed considerable variety in the severity of the phenotype: whether one or both forelimbs were affected, and in the extent of involvement of digits and/or wrist. In more severly affected *clp* mice, one or both hind limbs exhibit a mild weakness in active dorsiflexion in contrast to *Olig2-Cre^{+};Npn-1$^{cond-/-}$* mutants with no overt hind limb phenotype. The described abnormalities in fore- but not hind limbs is congruent with embryonic data showing that the ingrowth of distal-most motor and sensory projections is significantly reduced in fore- but not in hind limbs of *Olig2-Cre^{+};Npn-1$^{cond-/-}$* mutants relative to controls at

E12.5 (Fig. 3I in Huettl *et al.*, 2011). Thus, distinct forelimb nerves of *Olig2-Cre*$^{+}$*; Npn-1*$^{cond-/-}$ mutants possibly did not reach and innervate their peripheral target muscles in contrast to unaffected hind limbs displaying normal distal advancement of ingrowing axons.

Behavioural testing of general health parameters and overground locomotion in *clp* mutants revealed significant deficits in grooming, vertical and horizontal locomotion - impairments we did not detect in *Olig2-Cre*$^{+}$*;Npn-1*$^{cond-/-}$ mice (Henry *et al.*, 1991). *Olig2-Cre*$^{+}$*;Npn-1*$^{cond-/-}$ mutants possibly accustomed themselves to walking on their fists due to the permanent flexion in the forepaws. Alternatively, the underlying sensory projections for pain sensation in their forepaws may also be impaired. Noxious sensory functions in the hind limbs of *Olig2-Cre*$^{+}$*;Npn-1*$^{cond-/-}$ mutants were tested on the Hot Plate and did not reveal deficits. Notwithstanding, so far we have not addressed if affected forepaws are hyposensitive to touch or pain. This issue could be tested using Von Frey hairs to determine the threshold for sensation of pressure applied with fine needles of different sizes to the forepaws (Pearce, 2006).

However, more complex motor skills such as balance and motor coordination are severly impaired without improvement of locomotor performance during postnatal development (Fig. 17,18). Thus, *Olig2-Cre*$^{+}$*;Npn-1*$^{cond-/-}$ mice did not reveal deficits in stereotyped but in more complex locomotor tasks which seem incapable of compensatory, plastic adaptions to improve the locomotor performance postnatally.

V.2.2 Putative role of Npn-1 in radial sorting

The common underlying neurogenic cause for the congenital limb posture deficits in *clp* mutants was assigned to deficits in axonal sorting and myelination of the peripheral nervous system. Adult *clp* mice showed general hypomyelination and delayed onset of myelination with postnatal large diameter fibers stalled in the promyelin state (Henry *et al.*, 1991; Koszowski *et al.*, 1998; Darbas *et al.*, 2004).

Ultrastructural analysis of the *N.radial* innervating extensor muscles in affected paws of adult *Olig2-Cre*$^{+}$*;Npn-1*$^{cond-/-}$ mutants did not identify deficits in myelination properties nor abnormal unmyelinated, large diameter axons (Fig. 20). As the ultrastructural analysis of forelimb nerves in *Olig2-Cre*$^{+}$*;Npn-1*$^{cond-/-}$ mutants were conducted at adult stage only, we cannot exclude a delay in the onset of myelination

in neonatals that is later on corrected. In order to address this issue, the g-ratio and composition of forelimb nerves in young *Olig2-Cre^{+};Npn-1$^{cond-/-}$* mutants prior to 4 weeks of age should be analysed.

Although the forepaw posture abnormalities in *Olig2-Cre^{+};Npn-1$^{cond-/-}$* mutants highly resemble the phenotype described for *clp* mice, our ultrastructural data rather demonstrate a preference towards small diameter axons and suggests deficits in axonal sorting as seen by a roughly twofold increase of fibers incorporated per Remak bundle in the peripheral extensor nerves of affected paws (Fig. 21). During the process of radial sorting the axonal diameter determines the binary fate of the immature Schwann cell becoming an unmyelinating Schwann cell associated with several axon fibers in a Remak bundle or, alternatively, a pro-myelin and eventually myelinating Schwann cell associated with a single axon in a 1:1 ratio (Webster & Favilla, 1984; Jessen & Mirsky, 2005). Thereby, reciprocal axon-glia communication is crucial for this axonal sorting event prior to the onset of myelination. Available mouse mutants with particularly impaired radial sorting like *claw paw*, *laminin*, *beta1-integrin, DN-ErbB4* comprise defects in basal lamina components or expression of glial receptors ErbB4 or Lgi4 (Feltri *et al.*, 2002; Chen *et al.*, 2003; Darbas *et al.*, 2004; Pietri *et al.*, 2004; Yu *et al.*, 2005; Bermingham *et al.*, 2006). Among them *claw paw* resembles the described functional phenotype in *Olig2-Cre^{+};Npn-1$^{cond-/-}$* mutants best, as the *laminin* and *beta1-integrin* mutants showed a progressive and postnatal onset of peripheral motor neuropathy with symptoms such as muscle weakness, tremor or paralysis (Feltri *et al.*, 2002; Pietri *et al.*, 2004; Yu *et al.*, 2005). Furthermore, in *DN-ErbB4* mice solely sensory axons are affected resulting in their progressive degeneration and increasing insensitivity to noxious thermal stimuli (Chen *et al.*, 2003).

One cause for the increased number of fibers sorted into Remak bundles in *Olig2-Cre^{+};Npn-1$^{cond-/-}$* mutants could be aberrant axon-glia communication between the Npn-1 receptor normally expressed on motor neurons and its cognate interactor on the Schwann cell. Under normal conditions, Remak bundles are devoid of motor axons. Increased number of fibers per Remak bundle, however, could be due to aberrant sorting of some motor axons into Remak bundles. To test this hypothesis, the extensor nerve *N.radial* of affected paws in *Hb9::GFP^{+};Olig2-Cre^{+};Npn-1$^{cond-/-}$* mutants should be screened by immunohistochemistry for ectopic presence of *Hb9::GFP* labelled motor axons in unmyelinated Remak bundles instead of in single

myelinated large diameter axons. Preliminary data from the laboratory suggests that motor axons are not missorted into Remak bundles in *Hb9::GFP*$^{+}$*;Olig2-Cre*$^{+}$*; Npn-1*$^{cond-/-}$ mutants.

Alternatively, the axonal clusters ensheathed by Schwann cells are not Remak structures but immature Schwann cells stalled in maturation. To assess the question if expression of Npn-1 on motor neurons influences Schwann cell maturation, Schwann cell-axon bundles should be stained for maturation markers to distinguish immature (Krox20, Oct6) from non-myelinating mature (GFAP; NGFR^{P75}) Schwann cells (Jessen *et al.*, 1990; Blanchard *et al.*, 1996; Murphy *et al.*, 1996).

Putative Schwann cell-derived interactors for the Npn-1 receptor on motor neurons could be a Npn-1 receptor for homophilic interactions, L1, Lgi4 or yet unindentified ligands (Castellani, 2002; Jessen & Mirsky, 2005; Bannerman *et al.*, 2008). The Lgi4 protein is extracellularly expressed and its C-terminal ß-sheet structure shares striking similarities with integrins and semaphorins – both known ligands for Npn-1 receptors (Bermingham *et al.*, 2006; Nishino *et al.*, 2010). However, since peripheral nerves in *Npn-1*$^{Sema-}$ mice carrying three point mutations in the binding site for semaphorins are ultrastructurally unaffected, we rather propose a mechanism independent of binding to the Sema domain but instead to cell adhesion sites in the full length receptor (Shimizu *et al.*, 2000; Vander Kooi *et al.*, 2007).

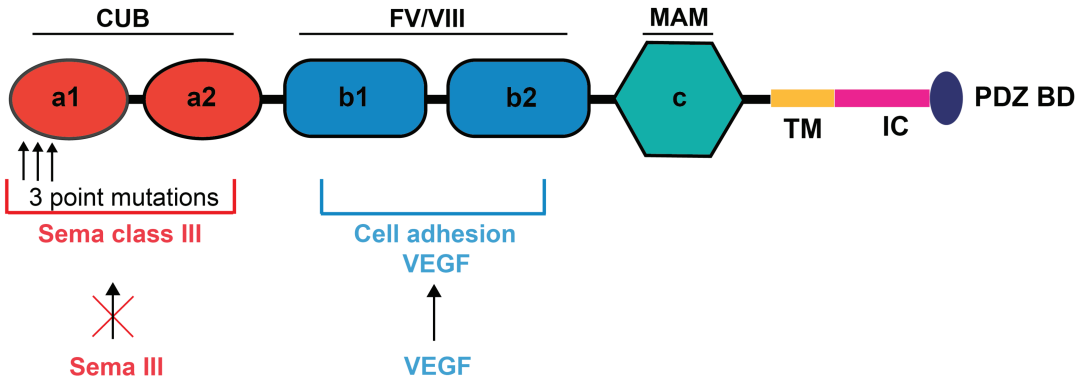


Figure 27: Schematic drawing of the full length Npn-1 receptor.

Besides the 2 CUB domains for binding of class III semaphorins, the Npn-1 receptor harbours 2 FV/VIII domains capable of binding cell adhesion molecules and VEGF. In *Npn-1*$^{Sema-}$ mice, the three point mutants inserted into the N-terminal located first CUB domain abolish binding of class III semaphorins. (Modified after Gu *et al.*, 2002).

V.2.3 Congenital muscle atrophy and postnatal muscle degeneration in *Olig2-Cre^{+};Npn-1$^{cond-/-}$* mice

Analysis of muscle volume in affected forelimbs of *Olig2-Cre^{+};Npn-1$^{cond-/-}$* mice revealed congenital muscle atrophy of forelimb extensors with progressive degeneration in neonatals during postnatal development (Fig. 16). Prolonged muscle denervation in degenerative motor neuron diseases like amyotrophic lateral sclerosis (ALS) or a mouse model of progressive motor neuronopathy (*pmn*) are parallelled by rapid and fatal muscle atrophy (Schmalbruch *et al.*, 1991; Boillee *et al.*, 2006). The reduced volume of extensor relative to antagonistic flexor muscles in the distal forelimb of *Olig2-Cre^{+};Npn-1$^{cond-/-}$* mutants might suggest a complete absence of innervation of extensor muscles, an ongoing denervation thereof or a reduction of neuromuscular transmission.

Embryonic skeletal muscles control motor neuron survival and numbers by providing a limited amount of trophic support (Phelan & Hollyday, 1991). A reduced muscle volume during embryonic development leads to reduced levels of trophic support and may cause programmed cell death of an increased amount of motor neurons. Thus, reduced extensor muscle generation during embryogenesis may be the underlying cause for alterations in extensor nerve innervation and survival. This issue could be addressed further by analysing aspects of muscle morphogenesis such as measuring the expansion of the myotome and onset of muscle differentiation in *Olig2-Cre^{+};Npn-1$^{cond-/-}$* mutants.

Additionally, particularly dorsal extensor muscles but not ventral forelimb flexors might have reduced innervation of motor projections. Data at embryonic stage E12.5 showed that motor projections in *Olig2-Cre^{+};Npn-1$^{cond-/-}$* mutants were less far advanced than in controls. Furthermore, backfills from dorsal muscles in the forelimbs of *Olig2-Cre^{+};Npn-1$^{cond-/-}$* embryos did not label motor projections in the brachial spinal cord where forelimb motor pools are located (Figs. 3I,4F in Huettl *et al.*, 2011). These findings suggest that particularly motor projections to dorsal forelimb muscles are stalled or delayed, causing their denervation or hypoinnervation and consequently result in muscle atrophy.

Besides correct innervation by motor projections, active forepaw extension requires functional neurotransmission at motor end plates. Mutations in genes encoding components of the neuromuscular junctions (NMJ) result in congenital myasthenic disorders (CMD) with symptoms such as muscle weakness, dropping

forelimbs and in severe cases neonatal lethality due to respiratory failure (reviewed in Engel & Sine, 2005). As *Olig2-Cre*$^{+}$*;Npn-1*$^{cond-/-}$ mutants also exhibit dropping in forepaws, we assessed the shape and spatial distribution of nicotinic acetylcholine receptors (AChR) at NMJs in 2 extensor muscles *Carpi Radialis longus* and *brevi*s. Experiments were performed by Tobias Gaisbauer, a Bachelor student I supervised (Gaisbauer, 2009). By the end of synaptogenesis (P30), the shape of mature AChR clusters, their spatial dispersion and the neuromuscular innervation pattern in *Olig2-Cre*$^{+}$*;Npn-1*$^{cond-/-}$ mutants are comparable to control littermates. These data suggest that morphologically normal NMJs are formed and maintained if Npn-1 is removed from motor neurons. It is therefore unlikely that abnormal NMJs are the underlying cause for the observed reduced extensor muscle volume in affected forelimbs. However, despite the morphology of synapses is unaltered in *Olig2-Cre*$^{+}$*;Npn-1*$^{cond-/-}$ mutants, their functional neurotransmission should be determined by assessing for example the onset and duration of postsynaptic potential (PSP) as readouts .

Together, congenital muscle atrophy with progressive postnatal degeneration in forelimb extensors of *Olig2-Cre*$^{+}$*;Npn-1*$^{cond-/-}$ mutants is likely due to embryonic hypoinnervation or denervation of the respective muscles. Although the morphology of NMJs and their distribution on forelimb extensor muscles is comparable among mutant and control animals, their functionality still needs to be assessed.

V.2.4 Oligodendrocyte precursors appear normal in *Olig2-Cre*$^{+}$*;Npn-1*$^{cond-/-}$ mutants

The basic helix-loop-helix transcription factor Olig2 is crucial for the generation of motor neurons and roughly 85% of all spinal oligodendrocyte precursors (OPC) via progenitors evolving from the pMN domain (Zhou *et al.*, 2001). Newly generated OPC migrate from their site of origin in the ventral spinal cord to their prospective targets, the future white matter, and mature into myelinating oligodendrocytes (Miller, 2002; Richardson *et al.*, 2006). Since expression of the Npn-1 receptor is reported in migrating OPC of the murine optic nerve and in mature oligodendrocytes (Ricard *et al.*, 2000; Ricard *et al.*, 2001; Spassky *et al.*, 2002), its loss on the surface of OPC in *Olig2-Cre*$^{+}$*;Npn-1*$^{cond-/-}$ mutants might impair essential functions of spinal cord oligodendrocytes or precursors. Thus, Anna Truckenbrodt, a bachelor student I supervised, addressed the migration and maturation of newly generated OPC and

the myelination capabilities of mature oligodendrocytes in the spinal cord. Preliminary results obtained by *in situ* stainings revealed no obvious differences in the generation and migration of spinal OPC at the time points E13.5 (after the switch from motor neuron to OPC generation in the pMN domain), E15.5 (when OPCs migrated dorsally and populated the entire spinal cord) or P0 (after differentiation into mature oligodendrocytes). Additionally, myelination properties of mature oligodendrocytes in the spinal cord of *Olig2-Cre*$^{+}$*;Npn-1*$^{cond-/-}$ mutants were indistinguishable from controls at P0 and adult stage (Truckenbrodt, 2009). For a more precise statement, the obtained qualitative data need to be further evaluated quantitatively. However, generation and migration of OPC as well es myelination by oligodendrocytes in the spinal cord seems to be independent of intrinsic Npn-1 expression.

V.3 Adaptive structural plasticity parallels motor recovery after *Sema3F-Npn-2* induced embryonic circuit miswiring

The function of the ligand-receptor pair Sema3F-Npn-2 in axon guidance during embryonic circuit wiring is well characterized in literature (Giger *et al.*, 2000; Marin *et al.*, 2001; Cloutier *et al.*, 2002; Sahay *et al.*, 2003; Huber *et al.*, 2005). However, its role in shaping early postnatal neural networks or in adaptive plasticity in adult mice is less clear. So far, there is compelling evidence that class 3 and 4 semaphorins in combination with their cognate receptors mediate synaptogenesis, axonal pruning, dendritic spine maturation and synaptic transmission (reviewed in Pasterkamp & Giger, 2009). My thesis focuses on postnatal adaptive rearrangements in miswired circuits after the loss of Sema3F-Npn-2 signalling. The data suggest possible mechanisms for structural and functional neuroplasticity in these mutants. Instead of a lesion-based model for adaptive plasticity, we used genetically induced wiring deficits in *Sema3F* or *Npn-2* mutants to unravel the response of the nervous system to embryonic neuronal miswiring. Hitherto, neuroplasticity was mainly studied after experimentally induced injury to the CNS. Due to their lesion-based nature, these injury models have numerous disadvantages such as standardization of lesion size and severity across laboratories. Additionally, pronounced side effects after experimentally induced CNS injury like inflammation, haemorrhage and scar formation confound obtained results and thus analysis of neuroplasticity.

V.3.1 Embryonic circuit miswiring in *Sema3F* and *Npn-2* mutants causes a distinct locomotor phenotype

Behavioural phenotyping in *Sema3F* or *Npn-2* mice demonstrated that absence of Sema3F-Npn-2 signalling during neuronal circuit formation leads to postnatal motor deficits - particularly in motor coordination. Poor motor performance is evidenced by the increased time it takes mutant mice to traverse a horizontal ladder and by the increased number of slips (Fig. 22). Interestingly, effects on speed have not been observed in *Sema3F* or *Npn-2* mutants subjected to tests analysing gross locomotion, anxiety or explorative behaviour. The locomotion speed in *Sema3F* or *Npn-2* mutants and anxiety-related parameters such as percentage of time spent in

the center of the open field do not differ significantly from wildtype controls (Table 1). Thus, the decreased crossing speed of mutants in tests assessing skilled locomotion might rather be due to motor slowness for voluntary movement initiation or execution (bradykinesia) and/or coordination deficits because of unsteady, wobbly stepping.

Compared to the phenotype observed in *Sema3F* mutants, locomotor deficits in absence of the receptor Npn-2 are slightly more severe and longer-lasting as seen in rotarod, wire climbing and beam walking tests (Fig. 23). These data suggest additional binding partners for Npn-2. Previous studies reported that Sema3C, an additional ligand for Npn-2, is expressed in specific subgroups of motor neurons in the developing spinal cord and thus might contribute to neuronal circuit wiring during embryogenesis (Chen *et al.*, 1997; Cohen *et al.*, 2005).

Interestingly, the mutant population segregated according to their motor performance into two groups of wildtype-like and poor performers by 4 weeks of age (Figs. 22B,23B). One explanation for this significant difference in motor skills might be the variable penetrance of the phenotype. Indeed, retrograde-tracing in embryos lacking Sema3F-Npn-2 signalling revealed variable penetrance of dorsal-ventral pathfinding defects among mutants (Huber, unpublished observations). Alternatively, the differential segregation observed in *Sema3F* and *Npn-2* mutants might be a consequence of variable compensatory adaptions in neonatals before behavioural testing started at 4 weeks. Voluntary locomotion among individual newborns varies in terms of quality and quantitiy and thus might be the underlying cause for high or low postnatal recovery in wildtype-like or poorly performing mutants, respectively. Available information on neurobehavioural testing of mice prior to weaning mainly focus on the appearance and development of milestones e.g. reflexes and early locomotion like pivoting and crawling (Tremml *et al.*, 1998; Branchi & Ricceri, 2002; Heyser, 2004). Furthermore, overground walking starts in infant rodents within a time range of 12 to 21 days postnatally (Heyser, 2004). Therefore, assessing motor coordination capabilities in mice prior to 4 weeks of age is technically hardly feasible and also not reliable due to the physiological range in the onset of walking.

During postnatal development from 4 to 12 weeks *Sema3F* and *Npn-2* mutants significantly improved their motor skills (Figs. 22,23). Previous data evidenced the positive effect of training on motor capabilities in mice after spinal cord injury (reviewed in Edgerton *et al.*, 2004). In order to rule out that the observed motor improvement in animals repetitively tested at 4, 8 and 12 weeks is solely induced by

repetitive testing, data of their locomotor performance was compared with the additional cohorts tested only at the single time points 8 or 12 weeks. No significant differences in motor skills among animals tested repetitively or at single time points (Table 1) suggest that the improvement, particularly in poor performers, is due to a native capacity for compensation in postnatal mutant mice.

V.3.2 Adaptive structural plasticity in *Sema3F* mutant mice

Previous studies in embryonic *Sema3F* and *Npn-2* mutants at E13.5 reported dorsal-ventral pathfinding errors of medial LMC neurons innervating ventral instead of their assigned dorsal muscles (Huber *et al.*, 2005). We found that forelimb motor pools compaction and localization in early postnatal (4 weeks) and adult (12 weeks) *Sema3F* mutants revealed increased dorsal-ventral spreading of medial LMC neurons exclusively in poor performers (Fig. 24). Correlation of the neuroanatomical data obtained from the distal forelimb to motor coordination skills revealed a tight and predictive coupling of these two parameters on a single animal level in *Sema3F* mice. Poorly performing *Sema3F* mutants exhibit increased spreading of ventrally projecting LMCm motor pools at 4 and 12 weeks which is not the case in wildtype-like mutants. Instead, the values of motor performance in the grid walk test and the scatter index of ventral projections in wildtype and wildtype-like mutants lie within two standard deviations from the wildtype mean (Fig. 24I).

A possible explanation for the observed correlation of neuroanatomy to skilled motor performance lies in the fact that spinal localization of motor pools determines their peripheral muscle innervation pattern (Landmesser, 1978a; b; Hollyday, 1980; Gutman *et al.*, 1993). An intriguing study by Romanes provided a topographic map linking the dorsal-ventral position of spinal motor pools to the proximo-distal location of innervated muscles in the cat hind limb (Romanes, 1951). A very recent elegant study built on these classical data showed that the precise connection of Ia sensory afferents to self spinal motor neurons critically depends on the correct positioning of the target motor pool in the dorsoventral tier domain in the spinal cord. Motor neurons of *FoxP1*$^{MN\Delta}$ mutants lost their pool identity and therefore settle randomly and in aberrant positions in the spinal cord. Consequently, the scrambled motor neurons are falsely innervated by nonself sensory afferents (Surmeli *et al.*, 2011). Thus, increased dorsal-ventral spreading of LMCm motor neurons of *Sema3F*

mutants into ectopic areas in the spinal cord may entail aberrant innervation of limb target muscles and eventually hindered motor coordination. More dorsally positioned motor neurons of distal flexors from the lower forelimb are presumably mis-innervated by Ia sensory afferents originally targeting motor pools from the more proximal located *Triceps brachii* extensor muscle. This issue can be addressed by making use of the fact that CTB is also transported in sensory axons and labels sensory boutons (Surmeli *et al.*, 2011). Injection of differentially labeled CTBs into distal forelimb flexors and the proximal *Triceps brachii* muscles can visualise nonself sensory input originally assigned for *Triceps brachii* motor neurons on dorsally mispositioned flexor motor neurons.

How are motor neurons compacted into muscle-specific pools? While a combinatorial transcription factor code has been identified for the specification, little is known about molecular cues involved in the compaction of motor pools (Jessell, 2000). Type II cadherins as well as β- and γ-catenins demarcate distinct spinal motor pools and influence positioning in the developing chick and mouse spinal cord. In addition, loss of cadherin-catenin signalling reduces the packaging density of spinal motor pools in the medial or lateral LMC (Price *et al.*, 2002; Patel *et al.*, 2006; Demireva *et al.*, 2011). Similarly, the combinatorial expression of axon guidance cues and their receptors, e.g. class 3 semaphorins, neuropilins and plexins, in spinal motor neurons may contribute to motor pool clustering and patterning of sensory-motor connections during embryonic development. Thereby, repulsive signalling triggers clustering of adjacent motor pools and prevents the intermixing of different motor neuron subpopulations (Cohen *et al.*, 2005; Zlatic *et al.*, 2009). Thus, under physiological conditions Sema3F expression might be involved in the tight compaction of homonymous motor nuclei into distinct pools and thereby prevent the LMCm motor pools from ectopic spreading. Consequently, loss of inhibitory Sema3F-Npn-2 signalling in subsets of spinal motor neurons allows for increased spreading in *Sema3F* mutant poor performers.

V.3.3 Role of supraspinal input in postnatal neural plasticity

More detailed analyses of locomotion and the neural circuits involved distinguish stereotyped, overground locomotion from skilled locomotion. While the first is mainly driven by spinal circuitry, the latter implies additional input from higher ordered

circuits such as corticospinal (CST) and rubrospinal (RST) tract (Goulding, 2009). Deficits in the accuracy of ipsilateral forelimb-hind limb foot placement on the grid walk in *Sema3F* mutants (Fig. 22D) may be an indication for defects in corticospinal connections (Metz & Whishaw, 2002). To investigate this possibility in *Sema3F* mutants, I analysed anteriogradely traced descending CST projections on defined spinal motor pools, which were retrogradely labelled from dorsal or ventral forelimb muscles. There were no obvious differences in the organisation and localization of the CST within the spinal cord or its projections to retrogradely labelled distal forelimb motor neurons between mutant and wildtype *Sema3F* mice (data not shown).

However, to determine the role of pyramidal and extrapyramidal tracts in postnatal neural plasticity after genetically-induced circuit miswiring, a more detailed analysis is required. This would involve using a neurotropic virus for retrograde trans-synaptic tracing such as Bartha Pseudorabies virus or Rabiesvirus CSV-11 (reviewed in Ugolini, 2010). The virus propagates from its site of injection, the muscles, to the spinal motor neurons innervating these muscles and via synaptically coupled neurons to the cortical neurons in layer V in the CNS (Coulon *et al.*, 1989; Babic *et al.*, 1993; Ugolini, 1995; Bareyre *et al.*, 2004; Rathelot & Strick, 2006). Thereby, the topographic representation of specific forelimb muscles in the motor cortex is visualised and can be compared among *Sema3F* or *Npn-2* mutants and control mice. Additionally the projection pattern of extrapyramidal tracts, such as the reticulospinal or rubrospinal tracts that are involved in initiation of movement and fine motor control, respectively, could be analysed following anterograde tracing by using biotinylated dextran amine (BDA; Raineteau *et al.*, 2001; Ballermann & Fouad, 2006).

V.3.4 Functional wiring of peripheral circuits in adult *Sema3F* mutants corroborates embryonic pathfinding deficits

The functional wiring of sensorimotor circuits innervating the forelimb of *Sema3F* mutants was assessed by EMG recordings in individual dorsal or ventral muscles. Owing to the close proximity of adjacent muscles, no EMGs from single muscles could be recorded in the distal forelimb, where the anatomical data was obtained from. Therefore, *Biceps* and *Triceps brachii* muscles in the proximal forelimb were chosen as ventral and dorsal antagonists, respectively. Our data suggest an aberrant muscle recruitment paradigm in all *Sema3F* mutants: stimulation of the normally

ventrally projecting *musculocutaneous* nerve elicits synchronous activity in *Biceps brachii* and antagonistic *Triceps* brachii muscles, which was never observed in wildtype littermates (Fig. 26C). The underlying cause for the synchronous activity in antagonistic forelimb muscles might be ectopic projections of medial LMC axons to dorsal limb muscles in addition to innervation of ventral muscles. Such pathfinding defects have been observed during embryonic circuit wiring in *Sema3F* mutants (Huber *et al.*, 2005). Therefore, the data on functional motor innervation of the distal forelimb in all adult *Sema3F* mutants indicates that the genetically induced peripheral circuit miswiring in *Sema3F* mutant embryos persists postnatally and that false connections were not simply eliminated.

Our data obtained from behavioural phenotyping and neuroanatomical analyses showed that motor coordination and spinal organisation of motor pools of the distal forelimb correlate on a single animal level and differ in the two mutant groups wildtype-like and poor performers (Figs. 22,24). However, the electrophysiological data in these mutants do not correlate with behavioural or anatomical results. We found synchronous EMG recordings of antagonistic *Biceps* and *Triceps brachii* in all *Sema3F* mutants. Interestingly, the neuroanatomical characterization of the *Biceps* and *Triceps* motor pool representation in *Sema3F* mutants did not reveal an aberrant spreading (data not shown). This may arise from differences in the applied neuronal tracing methods: retrograde tracings of distal forelimb motor pools were performed by injecting virtually all muscles while in the proximal limb only individual motor pools of *Biceps* and *Triceps brachii* muscles were analysed. Since no postnatal molecular markers of individual motor pools are known, we cannot exclude that both *Biceps* and *Triceps* motor pools in *Sema3F* mutants increased spreading or changed location with respect to each other. Alternatively, the clustering of *Biceps* and *Triceps brachii* motor pool may not be dependent on repulsive Sema3F-Npn-2 signalling. To test this hypothesis, the expression of the Npn-2 receptor should be assigned to specific motor pools by combining immunohistochemistry for visualization of Npn-2 expression with retrograde tracing of the motor pools from distal forelimb muscles or proximal *Biceps* and *Triceps brachii*.

Housing *Sema3F* mutants in an enriched environment boosted improvement of motor function and resolved the anatomical mislocation of distinct forelimb motor pools (Fig. 25). However, increased motor stimulation in an enriched environment had no impact on the synchronous muscle recruitment paradigm of *Biceps* and

Triceps brachii muscles in *Sema3F* mutants (Fig. 26). One possible explanation for the synchronous activation of antagonistic, proximal forelimb muscles in all mutants independent of their housing conditions could be that the control of *Biceps* and *Triceps brachii* muscle activation might not be essential for proper motor coordination in *Sema3F* mutants. *Biceps* and *Triceps brachii* are two large muscles in the proximal forelimb that control flexion of elbow, supination of the forearm as well as extension of the forearm, respectively. Contrary, the distal forelimb harbours numerous small muscles each required for a distinct, fine controlled movement such as *extensor minimi digiti* for extension of the little digit in all joints. Hence, fine grasping of objects such as the rungs of the horizontal ladder might rather depend critically on the fine control of the interplay of various small muscles innervating the paw than on the action of large proximal forelimb muscles.

Alternatively, modulatory input via extrapyramidal or pyramidal tracts from the CNS could shape the overall response despite persisting functional deficits in local peripheral sensorimotor circuits of the forelimb. Thus, the muscle activation deficit in *Sema3F* mutants characterized by EMGs persists in local spinal circuits independent of the housing conditions but higher-ordered modulatory input on these circuits ensures improvement of motor coordination capabilities. However, the tracts involved in modulation and the underlying mechanisms need to be determined.

V.3.5 Excitability of peripheral limb circuits is unchanged in *Sema3F* mutants

Besides structural changes on the anatomical level and functional alterations in the recruitment patterns of muscles in sensorimotor circuits, adaptive mechanisms may also occur on a synaptic level by modulating excitatory and inhibitory input for the fine tuning of neuronal circuits (Sanes & Yamagata, 2009).

Injury-induced neuroplastic rearrangements have been shown to go along with synaptogenesis, synaptic enhancement to strengthen certain circuits and changes in the excitability of spared neuronal circuits (Keller *et al.*, 1992; Kleim *et al.*, 1996; Nakazawa *et al.*, 2006). Sema3F acts as a negative regulator of excitatory synapse input in dentate gyrus neurons (Tran *et al.*, 2009). Additionally, recent studies reported a shift of the well-adjusted balance of inhibitory to excitatory input on α- and γ- motor neurons to increased inhibitory conditions after spinal cord injury (Ichiyama *et al.*, 2011).

To address the possibility of plasticity on the synaptic level, the density of excitatory glutamatergic synapses on lateral and medial LMC motor neurons which were identified by retrograde labelling from dorsal or ventral forelimb muscles, respectively, was assessed. Mean vGlut1$^+$ excitatory input on labelled lateral or medial LMC motor neurons was not altered in 4 weeks old *Sema3F* mutants compared to control animals (Fig. 26D,E). Although the excitatory input is unchanged in 4 weeks old *Sema3F* mutants compared to wildtype, the inhibitory input may still be altered and thus lead to a general hypo- or hyperexcitability of specific peripheral limb circuitries innervating distal forelimb muscles. To rule out this possibility, mean vGAT inhibitory input on traced motor neuron pools of dorsal and ventral forelimb muscles needs to be assessed.

Thus, alterations in excitatory synaptic input on sensorimotor networks innervating forelimb muscles are unlikely to contribute to the observed motor and functional deficits in *Sema3F* mutants. However, the role of synaptic inhibition in miswired peripheral sensorimotor circuitry in these mutants needs to be determined.

V.3.6 Enriched environment housing promotes structural plasticity paralleled by improvement of motor coordination in *Sema3F* mutants

Compelling evidence suggests that enhancing sensory, motor and cognitive stimulations in an enriched environment promote structural and functional changes in the nervous system including gliogenesis, neurogenesis, improved learning and positively influences the outcome of CNS damage or disorders such as stroke and Parkinson's disease (reviewed in van Praag *et al.*, 2000; Nithianantharajah & Hannan, 2006).

Our data show that enriched housing conditions that stimulate motor behaviour and social interaction starting at birth significantly boosts locomotor skills in *Sema3F* mutants to wildtype level within the first 8 to 12 postnatal weeks (Fig. 25). These data fit with prior publications reporting beneficial effects of physical and social enrichment on motor functions in rodents suffering from a neurodevelopmental disorder, the Rett syndrome, or CNS injury (Johansson & Ohlsson, 1996; Jadavji *et al.*, 2006; Kondo *et al.*, 2008). *Sema3F* wildtypes, however, do not improve their motor skills significantly during postnatal development as seen in the grid walk, beam walk or wire climbing tests (Fig. 25). The latter observation might be due to a ceiling

effect in wildtypes as previously reported for rodent spinal cord injury models. Thereby, in-cage-activity already triggered spontaneous functional recovery to a level that cannot be improved further by activity based training, e.g. on the treadmill, (Fouad *et al.*, 2000; Heng & de Leon, 2009; Kuerzi *et al.*, 2010).

During “critical periods” in early postnatal life, established neuronal networks are particularly receptive to experience-dependent circuit refinement as previously shown for the sensory and motor system (reviewed in Hensch, 2004). Moreover, housing rodents in an enriched environment during these definded time windows has profound impact on critical period plasticity (reviewed in Sale *et al.*, 2009). Experiencing enriched housing conditions from birth on promoted the physiological maturation of retinal and visual cortex circuitry - the latter even in the absence of visual experience in dark-reared animals (Bartoletti *et al.*, 2004; Cancedda *et al.*, 2004; Landi *et al.*, 2007). Even in adult rats with amblyopia due to monocular deprivation, enriched stimulation facilitates plastic changes that restore visual acuity and ocular dominance. Hereby one underlying mechanism to unmask neuroplasticity lies in the intracortical inhibition of GABAergic neurotransmission (Hensch *et al.*, 1998; Fagiolini & Hensch, 2000; Sale *et al.*, 2007).

At the neuroanatomical level, wildtype-like ventral forelimb pool distribution was observed in *Sema3F* mutants raised under enriched conditions already by 4 weeks whereas functional improvement of transient motor coordination deficits to wildtype-levels occurred between 8 to 12 weeks (Fig. 25A). Therefore, early enriched environment housing may accelerate structural refinement and adaption of embryonically miswired sensorimotor circuitry in *Sema3F* mutants resulting in spinal motor pool distribution indistinguishable among mutants and controls. One possible explanation for the delay in functional compared to neuranatomical improvements might be presented by the fact that neonatal mice start to walk at around 2 to 3 weeks of age and consequently are able to use the provided devices for motor stimulation like running wheel and mini step ladder for a short time prior to behavioural testing at 4 weeks (Heyser, 2004). However, from these data we cannot conclude if early stimulation of physical activity and social interaction from birth is required in *Sema3F* mutants to restore motor functions later on. To address the issue further, additional cohorts of *Sema3F* mice are housed under regular conditions during the first 4 postnatal weeks and subsequently subjected to an enriched environment housing period of 4 weeks. Behavioural phenotyping on a weekly basis

and structural analysis of the underlying neuroanatomy in peripheral sensorimotor circuitry at 8 and 12 weeks should give insights into the extent of beneficial impact of late versus early enriched environment housing and the exact time point of motor improvement to wildtype level.

Besides the environmental influence on neuroplasticity, there are reports on pharmacological compounds likewise promoting plasticity by reducing or neutralizing extrinsic inhibitory factors, such as myelin-associated inhibitors (MAIs) or chondroitin sulfate proteoglycans (CSPGs), that inhibit functional reorganisation of spinal circuits (Busch & Silver, 2007; Giger *et al.*, 2010). Degradation of perineuronal nets (PNNs) composed of CSPGs by Chondroitinase-ABC treatment restored plasticity in the adult visual cortex (Pizzorusso *et al.*, 2002; Pizzorusso *et al.*, 2006). Thus, it would be interesting to assess the effect of pharmacologically inhibiting these extrinsic factors by e.g. Chondroitinase-ABC alone and also in combination with physical and social stimulation in an enriched environment on structural and functional plasticity after developmental circuit miswiring in *Sema3F* mutants.

V.4 Neurodevelopmental circuit miswiring and postnatal consequences

During embryonic establishment of the nervous system, axons navigate to their peripheral - often distant targets - via instructive guidance cues. In the context of this thesis, three different mouse lines harbouring mutations in axon guidance cues or receptors were analysed postnatally to determine potential consequences of neural circuit miswiring and compensatory strategies in these animals. Hitherto insights into molecular and functional mechanisms to adapt to neurodevelopmental circuit miswiring are scarce - in contrary to the knowledge on neuroplasticity at spinal and supraspinal levels in CNS injury models (Bareyre *et al.*, 2004; Ballermann & Fouad, 2006; Barriere *et al.*, 2008; Courtine *et al.*, 2008; Rosenzweig *et al.*, 2010). However, experimental SCI models are associated with pronounced disadvantages such as low reproducibility of standardized lesions among different laboratories and unwanted side effects elicited in the tissue surrounding the lesion site. We circumvented these caveats by choosing genetically induced circuit miswiring to assess neuroplasticity.

The axon guidance cue-receptor pair Sema3F-Npn-2 instructs a specific dorsal-ventral innervation pattern onto motor axons. *Sema3F*$^{-/-}$ and *Npn-2*$^{-/-}$ embryos display specific pathfinding defects with medial LMC neurons misprojecting to dorsal in addition to their regular ventral limb targets (Huber *et al.*, 2005). Postnatally, *Sema3F* mutants are viable and revealed deficits in motor coordination, localization of distal forelimb motor pools in the spinal cord as well as in functional activation of antagonistic forelimb muscles.

In *Olig2-Cre*$^{+}$*;Npn-1*$^{cond-/-}$ mutants, the axon guidance receptor Npn-1 that is mainly involved in timing of axonal ingrowth and fasciculation status of peripheral motor and sensory projections, was specifically ablated in motor neurons. Mutant embryos displayed extensive defasciculation and reduced growth of motor projections into the limb (Huber *et al.*, 2005; Huettl *et al.*, 2011). Postnatally, these mutants suffered from permanent arthrogryposis-like forepaw impairments associated with a reduction in forelimb extensor muscles and further postnatal degeneration. Our data further suggest that the Npn-1 receptor is involved in Schwann cell-axon communication during radial sorting of axonal fibers.

Interestingly, we found structural and functional compensation of behavioural deficits in *Sema3F* mutants while the forelimb impairments observed in *Olig2-Cre*$^{+}$*;Npn-1*$^{cond-/-}$ mice are of permanent nature. One explanation for the differences in

postnatal plastic capabilities may lie in the underlying disturbances during embryonic circuit formation – dorsal-ventral circuit miswiring (*Sema3F* and *Npn-2* mutants) or defasciculation and reduced distal advancement of axonal projections to the limb (*Olig2-Cre*$^{+}$*;Npn-1*$^{cond-/-}$ mutants). In *Sema3F* and *Npn-2* embryos neuronal networks were established mainly correct with miswiring only in a subset of medial LMC motor neurons. In *Olig2-Cre*$^{+}$*;Npn-1*$^{cond-/-}$ mutants extensor forelimb muscles are likely not innervated and thus not incorporated into forming sensorimotor circuits. Thus, our data suggest that miswired neuronal networks are susceptible to compensation at structural and functional level to refine pre-extisting networks but are unable to newly establish sensorimotor circuits postnatally after embryonic hypoinnervation or denervation of specific muscles.

Although genetically induced circuit miswiring by mutations in axon guidance cues or corresponding receptors is the common basis in all three mouse lines analysed, the postnatal consequences differ significantly between structural and functional compensation in *Sema3F* or *Npn-2* mutants and permanent impairments in *Olig2-Cre*$^{+}$*;Npn-1*$^{cond-/-}$ mutants. Thus, I propose that *Sema3F* or *Npn-2* mutant mice are useful models to assess the underlying mechanisms of postnatal adaptive plasticity under non-injury based conditions. Moreover, also extrinsic factors such as environmental influence, motor training and pharmacological compounds promoting neuroplasticity can be analysed. *Olig2-Cre*$^{+}$*;Npn-1*$^{cond-/-}$ mutants did not reveal postnatal compensation but may serve as a model to analyse the consequences and mechanisms of congenital muscle atrophy in forelimb extensors followed by progressive degeneration postnatally.

VI REFERENCES

Aigouy, B., Van de Bor, V., Boeglin, M. & Giangrande, A. (2004) Time-lapse and cell ablation reveal the role of cell interactions in fly glia migration and proliferation. *Development*, **131**, 5127-5138.

Arber, S., Ladle, D.R., Lin, J.H., Frank, E. & Jessell, T.M. (2000) ETS gene Er81 controls the formation of functional connections between group Ia sensory afferents and motor neurons. *Cell*, **101**, 485-498.

Armstrong, D.M. (1988) The supraspinal control of mammalian locomotion. *The Journal of physiology*, **405**, 1-37.

Baatz, M., Arini, N., Schape, A., Binnig, G. & Linssen, B. (2006) Object-oriented image analysis for high content screening: detailed quantification of cells and sub cellular structures with the Cellenger software. *Cytometry. Part A : the journal of the International Society for Analytical Cytology*, **69**, 652-658.

Baatz, M., Zimmermann, J. & Blackmore, C.G. (2009) Automated analysis and detailed quantification of biomedical images using Definiens Cognition Network Technology. *Combinatorial chemistry & high throughput screening*, **12**, 908-916.

Babic, N., Mettenleiter, T.C., Flamand, A. & Ugolini, G. (1993) Role of essential glycoproteins gII and gp50 in transneuronal transfer of pseudorabies virus from the hypoglossal nerves of mice. *Journal of virology*, **67**, 4421-4426.

Bailey, M.S., Puche, A.C. & Shipley, M.T. (1999) Development of the olfactory bulb: evidence for glia-neuron interactions in glomerular formation. *The Journal of comparative neurology*, **415**, 423-448.

Ballermann, M. & Fouad, K. (2006) Spontaneous locomotor recovery in spinal cord injured rats is accompanied by anatomical plasticity of reticulospinal fibers. *The European journal of neuroscience*, **23**, 1988-1996.

Bannerman, P., Ara, J., Hahn, A., Hong, L., McCauley, E., Friesen, K. & Pleasure, D. (2008) Peripheral nerve regeneration is delayed in neuropilin 2-deficient mice. *Journal of neuroscience research*, **86**, 3163-3169.

Barbacid, M. (1994) The Trk family of neurotrophin receptors. *Journal of neurobiology*, **25**, 1386-1403.

Barbeau, H. & Rossignol, S. (1987) Recovery of locomotion after chronic spinalization in the adult cat. *Brain research*, **412**, 84-95.

Bareyre, F.M., Kerschensteiner, M., Raineteau, O., Mettenleiter, T.C., Weinmann, O. & Schwab, M.E. (2004) The injured spinal cord spontaneously forms a new intraspinal circuit in adult rats. *Nature neuroscience*, **7**, 269-277.

Barneoud, P., Lolivier, J., Sanger, D.J., Scatton, B. & Moser, P. (1997) Quantitative motor assessment in FALS mice: a longitudinal study. *Neuroreport*, **8**, 2861-2865.

Barriere, G., Leblond, H., Provencher, J. & Rossignol, S. (2008) Prominent role of the spinal central pattern generator in the recovery of locomotion after partial spinal cord injuries. *The Journal of neuroscience : the official journal of the Society for Neuroscience*, **28**, 3976-3987.

Bartoletti, A., Medini, P., Berardi, N. & Maffei, L. (2004) Environmental enrichment prevents effects of dark-rearing in the rat visual cortex. *Nature neuroscience*, **7**, 215-216.

Bastiani, M.J., Raper, J.A. & Goodman, C.S. (1984) Pathfinding by neuronal growth cones in grasshopper embryos. III. Selective affinity of the G growth cone for the P cells within the A/P fascicle. *The Journal of neuroscience : the official journal of the Society for Neuroscience*, **4**, 2311-2328.

Behar, O., Golden, J.A., Mashimo, H., Schoen, F.J. & Fishman, M.C. (1996) Semaphorin III is needed for normal patterning and growth of nerves, bones and heart. *Nature*, **383**, 525-528.

Belhaj-Saif, A. & Cheney, P.D. (2000) Plasticity in the distribution of the red nucleus output to forearm muscles after unilateral lesions of the pyramidal tract. *Journal of neurophysiology*, **83**, 3147-3153.

Ben-Zvi, A., Manor, O., Schachner, M., Yaron, A., Tessier-Lavigne, M. & Behar, O. (2008) The Semaphorin receptor PlexinA3 mediates neuronal apoptosis during dorsal root ganglia development. *The Journal of neuroscience : the official journal of the Society for Neuroscience*, **28**, 12427-12432.

Ben-Zvi, A., Yagil, Z., Hagalili, Y., Klein, H., Lerman, O. & Behar, O. (2006) Semaphorin 3A and neurotrophins: a balance between apoptosis and survival signaling in embryonic DRG neurons. *Journal of neurochemistry*, **96**, 585-597.

Benecke, R., Meyer, B.U. & Freund, H.J. (1991) Reorganisation of descending motor pathways in patients after hemispherectomy and severe hemispheric lesions demonstrated by magnetic brain stimulation. *Experimental brain research. Experimentelle Hirnforschung. Experimentation cerebrale*, **83**, 419-426.

Bermingham, J.R., Jr., Shearin, H., Pennington, J., O'Moore, J., Jaegle, M., Driegen, S., van Zon, A., Darbas, A., Ozkaynak, E., Ryu, E.J., Milbrandt, J. & Meijer, D. (2006) The claw paw mutation reveals a role for Lgi4 in peripheral nerve development. *Nature neuroscience*, **9**, 76-84.

Bibel, M. & Barde, Y.A. (2000) Neurotrophins: key regulators of cell fate and cell shape in the vertebrate nervous system. *Genes & development*, **14**, 2919-2937.

Bjursten, L.M., Norrsell, K. & Norrsell, U. (1976) Behavioural repertory of cats without cerebral cortex from infancy. *Experimental brain research. Experimentelle Hirnforschung. Experimentation cerebrale*, **25**, 115-130.

Blanchard, A.D., Sinanan, A., Parmantier, E., Zwart, R., Broos, L., Meijer, D., Meier, C., Jessen, K.R. & Mirsky, R. (1996) Oct-6 (SCIP/Tst-1) is expressed in Schwann cell precursors, embryonic Schwann cells, and postnatal myelinating Schwann cells: comparison with Oct-1, Krox-20, and Pax-3. *Journal of neuroscience research*, **46**, 630-640.

Boillee, S., Vande Velde, C. & Cleveland, D.W. (2006) ALS: a disease of motor neurons and their nonneuronal neighbors. *Neuron*, **52**, 39-59.

Bolam, J.P., Hanley, J.J., Booth, P.A. & Bevan, M.D. (2000) Synaptic organisation of the basal ganglia. *Journal of anatomy*, **196 (Pt 4)**, 527-542.

Bonanomi, D. & Pfaff, S.L. (2010) Motor axon pathfinding. *Cold Spring Harbor perspectives in biology*, **2**, a001735.

Branchi, I. & Ricceri, L. (2002) Transgenic and knock-out mouse pups: the growing need for behavioral analysis. *Genes, brain, and behavior*, **1**, 135-141.

Briscoe, J. & Novitch, B.G. (2008) Regulatory pathways linking progenitor patterning, cell fates and neurogenesis in the ventral neural tube. *Philosophical transactions of the Royal Society of London. Series B, Biological sciences*, **363**, 57-70.

Briscoe, J., Pierani, A., Jessell, T.M. & Ericson, J. (2000) A homeodomain protein code specifies progenitor cell identity and neuronal fate in the ventral neural tube. *Cell*, **101**, 435-445.

Briscoe, J., Sussel, L., Serup, P., Hartigan-O'Connor, D., Jessell, T.M., Rubenstein, J.L. & Ericson, J. (1999) Homeobox gene Nkx2.2 and specification of neuronal identity by graded Sonic hedgehog signalling. *Nature*, **398**, 622-627.

Brittis, P.A., Lu, Q. & Flanagan, J.G. (2002) Axonal protein synthesis provides a mechanism for localized regulation at an intermediate target. *Cell*, **110**, 223-235.

Brockschnieder, D., Lappe-Siefke, C., Goebbels, S., Boesl, M.R., Nave, K.A. & Riethmacher, D. (2004) Cell depletion due to diphtheria toxin fragment A after Cre-mediated recombination. *Molecular and cellular biology*, **24**, 7636-7642.

Brockschnieder, D., Pechmann, Y., Sonnenberg-Riethmacher, E. & Riethmacher, D. (2006) An improved mouse line for Cre-induced cell ablation due to diphtheria toxin A, expressed from the Rosa26 locus. *Genesis*, **44**, 322-327.

Brown, G.T. (1911) The intrinsic factors in the act of progression in the mammal. *Proc R Soc Lond B Biol Sci*, **84**, 308-319.

Brown, G.T. (1914) On the nature of the fundamental activity of the nervous centres; together with an analysis of the conditioning of rhythmic activity in progression, and a theory of the evolution of function in the nervous system. *The Journal of physiology*, **48**, 18-46.

Brushart, T.M., Henry, E.W. & Mesulam, M.M. (1981) Reorganization of muscle afferent projections accompanies peripheral nerve regeneration. *Neuroscience*, **6**, 2053-2061.

Brushart, T.M. & Mesulam, M.M. (1980) Alteration in connections between muscle and anterior horn motoneurons after peripheral nerve repair. *Science*, **208**, 603-605.

Busch, S.A. & Silver, J. (2007) The role of extracellular matrix in CNS regeneration. *Current opinion in neurobiology*, **17**, 120-127.

Cai, L.L., Courtine, G., Fong, A.J., Burdick, J.W., Roy, R.R. & Edgerton, V.R. (2006) Plasticity of functional connectivity in the adult spinal cord. *Philosophical transactions of the Royal Society of London. Series B, Biological sciences*, **361**, 1635-1646.

Cancedda, L., Putignano, E., Sale, A., Viegi, A., Berardi, N. & Maffei, L. (2004) Acceleration of visual system development by environmental enrichment. *The Journal of neuroscience : the official journal of the Society for Neuroscience*, **24**, 4840-4848.

Cangiano, L. & Grillner, S. (2003) Fast and slow locomotor burst generation in the hemispinal cord of the lamprey. *Journal of neurophysiology*, **89**, 2931-2942.

Cangiano, L. & Grillner, S. (2005) Mechanisms of rhythm generation in a spinal locomotor network deprived of crossed connections: the lamprey hemicord. *The Journal of neuroscience : the official journal of the Society for Neuroscience*, **25**, 923-935.

Carlstedt, T. (2000) Approaches permitting and enhancing motoneuron regeneration after spinal cord, ventral root, plexus and peripheral nerve injuries. *Current opinion in neurology*, **13**, 683-686.

Carr, L.J., Harrison, L.M., Evans, A.L. & Stephens, J.A. (1993) Patterns of central motor reorganization in hemiplegic cerebral palsy. *Brain : a journal of neurology*, **116 (Pt 5)**, 1223-1247.

Castellani, V. (2002) The function of neuropilin/L1 complex. *Advances in experimental medicine and biology*, **515**, 91-102.

Chen, H., Chedotal, A., He, Z., Goodman, C.S. & Tessier-Lavigne, M. (1997) Neuropilin-2, a novel member of the neuropilin family, is a high affinity receptor for the semaphorins Sema E and Sema IV but not Sema III. *Neuron*, **19**, 547-559.

Chen, H.H. & Frank, E. (1999) Development and specification of muscle sensory neurons. *Current opinion in neurobiology*, **9**, 405-409.

Chen, S., Rio, C., Ji, R.R., Dikkes, P., Coggeshall, R.E., Woolf, C.J. & Corfas, G. (2003) Disruption of ErbB receptor signaling in adult non-myelinating Schwann cells causes progressive sensory loss. *Nature neuroscience*, **6**, 1186-1193.

Cheng, H.J., Bagri, A., Yaron, A., Stein, E., Pleasure, S.J. & Tessier-Lavigne, M. (2001) Plexin-A3 mediates semaphorin signaling and regulates the development of hippocampal axonal projections. *Neuron*, **32**, 249-263.

Clarac, F. (2008) Some historical reflections on the neural control of locomotion. *Brain research reviews*, **57**, 13-21.

Cloutier, J.F., Giger, R.J., Koentges, G., Dulac, C., Kolodkin, A.L. & Ginty, D.D. (2002) Neuropilin-2 mediates axonal fasciculation, zonal segregation, but not axonal convergence, of primary accessory olfactory neurons. *Neuron*, **33**, 877-892.

Cohen, S., Funkelstein, L., Livet, J., Rougon, G., Henderson, C.E., Castellani, V. & Mann, F. (2005) A semaphorin code defines subpopulations of spinal motor neurons during mouse development. *The European journal of neuroscience*, **21**, 1767-1776.

Corti, S., Nizzardo, M., Nardini, M., Donadoni, C., Salani, S., Ronchi, D., Saladino, F., Bordoni, A., Fortunato, F., Del Bo, R., Papadimitriou, D., Locatelli, F., Menozzi, G., Strazzer, S., Bresolin, N. & Comi, G.P. (2008) Neural stem cell transplantation can ameliorate the phenotype of a mouse model of spinal muscular atrophy. *The Journal of clinical investigation*, **118**, 3316-3330.

Coulon, P., Derbin, C., Kucera, P., Lafay, F., Prehaud, C. & Flamand, A. (1989) Invasion of the peripheral nervous systems of adult mice by the CVS strain of rabies virus and its avirulent derivative AvO1. *Journal of virology*, **63**, 3550-3554.

Courtine, G., Song, B., Roy, R.R., Zhong, H., Herrmann, J.E., Ao, Y., Qi, J., Edgerton, V.R. & Sofroniew, M.V. (2008) Recovery of supraspinal control of stepping via indirect propriospinal relay connections after spinal cord injury. *Nature medicine*, **14**, 69-74.

Cowan, W.M. (2001) Viktor Hamburger and Rita Levi-Montalcini: the path to the discovery of nerve growth factor. *Annual review of neuroscience*, **24**, 551-600.

Crews, L.L. & Wigston, D.J. (1990) The dependence of motoneurons on their target muscle during postnatal development of the mouse. *J Neurosci*, **10**, 1643-1653.

Darbas, A., Jaegle, M., Walbeehm, E., van den Burg, H., Driegen, S., Broos, L., Uyl, M., Visser, P., Grosveld, F. & Meijer, D. (2004) Cell autonomy of the mouse claw paw mutation. *Developmental biology*, **272**, 470-482.

Dasen, J.S., De Camilli, A., Wang, B., Tucker, P.W. & Jessell, T.M. (2008) Hox repertoires for motor neuron diversity and connectivity gated by a single accessory factor, FoxP1. *Cell*, **134**, 304-316.

Dasen, J.S., Liu, J.P. & Jessell, T.M. (2003) Motor neuron columnar fate imposed by sequential phases of Hox-c activity. *Nature*, **425**, 926-933.

Dasen, J.S., Tice, B.C., Brenner-Morton, S. & Jessell, T.M. (2005) A Hox regulatory network establishes motor neuron pool identity and target-muscle connectivity. *Cell*, **123**, 477-491.

De Leon, R.D., Hodgson, J.A., Roy, R.R. & Edgerton, V.R. (1998a) Full weight-bearing hindlimb standing following stand training in the adult spinal cat. *Journal of neurophysiology*, **80**, 83-91.

De Leon, R.D., Hodgson, J.A., Roy, R.R. & Edgerton, V.R. (1998b) Locomotor capacity attributable to step training versus spontaneous recovery after spinalization in adult cats. *Journal of neurophysiology*, **79**, 1329-1340.

Demireva, E.Y., Shapiro, L.S., Jessell, T.M. & Zampieri, N. (2011) Motor neuron position and topographic order imposed by beta- and gamma-catenin activities. *Cell*, **147**, 641-652.

DeSantis, M., Berger, P.K., Laskowski, M.B. & Norton, A.S. (1992) Regeneration by skeletomotor axons in neonatal rats is topographically selective at an early stage of reinnervation. *Experimental neurology*, **116**, 229-239.

DeSantis, M. & Norman, W.P. (1993) Location and completeness of reinnervation by two types of neurons at a single target: the feline muscle spindle. *The Journal of comparative neurology*, **336**, 66-76.

Dessaud, E., Yang, L.L., Hill, K., Cox, B., Ulloa, F., Ribeiro, A., Mynett, A., Novitch, B.G. & Briscoe, J. (2007) Interpretation of the sonic hedgehog morphogen gradient by a temporal adaptation mechanism. *Nature*, **450**, 717-720.

Dickson, B.J. (2002) Molecular mechanisms of axon guidance. *Science*, **298**, 1959-1964.

Dietz, V., Colombo, G. & Jensen, L. (1994) Locomotor activity in spinal man. *Lancet*, **344**, 1260-1263.

Dietz, V., Colombo, G., Jensen, L. & Baumgartner, L. (1995) Locomotor capacity of spinal cord in paraplegic patients. *Annals of neurology*, **37**, 574-582.

Dodd, J., Morton, S.B., Karagogeos, D., Yamamoto, M. & Jessell, T.M. (1988) Spatial regulation of axonal glycoprotein expression on subsets of embryonic spinal neurons. *Neuron*, **1**, 105-116.

Dong, Z., Brennan, A., Liu, N., Yarden, Y., Lefkowitz, G., Mirsky, R. & Jessen, K.R. (1995) Neu differentiation factor is a neuron-glia signal and regulates survival,

proliferation, and maturation of rat Schwann cell precursors. *Neuron*, **15**, 585-596.

Donoghue, J.P. & Sanes, J.N. (1987) Peripheral nerve injury in developing rats reorganizes representation pattern in motor cortex. *Proceedings of the National Academy of Sciences of the United States of America*, **84**, 1123-1126.

Drew, T., Prentice, S. & Schepens, B. (2004) Cortical and brainstem control of locomotion. *Progress in brain research*, **143**, 251-261.

Duband, J.L., Tucker, G.C., Poole, T.J., Vincent, M., Aoyama, H. & Thiery, J.P. (1985) How do the migratory and adhesive properties of the neural crest govern ganglia formation in the avian peripheral nervous system? *Journal of cellular biochemistry*, **27**, 189-203.

Eccles, J.C., Eccles, R.M. & Lundberg, A. (1957) The convergence of monosynaptic excitatory afferents on to many different species of alpha motoneurones. *The Journal of physiology*, **137**, 22-50.

Edgerton, V.R., Tillakaratne, N.J., Bigbee, A.J., de Leon, R.D. & Roy, R.R. (2004) Plasticity of the spinal neural circuitry after injury. *Annual review of neuroscience*, **27**, 145-167.

Engel, A.G. & Sine, S.M. (2005) Current understanding of congenital myasthenic syndromes. *Current opinion in pharmacology*, **5**, 308-321.

Ensini, M., Tsuchida, T.N., Belting, H.G. & Jessell, T.M. (1998) The control of rostrocaudal pattern in the developing spinal cord: specification of motor neuron subtype identity is initiated by signals from paraxial mesoderm. *Development*, **125**, 969-982.

Ericson, J., Briscoe, J., Rashbass, P., van Heyningen, V. & Jessell, T.M. (1997a) Graded sonic hedgehog signaling and the specification of cell fate in the ventral neural tube. *Cold Spring Harbor symposia on quantitative biology*, **62**, 451-466.

Ericson, J., Rashbass, P., Schedl, A., Brenner-Morton, S., Kawakami, A., van Heyningen, V., Jessell, T.M. & Briscoe, J. (1997b) Pax6 controls progenitor cell identity and neuronal fate in response to graded Shh signaling. *Cell*, **90**, 169-180.

Ericson, J., Thor, S., Edlund, T., Jessell, T.M. & Yamada, T. (1992) Early stages of motor neuron differentiation revealed by expression of homeobox gene Islet-1. *Science*, **256**, 1555-1560.

Fagiolini, M. & Hensch, T.K. (2000) Inhibitory threshold for critical-period activation in primary visual cortex. *Nature*, **404**, 183-186.

Fekete, D.M. & Campero, A.M. (2007) Axon guidance in the inner ear. *The International journal of developmental biology*, **51**, 549-556.

Feltri, M.L., D'Antonio, M., Previtali, S., Fasolini, M., Messing, A. & Wrabetz, L. (1999) P0-Cre transgenic mice for inactivation of adhesion molecules in Schwann cells. *Annals of the New York Academy of Sciences*, **883**, 116-123.

Feltri, M.L., Graus Porta, D., Previtali, S.C., Nodari, A., Migliavacca, B., Cassetti, A., Littlewood-Evans, A., Reichardt, L.F., Messing, A., Quattrini, A., Mueller, U. & Wrabetz, L. (2002) Conditional disruption of beta 1 integrin in Schwann cells impedes interactions with axons. *The Journal of cell biology*, **156**, 199-209.

Feng, G., Laskowski, M.B., Feldheim, D.A., Wang, H., Lewis, R., Frisen, J., Flanagan, J.G. & Sanes, J.R. (2000) Roles for ephrins in positionally selective synaptogenesis between motor neurons and muscle fibers. *Neuron*, **25**, 295-306.

Ferguson, B.A. (1983) Development of motor innervation of the chick following dorsal-ventral limb bud rotations. *The Journal of neuroscience : the official journal of the Society for Neuroscience*, **3**, 1760-1772.

Field-Fote, E.C. (2001) Combined use of body weight support, functional electric stimulation, and treadmill training to improve walking ability in individuals with chronic incomplete spinal cord injury. *Archives of physical medicine and rehabilitation*, **82**, 818-824.

Fischer, F.R. & Peduzzi, J.D. (2007) Functional recovery in rats with chronic spinal cord injuries after exposure to an enriched environment. *J Spinal Cord Med*, **30**, 147-155.

Forssberg, H., Grillner, S. & Halbertsma, J. (1980a) The locomotion of the low spinal cat. I. Coordination within a hindlimb. *Acta physiologica Scandinavica*, **108**, 269-281.

Forssberg, H., Grillner, S., Halbertsma, J. & Rossignol, S. (1980b) The locomotion of the low spinal cat. II. Interlimb coordination. *Acta physiologica Scandinavica*, **108**, 283-295.

Fortier, P.A., Smith, A.M. & Rossignol, S. (1987) Locomotor deficits in the mutant mouse, Lurcher. *Experimental brain research. Experimentelle Hirnforschung. Experimentation cerebrale*, **66**, 271-286.

Fouad, K., Metz, G.A., Merkler, D., Dietz, V. & Schwab, M.E. (2000) Treadmill training in incomplete spinal cord injured rats. *Behavioural brain research*, **115**, 107-113.

Fouad, K., Pedersen, V., Schwab, M.E. & Brosamle, C. (2001) Cervical sprouting of corticospinal fibers after thoracic spinal cord injury accompanies shifts in evoked motor responses. *Current biology : CB*, **11**, 1766-1770.

Fridman, E.A., Hanakawa, T., Chung, M., Hummel, F., Leiguarda, R.C. & Cohen, L.G. (2004) Reorganization of the human ipsilesional premotor cortex after stroke. *Brain : a journal of neurology*, **127**, 747-758.

Gaisbauer, T. (2009) The role of Neuropilin-1 in establishing motor function. (Bachelor thesis) *Helmholtz Zentrum München - German Research Center for Environmental Health; Institute of Developmental Genetics*. Technical University Munich, pp. 42.

Gallarda, B.W., Bonanomi, D., Muller, D., Brown, A., Alaynick, W.A., Andrews, S.E., Lemke, G., Pfaff, S.L. & Marquardt, T. (2008) Segregation of axial motor and sensory pathways via heterotypic trans-axonal signaling. *Science*, **320**, 233-236.

Ghosh, A., Antonini, A., McConnell, S.K. & Shatz, C.J. (1990) Requirement for subplate neurons in the formation of thalamocortical connections. *Nature*, **347**, 179-181.

Giangrande, A. (1994) Glia in the fly wing are clonally related to epithelial cells and use the nerve as a pathway for migration. *Development*, **120**, 523-534.

Giger, R.J., Cloutier, J.F., Sahay, A., Prinjha, R.K., Levengood, D.V., Moore, S.E., Pickering, S., Simmons, D., Rastan, S., Walsh, F.S., Kolodkin, A.L., Ginty, D.D. & Geppert, M. (2000) Neuropilin-2 is required in vivo for selective axon guidance responses to secreted semaphorins. *Neuron*, **25**, 29-41.

Giger, R.J., Hollis, E.R., 2nd & Tuszynski, M.H. (2010) Guidance molecules in axon regeneration. *Cold Spring Harbor perspectives in biology*, **2**, a001867.

Gilmour, D.T., Maischein, H.M. & Nusslein-Volhard, C. (2002) Migration and function of a glial subtype in the vertebrate peripheral nervous system. *Neuron*, **34**, 577-588.

Giovannini, M., Robanus-Maandag, E., van der Valk, M., Niwa-Kawakita, M., Abramowski, V., Goutebroze, L., Woodruff, J.M., Berns, A. & Thomas, G. (2000) Conditional biallelic Nf2 mutation in the mouse promotes manifestations of human neurofibromatosis type 2. *Genes & development*, **14**, 1617-1630.

Girgis, J., Merrett, D., Kirkland, S., Metz, G.A., Verge, V. & Fouad, K. (2007) Reaching training in rats with spinal cord injury promotes plasticity and task specific recovery. *Brain : a journal of neurology*, **130**, 2993-3003.

Gomez-Pinilla, F., Villablanca, J.R., Sonnier, B.J. & Levine, M.S. (1986) Reorganization of pericruciate cortical projections to the spinal cord and dorsal column nuclei after neonatal or adult cerebral hemispherectomy in cats. *Brain research*, **385**, 343-355.

Gomez-Pinilla, F., Ying, Z., Opazo, P., Roy, R.R. & Edgerton, V.R. (2001) Differential regulation by exercise of BDNF and NT-3 in rat spinal cord and skeletal muscle. *The European journal of neuroscience*, **13**, 1078-1084.

Goodman, C.S. & Shatz, C.J. (1993) Developmental mechanisms that generate precise patterns of neuronal connectivity. *Cell*, **72 Suppl**, 77-98.

Gosgnach, S., Lanuza, G.M., Butt, S.J., Saueressig, H., Zhang, Y., Velasquez, T., Riethmacher, D., Callaway, E.M., Kiehn, O. & Goulding, M. (2006) V1 spinal neurons regulate the speed of vertebrate locomotor outputs. *Nature*, **440**, 215-219.

Goulding, M. (2009) Circuits controlling vertebrate locomotion: moving in a new direction. *Nature reviews. Neuroscience*, **10**, 507-518.

Graybiel, A.M., Aosaki, T., Flaherty, A.W. & Kimura, M. (1994) The basal ganglia and adaptive motor control. *Science*, **265**, 1826-1831.

Grillner, S. (1985) Neurobiological bases of rhythmic motor acts in vertebrates. *Science*, **228**, 143-149.

Grillner, S. (2003) The motor infrastructure: from ion channels to neuronal networks. *Nature reviews. Neuroscience*, **4**, 573-586.

Grillner, S. (2006) Biological pattern generation: the cellular and computational logic of networks in motion. *Neuron*, **52**, 751-766.

Grillner, S. & Zangger, P. (1979) On the central generation of locomotion in the low spinal cat. *Experimental brain research. Experimentelle Hirnforschung. Experimentation cerebrale*, **34**, 241-261.

Gross, T.S., Poliachik, S.L., Prasad, J. & Bain, S.D. (2010) The effect of muscle dysfunction on bone mass and morphology. *Journal of musculoskeletal & neuronal interactions*, **10**, 25-34.

Gu, C., Limberg, B.J., Whitaker, G.B., Perman, B., Leahy, D.J., Rosenbaum, J.S., Ginty, D.D. & Kolodkin, A.L. (2002) Characterization of neuropilin-1 structural features that confer binding to semaphorin 3A and vascular endothelial growth factor 165. *The Journal of biological chemistry*, **277**, 18069-18076.

Gu, C., Rodriguez, E.R., Reimert, D.V., Shu, T., Fritzsch, B., Richards, L.J., Kolodkin, A.L. & Ginty, D.D. (2003) Neuropilin-1 Conveys Semaphorin and VEGF Signaling during Neural and Cardiovascular Development. *Developmental cell*, **5**, 45-57.

Guertin, P.A. (2009) The mammalian central pattern generator for locomotion. *Brain research reviews*, **62**, 45-56.

Gutman, C.R., Ajmera, M.K. & Hollyday, M. (1993) Organization of motor pools supplying axial muscles in the chicken. *Brain research*, **609**, 129-136.

Harel, N.Y. & Strittmatter, S.M. (2006) Can regenerating axons recapitulate developmental guidance during recovery from spinal cord injury? *Nature reviews. Neuroscience*, **7**, 603-616.

Harper, J.M., Krishnan, C., Darman, J.S., Deshpande, D.M., Peck, S., Shats, I., Backovic, S., Rothstein, J.D. & Kerr, D.A. (2004) Axonal growth of embryonic

stem cell-derived motoneurons in vitro and in motoneuron-injured adult rats. *Proceedings of the National Academy of Sciences of the United States of America*, **101**, 7123-7128.

Hartmann, C. (2009) Transcriptional networks controlling skeletal development. *Current opinion in genetics & development*, **19**, 437-443.

Haupt, C., Kloos, K., Faus-Kessler, T. & Huber, A.B. (2010) Semaphorin 3A-Neuropilin-1 signaling regulates peripheral axon fasciculation and pathfinding but not developmental cell death patterns. *The European journal of neuroscience*, **31**, 1164-1172.

Helmbacher, F., Schneider-Maunoury, S., Topilko, P., Tiret, L. & Charnay, P. (2000) Targeting of the EphA4 tyrosine kinase receptor affects dorsal/ventral pathfinding of limb motor axons. *Development*, **127**, 3313-3324.

Heng, C. & de Leon, R.D. (2009) Treadmill training enhances the recovery of normal stepping patterns in spinal cord contused rats. *Experimental neurology*, **216**, 139-147.

Henry, E.W., Eicher, E.M. & Sidman, R.L. (1991) The mouse mutation claw paw: forelimb deformity and delayed myelination throughout the peripheral nervous system. *The Journal of heredity*, **82**, 287-294.

Hensch, T.K. (2004) Critical period regulation. *Annual review of neuroscience*, **27**, 549-579.

Hensch, T.K., Fagiolini, M., Mataga, N., Stryker, M.P., Baekkeskov, S. & Kash, S.F. (1998) Local GABA circuit control of experience-dependent plasticity in developing visual cortex. *Science*, **282**, 1504-1508.

Heyser, C.J. (2004) Assessment of developmental milestones in rodents. *Current protocols in neuroscience / editorial board, Jacqueline N. Crawley ... [et al.]*, **Chapter 8**, Unit 8 18.

Hickey, M.A., Kosmalska, A., Enayati, J., Cohen, R., Zeitlin, S., Levine, M.S. & Chesselet, M.F. (2008) Extensive early motor and non-motor behavioral deficits are followed by striatal neuronal loss in knock-in Huntington's disease mice. *Neuroscience*, **157**, 280-295.

Hjorth, J. & Key, B. (2002) Development of axon pathways in the zebrafish central nervous system. *The International journal of developmental biology*, **46**, 609-619.

Ho, R.K. & Goodman, C.S. (1982) Peripheral pathways are pioneered by an array of central and peripheral neurones in grasshopper embryos. *Nature*, **297**, 404-406.

Ho, S.M. & Waite, P.M. (2002) Effects of different anesthetics on the paired-pulse depression of the h reflex in adult rat. *Experimental neurology*, **177**, 494-502.

Hollyday, M. (1980) Organization of motor pools in the chick lumbar lateral motor column. *The Journal of comparative neurology*, **194**, 143-170.

Hollyday, M. & Jacobson, R.D. (1990) Location of motor pools innervating chick wing. *The Journal of comparative neurology*, **302**, 575-588.

Holtmaat, A. & Svoboda, K. (2009) Experience-dependent structural synaptic plasticity in the mammalian brain. *Nature reviews. Neuroscience*, **10**, 647-658.

Honig, M.G., Lance-Jones, C. & Landmesser, L. (1986) The development of sensory projection patterns in embryonic chick hindlimb under experimental conditions. *Developmental biology*, **118**, 532-548.

Huang, E.J. & Reichardt, L.F. (2001) Neurotrophins: roles in neuronal development and function. *Annual review of neuroscience*, **24**, 677-736.

Huber, A.B., Kania, A., Tran, T.S., Gu, C., De Marco Garcia, N., Lieberam, I., Johnson, D., Jessell, T.M., Ginty, D.D. & Kolodkin, A.L. (2005) Distinct roles for secreted semaphorin signaling in spinal motor axon guidance. *Neuron*, **48**, 949-964.

Huettl, R.E., Soellner, H., Bianchi, E., Novitch, B.G. & Huber, A.B. (2011) Npn-1 contributes to axon-axon interactions that differentially control sensory and motor innervation of the limb. *PLoS biology*, **9**, e1001020.

Ichiyama, R.M., Broman, J., Roy, R.R., Zhong, H., Edgerton, V.R. & Havton, L.A. (2011) Locomotor training maintains normal inhibitory influence on both alpha- and gamma-motoneurons after neonatal spinal cord transection. *J Neurosci*, **31**, 26-33.

Imai, T., Yamazaki, T., Kobayakawa, R., Kobayakawa, K., Abe, T., Suzuki, M. & Sakano, H. (2009) Pre-target axon sorting establishes the neural map topography. *Science*, **325**, 585-590.

Islam, S.M., Shinmyo, Y., Okafuji, T., Su, Y., Naser, I.B., Ahmed, G., Zhang, S., Chen, S., Ohta, K., Kiyonari, H., Abe, T., Tanaka, S., Nishinakamura, R., Terashima, T., Kitamura, T. & Tanaka, H. (2009) Draxin, a repulsive guidance protein for spinal cord and forebrain commissures. *Science*, **323**, 388-393.

Ivanova, A., Signore, M., Caro, N., Greene, N.D., Copp, A.J. & Martinez-Barbera, J.P. (2005) In vivo genetic ablation by Cre-mediated expression of diphtheria toxin fragment A. *Genesis*, **43**, 129-135.

Jacobs, K.M. & Donoghue, J.P. (1991) Reshaping the cortical motor map by unmasking latent intracortical connections. *Science*, **251**, 944-947.

Jadavji, N.M., Kolb, B. & Metz, G.A. (2006) Enriched environment improves motor function in intact and unilateral dopamine-depleted rats. *Neuroscience*, **140**, 1127-1138.

Jessell, T.M. (2000) Neuronal specification in the spinal cord: inductive signals and transcriptional codes. *Nature reviews. Genetics*, **1**, 20-29.

Jessen, K.R. & Mirsky, R. (2005) The origin and development of glial cells in peripheral nerves. *Nature reviews. Neuroscience*, **6**, 671-682.

Jessen, K.R., Morgan, L., Stewart, H.J. & Mirsky, R. (1990) Three markers of adult non-myelin-forming Schwann cells, 217c(Ran-1), A5E3 and GFAP: development and regulation by neuron-Schwann cell interactions. *Development*, **109**, 91-103.

Johansson, B.B. & Ohlsson, A.L. (1996) Environment, social interaction, and physical activity as determinants of functional outcome after cerebral infarction in the rat. *Experimental neurology*, **139**, 322-327.

Jurata, L.W., Pfaff, S.L. & Gill, G.N. (1998) The nuclear LIM domain interactor NLI mediates homo- and heterodimerization of LIM domain transcription factors. *The Journal of biological chemistry*, **273**, 3152-3157.

Kaas, J.H. (1991) Plasticity of sensory and motor maps in adult mammals. *Annual review of neuroscience*, **14**, 137-167.

Kaas, J.H., Qi, H.X., Burish, M.J., Gharbawie, O.A., Onifer, S.M. & Massey, J.M. (2008) Cortical and subcortical plasticity in the brains of humans, primates, and rats after damage to sensory afferents in the dorsal columns of the spinal cord. *Experimental neurology*, **209**, 407-416.

Kalcheim, C. & Le Douarin, N.M. (1986) Requirement of a neural tube signal for the differentiation of neural crest cells into dorsal root ganglia. *Developmental biology*, **116**, 451-466.

Kania, A. & Jessell, T.M. (2003) Topographic motor projections in the limb imposed by LIM homeodomain protein regulation of ephrin-A:EphA interactions. *Neuron*, **38**, 581-596.

Kania, A., Johnson, R.L. & Jessell, T.M. (2000) Coordinate roles for LIM homeobox genes in directing the dorsoventral trajectory of motor axons in the vertebrate limb. *Cell*, **102**, 161-173.

Kaplan, D.R., Hempstead, B.L., Martin-Zanca, D., Chao, M.V. & Parada, L.F. (1991) The trk proto-oncogene product: a signal transducing receptor for nerve growth factor. *Science*, **252**, 554-558.

Keller, A., Arissian, K. & Asanuma, H. (1992) Synaptic proliferation in the motor cortex of adult cats after long-term thalamic stimulation. *J Neurophysiol*, **68**, 295-308.

Kingery, W.S., Offley, S.C., Guo, T.Z., Davies, M.F., Clark, J.D. & Jacobs, C.R. (2003) A substance P receptor (NK1) antagonist enhances the widespread osteoporotic effects of sciatic nerve section. *Bone*, **33**, 927-936.

Kleim, J.A., Lussnig, E., Schwarz, E.R., Comery, T.A. & Greenough, W.T. (1996) Synaptogenesis and Fos expression in the motor cortex of the adult rat after motor skill learning. *J Neurosci*, **16**, 4529-4535.

Klein, R., Jing, S.Q., Nanduri, V., O'Rourke, E. & Barbacid, M. (1991) The trk proto-oncogene encodes a receptor for nerve growth factor. *Cell*, **65**, 189-197.

Klose, M. & Bentley, D. (1989) Transient pioneer neurons are essential for formation of an embryonic peripheral nerve. *Science*, **245**, 982-984.

Kolodkin, A.L. & Tessier-Lavigne, M. (2011) Mechanisms and molecules of neuronal wiring: a primer. *Cold Spring Harbor perspectives in biology*, **3**.

Kondo, M., Gray, L.J., Pelka, G.J., Christodoulou, J., Tam, P.P. & Hannan, A.J. (2008) Environmental enrichment ameliorates a motor coordination deficit in a mouse model of Rett syndrome--Mecp2 gene dosage effects and BDNF expression. *The European journal of neuroscience*, **27**, 3342-3350.

Koszowski, A.G., Owens, G.C. & Levinson, S.R. (1998) The effect of the mouse mutation claw paw on myelination and nodal frequency in sciatic nerves. *The Journal of neuroscience : the official journal of the Society for Neuroscience*, **18**, 5859-5868.

Kramer, E.R., Knott, L., Su, F., Dessaud, E., Krull, C.E., Helmbacher, F. & Klein, R. (2006) Cooperation between GDNF/Ret and ephrinA/EphA4 signals for motor-axon pathway selection in the limb. *Neuron*, **50**, 35-47.

Kravitz, A.V., Freeze, B.S., Parker, P.R., Kay, K., Thwin, M.T., Deisseroth, K. & Kreitzer, A.C. (2010) Regulation of parkinsonian motor behaviours by optogenetic control of basal ganglia circuitry. *Nature*, **466**, 622-626.

Krull, C.E. (2001) Segmental organization of neural crest migration. *Mechanisms of development*, **105**, 37-45.

Kuerzi, J., Brown, E.H., Shum-Siu, A., Siu, A., Burke, D., Morehouse, J., Smith, R.R. & Magnuson, D.S. (2010) Task-specificity vs. ceiling effect: step-training in shallow water after spinal cord injury. *Experimental neurology*, **224**, 178-187.

Kullander, K., Butt, S.J., Lebret, J.M., Lundfald, L., Restrepo, C.E., Rydstrom, A., Klein, R. & Kiehn, O. (2003) Role of EphA4 and EphrinB3 in local neuronal circuits that control walking. *Science*, **299**, 1889-1892.

Kuwada, J.Y. (1986) Cell recognition by neuronal growth cones in a simple vertebrate embryo. *Science*, **233**, 740-746.

Ladle, D.R., Pecho-Vrieseling, E. & Arber, S. (2007) Assembly of motor circuits in the spinal cord: driven to function by genetic and experience-dependent mechanisms. *Neuron*, **56**, 270-283.

Lampa, S.J., Potluri, S., Norton, A.S., Fusco, W. & Laskowski, M.B. (2004) Ephrin-A5 overexpression degrades topographic specificity in the mouse gluteus

maximus muscle. *Brain research. Developmental brain research*, **153**, 271-274.

Lance-Jones, C. & Landmesser, L. (1980a) Motoneurone projection patterns in embryonic chick limbs following partial deletions of the spinal cord. *The Journal of physiology*, **302**, 559-580.

Lance-Jones, C. & Landmesser, L. (1980b) Motoneurone projection patterns in the chick hind limb following early partial reversals of the spinal cord. *The Journal of physiology*, **302**, 581-602.

Lance-Jones, C. & Landmesser, L. (1981a) Pathway selection by chick lumbosacral motoneurons during normal development. *Proc R Soc Lond B Biol Sci*, **214**, 1-18.

Lance-Jones, C. & Landmesser, L. (1981b) Pathway selection by embryonic chick motoneurons in an experimentally altered environment. *Proc R Soc Lond B Biol Sci*, **214**, 19-52.

Landi, S., Sale, A., Berardi, N., Viegi, A., Maffei, L. & Cenni, M.C. (2007) Retinal functional development is sensitive to environmental enrichment: a role for BDNF. *The FASEB journal : official publication of the Federation of American Societies for Experimental Biology*, **21**, 130-139.

Landmesser, L. (1978a) The development of motor projection patterns in the chick hind limb. *The Journal of physiology*, **284**, 391-414.

Landmesser, L. (1978b) The distribution of motoneurones supplying chick hind limb muscles. *The Journal of physiology*, **284**, 371-389.

Landmesser, L. & Honig, M.G. (1986) Altered sensory projections in the chick hind limb following the early removal of motoneurons. *Developmental biology*, **118**, 511-531.

Landmesser, L.T. (2001) The acquisition of motoneuron subtype identity and motor circuit formation. *International journal of developmental neuroscience : the official journal of the International Society for Developmental Neuroscience*, **19**, 175-182.

Landmesser, L.T., O'Donovan, M.J. & Honig, M. (1983) The response of avian hindlimb motor and sensory neurons to an altered periphery. *Progress in clinical and biological research*, **110 Pt A**, 207-216.

Lanuza, G.M., Gosgnach, S., Pierani, A., Jessell, T.M. & Goulding, M. (2004) Genetic identification of spinal interneurons that coordinate left-right locomotor activity necessary for walking movements. *Neuron*, **42**, 375-386.

Laskowski, M.B. & Sanes, J.R. (1988) Topographically selective reinnervation of adult mammalian skeletal muscles. *The Journal of neuroscience : the official journal of the Society for Neuroscience*, **8**, 3094-3099.

Lawrence, D.G. & Kuypers, H.G. (1968a) The functional organization of the motor system in the monkey. I. The effects of bilateral pyramidal lesions. *Brain : a journal of neurology*, **91**, 1-14.

Lawrence, D.G. & Kuypers, H.G. (1968b) The functional organization of the motor system in the monkey. II. The effects of lesions of the descending brain-stem pathways. *Brain : a journal of neurology*, **91**, 15-36.

Le Douarin, N.M. (1986) Cell line segregation during peripheral nervous system ontogeny. *Science*, **231**, 1515-1522.

Learte, A.R. & Hidalgo, A. (2007) The role of glial cells in axon guidance, fasciculation and targeting. *Advances in experimental medicine and biology*, **621**, 156-166.

Lichtman, J.W. & Colman, H. (2000) Synapse elimination and indelible memory. *Neuron*, **25**, 269-278.

Lin, J.H., Saito, T., Anderson, D.J., Lance-Jones, C., Jessell, T.M. & Arber, S. (1998) Functionally related motor neuron pool and muscle sensory afferent subtypes defined by coordinate ETS gene expression. *Cell*, **95**, 393-407.

Lin, W., Sanchez, H.B., Deerinck, T., Morris, J.K., Ellisman, M. & Lee, K.F. (2000) Aberrant development of motor axons and neuromuscular synapses in erbB2-deficient mice. *Proceedings of the National Academy of Sciences of the United States of America*, **97**, 1299-1304.

Livet, J., Sigrist, M., Stroebel, S., De Paola, V., Price, S.R., Henderson, C.E., Jessell, T.M. & Arber, S. (2002) ETS gene Pea3 controls the central position and terminal arborization of specific motor neuron pools. *Neuron*, **35**, 877-892.

Lloyd, D.P. (1943a) Conduction and synaptic transmission of the reflex response to stretch in spinal cats. *Journal of neurophysiology*, **6**, 317-326.

Lloyd, D.P. (1943b) Neuron patterns controlling transmission of ipsilateral hind limb reflexes in cat. *Journal of neurophysiology*, **6**, 293-215.

Loring, J.F. & Erickson, C.A. (1987) Neural crest cell migratory pathways in the trunk of the chick embryo. *Developmental biology*, **121**, 220-236.

Lovely, R.G., Gregor, R.J., Roy, R.R. & Edgerton, V.R. (1990) Weight-bearing hindlimb stepping in treadmill-exercised adult spinal cats. *Brain research*, **514**, 206-218.

Low, L.K., Liu, X.B., Faulkner, R.L., Coble, J. & Cheng, H.J. (2008) Plexin signaling selectively regulates the stereotyped pruning of corticospinal axons from visual cortex. *Proceedings of the National Academy of Sciences of the United States of America*, **105**, 8136-8141.

Lupo, G., Harris, W.A. & Lewis, K.E. (2006) Mechanisms of ventral patterning in the vertebrate nervous system. *Nature reviews. Neuroscience*, **7**, 103-114.

Luria, V., Krawchuk, D., Jessell, T.M., Laufer, E. & Kania, A. (2008) Specification of motor axon trajectory by ephrin-B:EphB signaling: symmetrical control of axonal patterning in the developing limb. *Neuron*, **60**, 1039-1053.

Ma, Q., Fode, C., Guillemot, F. & Anderson, D.J. (1999) Neurogenin1 and neurogenin2 control two distinct waves of neurogenesis in developing dorsal root ganglia. *Genes & development*, **13**, 1717-1728.

Madronal, N., Lopez-Aracil, C., Rangel, A., del Rio, J.A., Delgado-Garcia, J.M. & Gruart, A. (2010) Effects of enriched physical and social environments on motor performance, associative learning, and hippocampal neurogenesis in mice. *PloS one*, **5**, e11130.

Mahanthappa, N.K., Anton, E.S. & Matthew, W.D. (1996) Glial growth factor 2, a soluble neuregulin, directly increases Schwann cell motility and indirectly promotes neurite outgrowth. *The Journal of neuroscience : the official journal of the Society for Neuroscience*, **16**, 4673-4683.

Maier, I.C. & Schwab, M.E. (2006) Sprouting, regeneration and circuit formation in the injured spinal cord: factors and activity. *Philosophical transactions of the Royal Society of London. Series B, Biological sciences*, **361**, 1611-1634.

Marin, O., Yaron, A., Bagri, A., Tessier-Lavigne, M. & Rubenstein, J.L. (2001) Sorting of striatal and cortical interneurons regulated by semaphorin-neuropilin interactions. *Science*, **293**, 872-875.

Marquardt, T., Shirasaki, R., Ghosh, S., Andrews, S.E., Carter, N., Hunter, T. & Pfaff, S.L. (2005) Coexpressed EphA receptors and ephrin-A ligands mediate opposing actions on growth cone navigation from distinct membrane domains. *Cell*, **121**, 127-139.

Martin, J.H. (2005) The corticospinal system: from development to motor control. *The Neuroscientist : a review journal bringing neurobiology, neurology and psychiatry*, **11**, 161-173.

McKinley, P.A., Jenkins, W.M., Smith, J.L. & Merzenich, M.M. (1987) Age-dependent capacity for somatosensory cortex reorganization in chronic spinal cats. *Brain research*, **428**, 136-139.

Metz, G.A. & Whishaw, I.Q. (2002) Cortical and subcortical lesions impair skilled walking in the ladder rung walking test: a new task to evaluate fore- and hindlimb stepping, placing, and co-ordination. *Journal of neuroscience methods*, **115**, 169-179.

Miller, R.H. (2002) Regulation of oligodendrocyte development in the vertebrate CNS. *Prog Neurobiol*, **67**, 451-467.

Mizuguchi, R., Sugimori, M., Takebayashi, H., Kosako, H., Nagao, M., Yoshida, S., Nabeshima, Y., Shimamura, K. & Nakafuku, M. (2001) Combinatorial roles of olig2 and neurogenin2 in the coordinated induction of pan-neuronal and subtype-specific properties of motoneurons. *Neuron*, **31**, 757-771.

Morse, L., Teng, Y.D., Pham, L., Newton, K., Yu, D., Liao, W.L., Kohler, T., Muller, R., Graves, D., Stashenko, P. & Battaglino, R. (2008) Spinal cord injury causes rapid osteoclastic resorption and growth plate abnormalities in growing rats (SCI-induced bone loss in growing rats). *Osteoporosis international : a journal established as result of cooperation between the European Foundation for Osteoporosis and the National Osteoporosis Foundation of the USA*, **19**, 645-652.

Murase, N., Duque, J., Mazzocchio, R. & Cohen, L.G. (2004) Influence of interhemispheric interactions on motor function in chronic stroke. *Annals of neurology*, **55**, 400-409.

Murphy, P., Topilko, P., Schneider-Maunoury, S., Seitanidou, T., Baron-Van Evercooren, A. & Charnay, P. (1996) The regulation of Krox-20 expression reveals important steps in the control of peripheral glial cell development. *Development*, **122**, 2847-2857.

Nakazawa, T., Komai, S., Watabe, A.M., Kiyama, Y., Fukaya, M., Arima-Yoshida, F., Horai, R., Sudo, K., Ebine, K., Delawary, M., Goto, J., Umemori, H., Tezuka, T., Iwakura, Y., Watanabe, M., Yamamoto, T. & Manabe, T. (2006) NR2B tyrosine phosphorylation modulates fear learning as well as amygdaloid synaptic plasticity. *Embo J*, **25**, 2867-2877.

Nguyen, Q.T., Sanes, J.R. & Lichtman, J.W. (2002) Pre-existing pathways promote precise projection patterns. *Nature neuroscience*, **5**, 861-867.

Niquille, M., Garel, S., Mann, F., Hornung, J.P., Otsmane, B., Chevalley, S., Parras, C., Guillemot, F., Gaspar, P., Yanagawa, Y. & Lebrand, C. (2009) Transient neuronal populations are required to guide callosal axons: a role for semaphorin 3C. *PLoS biology*, **7**, e1000230.

Nishino, J., Saunders, T.L., Sagane, K. & Morrison, S.J. (2010) Lgi4 promotes the proliferation and differentiation of glial lineage cells throughout the developing peripheral nervous system. *The Journal of neuroscience : the official journal of the Society for Neuroscience*, **30**, 15228-15240.

Nithianantharajah, J. & Hannan, A.J. (2006) Enriched environments, experience-dependent plasticity and disorders of the nervous system. *Nature reviews. Neuroscience*, **7**, 697-709.

Novitch, B.G., Chen, A.I. & Jessell, T.M. (2001) Coordinate regulation of motor neuron subtype identity and pan-neuronal properties by the bHLH repressor Olig2. *Neuron*, **31**, 773-789.

Novitch, B.G., Wichterle, H., Jessell, T.M. & Sockanathan, S. (2003) A Requirement for Retinoic Acid-Mediated Transcriptional Activation in Ventral Neural Patterning and Motor Neuron Specification. *Neuron*, **40**, 81-95.

O'Callaghan, R.M., Griffin, E.W. & Kelly, A.M. (2009) Long-term treadmill exposure protects against age-related neurodegenerative change in the rat hippocampus. *Hippocampus*, **19**, 1019-1029.

Oppenheim, R.W. (1991) Cell death during development of the nervous system. *Annual review of neuroscience*, **14**, 453-501.

Oppenheim, R.W., Prevette, D., Yin, Q.W., Collins, F. & MacDonald, J. (1991) Control of embryonic motoneuron survival in vivo by ciliary neurotrophic factor. *Science*, **251**, 1616-1618.

Pasterkamp, R.J. & Giger, R.J. (2009) Semaphorin function in neural plasticity and disease. *Current opinion in neurobiology*, **19**, 263-274.

Patel, S.D., Ciatto, C., Chen, C.P., Bahna, F., Rajebhosale, M., Arkus, N., Schieren, I., Jessell, T.M., Honig, B., Price, S.R. & Shapiro, L. (2006) Type II cadherin ectodomain structures: implications for classical cadherin specificity. *Cell*, **124**, 1255-1268.

Pearce, J.M. (2006) Von Frey's pain spots. *Journal of neurology, neurosurgery, and psychiatry*, **77**, 1317.

Pearson, K.G., Acharya, H. & Fouad, K. (2005) A new electrode configuration for recording electromyographic activity in behaving mice. *Journal of neuroscience methods*, **148**, 36-42.

Pfaff, S.L., Mendelsohn, M., Stewart, C.L., Edlund, T. & Jessell, T.M. (1996) Requirement for LIM homeobox gene Isl1 in motor neuron generation reveals a motor neuron-dependent step in interneuron differentiation. *Cell*, **84**, 309-320.

Phelan, K.A. & Hollyday, M. (1991) Embryonic development and survival of brachial motoneurons projecting to muscleless chick wings. *The Journal of comparative neurology*, **311**, 313-320.

Pierani, A., Brenner-Morton, S., Chiang, C. & Jessell, T.M. (1999) A sonic hedgehog-independent, retinoid-activated pathway of neurogenesis in the ventral spinal cord. *Cell*, **97**, 903-915.

Pietri, T. (2003) The human tissue plasminogen activator-Cre mouse: a new tool for targeting specifically neural crest cells and their derivatives in vivo. *Developmental biology*, **259**, 176-187.

Pietri, T., Eder, O., Breau, M.A., Topilko, P., Blanche, M., Brakebusch, C., Fassler, R., Thiery, J.P. & Dufour, S. (2004) Conditional beta1-integrin gene deletion in neural crest cells causes severe developmental alterations of the peripheral nervous system. *Development*, **131**, 3871-3883.

Pike, S.H., Melancon, E.F. & Eisen, J.S. (1992) Pathfinding by zebrafish motoneurons in the absence of normal pioneer axons. *Development*, **114**, 825-831.

Pittman, A.J., Law, M.Y. & Chien, C.B. (2008) Pathfinding in a large vertebrate axon tract: isotypic interactions guide retinotectal axons at multiple choice points. *Development*, **135**, 2865-2871.

Pizzorusso, T., Medini, P., Berardi, N., Chierzi, S., Fawcett, J.W. & Maffei, L. (2002) Reactivation of ocular dominance plasticity in the adult visual cortex. *Science*, **298**, 1248-1251.

Pizzorusso, T., Medini, P., Landi, S., Baldini, S., Berardi, N. & Maffei, L. (2006) Structural and functional recovery from early monocular deprivation in adult rats. *Proceedings of the National Academy of Sciences of the United States of America*, **103**, 8517-8522.

Placzek, M., Yamada, T., Tessier-Lavigne, M., Jessell, T. & Dodd, J. (1991) Control of dorsoventral pattern in vertebrate neural development: induction and polarizing properties of the floor plate. *Development*, **Suppl 2**, 105-122.

Poewe, W. & Mahlknecht, P. (2009) The clinical progression of Parkinson's disease. *Parkinsonism & related disorders*, **15 Suppl 4**, S28-32.

Polleux, F., Morrow, T. & Ghosh, A. (2000) Semaphorin 3A is a chemoattractant for cortical apical dendrites. *Nature*, **404**, 567-573.

Price, S.R., De Marco Garcia, N.V., Ranscht, B. & Jessell, T.M. (2002) Regulation of motor neuron pool sorting by differential expression of type II cadherins. *Cell*, **109**, 205-216.

Raineteau, O., Fouad, K., Bareyre, F.M. & Schwab, M.E. (2002) Reorganization of descending motor tracts in the rat spinal cord. *The European journal of neuroscience*, **16**, 1761-1771.

Raineteau, O., Fouad, K., Noth, P., Thallmair, M. & Schwab, M.E. (2001) Functional switch between motor tracts in the presence of the mAb IN-1 in the adult rat. *Proceedings of the National Academy of Sciences of the United States of America*, **98**, 6929-6934.

Raineteau, O. & Schwab, M.E. (2001) Plasticity of motor systems after incomplete spinal cord injury. *Nature reviews. Neuroscience*, **2**, 263-273.

Raper, J. & Mason, C. (2010) Cellular strategies of axonal pathfinding. *Cold Spring Harbor perspectives in biology*, **2**, a001933.

Raper, J.A., Bastiani, M.J. & Goodman, C.S. (1984) Pathfinding by neuronal growth cones in grasshopper embryos. IV. The effects of ablating the A and P axons upon the behavior of the G growth cone. *The Journal of neuroscience : the official journal of the Society for Neuroscience*, **4**, 2329-2345.

Rathelot, J.A. & Strick, P.L. (2006) Muscle representation in the macaque motor cortex: an anatomical perspective. *Proceedings of the National Academy of Sciences of the United States of America*, **103**, 8257-8262.

Ricard, D., Rogemond, V., Charrier, E., Aguera, M., Bagnard, D., Belin, M.F., Thomasset, N. & Honnorat, J. (2001) Isolation and expression pattern of human Unc-33-like phosphoprotein 6/collapsin response mediator protein 5 (Ulip6/CRMP5): coexistence with Ulip2/CRMP2 in Sema3a- sensitive oligodendrocytes. *The Journal of neuroscience : the official journal of the Society for Neuroscience*, **21**, 7203-7214.

Ricard, D., Stankoff, B., Bagnard, D., Aguera, M., Rogemond, V., Antoine, J.C., Spassky, N., Zalc, B., Lubetzki, C., Belin, M.F. & Honnorat, J. (2000) Differential expression of collapsin response mediator proteins (CRMP/ULIP) in subsets of oligodendrocytes in the postnatal rodent brain. *Molecular and cellular neurosciences*, **16**, 324-337.

Richardson, W.D., Kessaris, N. & Pringle, N. (2006) Oligodendrocyte wars. *Nature reviews. Neuroscience*, **7**, 11-18.

Rickmann, M., Fawcett, J.W. & Keynes, R.J. (1985) The migration of neural crest cells and the growth of motor axons through the rostral half of the chick somite. *Journal of embryology and experimental morphology*, **90**, 437-455.

Roelink, H., Porter, J.A., Chiang, C., Tanabe, Y., Chang, D.T., Beachy, P.A. & Jessell, T.M. (1995) Floor plate and motor neuron induction by different concentrations of the amino-terminal cleavage product of sonic hedgehog autoproteolysis. *Cell*, **81**, 445-455.

Rogers, D.C., Fisher, E.M., Brown, S.D., Peters, J., Hunter, A.J. & Martin, J.E. (1997) Behavioral and functional analysis of mouse phenotype: SHIRPA, a proposed protocol for comprehensive phenotype assessment. *Mammalian genome : official journal of the International Mammalian Genome Society*, **8**, 711-713.

Romanes, G.J. (1951) The motor cell columns of the lumbo-sacral spinal cord of the cat. *The Journal of comparative neurology*, **94**, 313-363.

Romanes, G.J. (1964) The Motor Pools of the Spinal Cord. *Progress in brain research*, **11**, 93-119.

Rosenzweig, E.S., Courtine, G., Jindrich, D.L., Brock, J.H., Ferguson, A.R., Strand, S.C., Nout, Y.S., Roy, R.R., Miller, D.M., Beattie, M.S., Havton, L.A., Bresnahan, J.C., Edgerton, V.R. & Tuszynski, M.H. (2010) Extensive spontaneous plasticity of corticospinal projections after primate spinal cord injury. *Nature neuroscience*, **13**, 1505-1510.

Rossignol, S. (1996) Neural control of stereotypic limb movements. In Rowell, L.B., Sheperd, J.T. (eds) *Handbook of physiology*. Oxford University Press, New York, pp. 173-216.

Rossignol, S. (2006) Plasticity of connections underlying locomotor recovery after central and/or peripheral lesions in the adult mammals. *Philosophical transactions of the Royal Society of London. Series B, Biological sciences*, **361**, 1647-1671.

Rossignol, S., Dubuc, R. & Gossard, J.P. (2006) Dynamic sensorimotor interactions in locomotion. *Physiological reviews*, **86**, 89-154.

Rowitch, D.H., Lu, Q.R., Kessaris, N. & Richardson, W.D. (2002) An 'oligarchy' rules neural development. *Trends in neurosciences*, **25**, 417-422.

Sahay, A., Molliver, M.E., Ginty, D.D. & Kolodkin, A.L. (2003) Semaphorin 3F is critical for development of limbic system circuitry and is required in neurons for selective CNS axon guidance events. *The Journal of neuroscience : the official journal of the Society for Neuroscience*, **23**, 6671-6680.

Sale, A., Berardi, N. & Maffei, L. (2009) Enrich the environment to empower the brain. *Trends in neurosciences*, **32**, 233-239.

Sale, A., Maya Vetencourt, J.F., Medini, P., Cenni, M.C., Baroncelli, L., De Pasquale, R. & Maffei, L. (2007) Environmental enrichment in adulthood promotes amblyopia recovery through a reduction of intracortical inhibition. *Nature neuroscience*, **10**, 679-681.

Sanes, J.R. & Lichtman, J.W. (1999) Development of the vertebrate neuromuscular junction. *Annual review of neuroscience*, **22**, 389-442.

Sanes, J.R. & Yamagata, M. (2009) Many paths to synaptic specificity. *Annu Rev Cell Dev Biol*, **25**, 161-195.

Sauka-Spengler, T. & Bronner-Fraser, M. (2008) A gene regulatory network orchestrates neural crest formation. *Nature reviews. Molecular cell biology*, **9**, 557-568.

Schmalbruch, H., Jensen, H.J., Bjaerg, M., Kamieniecka, Z. & Kurland, L. (1991) A new mouse mutant with progressive motor neuronopathy. *Journal of neuropathology and experimental neurology*, **50**, 192-204.

Sepp, K.J. & Auld, V.J. (2003) Reciprocal interactions between neurons and glia are required for Drosophila peripheral nervous system development. *The Journal of neuroscience : the official journal of the Society for Neuroscience*, **23**, 8221-8230.

Sepp, K.J., Schulte, J. & Auld, V.J. (2001) Peripheral glia direct axon guidance across the CNS/PNS transition zone. *Developmental biology*, **238**, 47-63.

Shah, V., Drill, E. & Lance-Jones, C. (2004) Ectopic expression of Hoxd10 in thoracic spinal segments induces motoneurons with a lumbosacral molecular profile and axon projections to the limb. *Developmental dynamics : an official publication of the American Association of Anatomists*, **231**, 43-56.

Shanmugarajan, S., Tsuruga, E., Swoboda, K.J., Maria, B.L., Ries, W.L. & Reddy, S.V. (2009) Bone loss in survival motor neuron (Smn(-/-) SMN2) genetic mouse model of spinal muscular atrophy. *The Journal of pathology*, **219**, 52-60.

Sharma, K., Leonard, A.E., Lettieri, K. & Pfaff, S.L. (2000) Genetic and epigenetic mechanisms contribute to motor neuron pathfinding. *Nature*, **406**, 515-519.

Shimizu, M., Murakami, Y., Suto, F. & Fujisawa, H. (2000) Determination of cell adhesion sites of neuropilin-1. *The Journal of cell biology*, **148**, 1283-1293.

Song, H., Ming, G., He, Z., Lehmann, M., McKerracher, L., Tessier-Lavigne, M. & Poo, M. (1998) Conversion of neuronal growth cone responses from repulsion to attraction by cyclic nucleotides. *Science*, **281**, 1515-1518.

Spassky, N., de Castro, F., Le Bras, B., Heydon, K., Queraud-LeSaux, F., Bloch-Gallego, E., Chedotal, A., Zalc, B. & Thomas, J.L. (2002) Directional guidance of oligodendroglial migration by class 3 semaphorins and netrin-1. *The Journal of neuroscience : the official journal of the Society for Neuroscience*, **22**, 5992-6004.

Sullivan, G.E. (1962) Anatomy and embryology of the wing musculature of the domestic fowl (Gallus). *Australian J Zool*, **10**, 458-518.

Sundermeier, J. (2009) Analysis of molecular mechanisms of adaptive plasticity: Anatomical basis. (Bachelor thesis) *Helmholtz Zentrum München - German Research Center for Environmental Health; Institute of Developmental Genetics*. University of Osnabrück, pp. 42.

Surmeli, G., Akay, T., Ippolito, G.C., Tucker, P.W. & Jessell, T.M. (2011) Patterns of spinal sensory-motor connectivity prescribed by a dorsoventral positional template. *Cell*, **147**, 653-665.

Suster, M.L. & Bate, M. (2002) Embryonic assembly of a central pattern generator without sensory input. *Nature*, **416**, 174-178.

Swanson, G.J. & Lewis, J. (1986) Sensory nerve routes in chick wing buds deprived of motor innervation. *Journal of embryology and experimental morphology*, **95**, 37-52.

Sweeney, L.B., Couto, A., Chou, Y.H., Berdnik, D., Dickson, B.J., Luo, L. & Komiyama, T. (2007) Temporal target restriction of olfactory receptor neurons by Semaphorin-1a/PlexinA-mediated axon-axon interactions. *Neuron*, **53**, 185-200.

Tada, K., Ohshita, S., Yonenobu, K., Ono, K., Satoh, K. & Shimizu, N. (1979) Development of spinal motoneuron innervation of the upper limb muscle in the rat. *Exp Brain Res*, **35**, 287-293.

Tanabe, Y., William, C. & Jessell, T.M. (1998) Specification of motor neuron identity by the MNR2 homeodomain protein. *Cell*, **95**, 67-80.

Taylor, A.C. (1944) Selectivity of nerve fibers from the dorsal and ventral root in the development of the frog limb. *The Journal of experimental zoology*, **96**, 159-185.

Teillet, M.A., Kalcheim, C. & Le Douarin, N.M. (1987) Formation of the dorsal root ganglia in the avian embryo: segmental origin and migratory behavior of neural crest progenitor cells. *Developmental biology*, **120**, 329-347.

Tessier-Lavigne, M. & Goodman, C.S. (1996) The molecular biology of axon guidance. *Science*, **274**, 1123-1133.

Tillakaratne, N.J., de Leon, R.D., Hoang, T.X., Roy, R.R., Edgerton, V.R. & Tobin, A.J. (2002) Use-dependent modulation of inhibitory capacity in the feline lumbar spinal cord. *The Journal of neuroscience : the official journal of the Society for Neuroscience*, **22**, 3130-3143.

Tosney, K.W. & Hageman, M.S. (1989) Different subsets of axonal guidance cues are essential for sensory neurite outgrowth to cutaneous and muscle targets in the dorsal ramus of the embryonic chick. *The Journal of experimental zoology*, **251**, 232-244.

Tosney, K.W. & Landmesser, L.T. (1985a) Development of the major pathways for neurite outgrowth in the chick hindlimb. *Developmental biology*, **109**, 193-214.

Tosney, K.W. & Landmesser, L.T. (1985b) Specificity of early motoneuron growth cone outgrowth in the chick embryo. *The Journal of neuroscience : the official journal of the Society for Neuroscience*, **5**, 2336-2344.

Tran, T.S., Rubio, M.E., Clem, R.L., Johnson, D., Case, L., Tessier-Lavigne, M., Huganir, R.L., Ginty, D.D. & Kolodkin, A.L. (2009) Secreted semaphorins control spine distribution and morphogenesis in the postnatal CNS. *Nature*, **462**, 1065-1069.

Tremml, P., Lipp, H.P., Muller, U., Ricceri, L. & Wolfer, D.P. (1998) Neurobehavioral development, adult openfield exploration and swimming navigation learning in mice with a modified beta-amyloid precursor protein gene. *Behavioural brain research*, **95**, 65-76.

Truckenbrodt, A. (2009) The role of the axon guidance receptor Neuropilin-1 in oligodendrocytes during mouse development. (Bachelor thesis) *Helmholtz Zentrum München - German Research Center for Environmental Health; Institute of Developmental Genetics*. Technical University Munich, pp. 38.

Tsuchida, T., Ensini, M., Morton, S.B., Baldassare, M., Edlund, T., Jessell, T.M. & Pfaff, S.L. (1994) Topographic organization of embryonic motor neurons defined by expression of LIM homeobox genes. *Cell*, **79**, 957-970.

Ugolini, G. (1995) Specificity of rabies virus as a transneuronal tracer of motor networks: transfer from hypoglossal motoneurons to connected second-order

and higher order central nervous system cell groups. *The Journal of comparative neurology*, **356**, 457-480.

Ugolini, G. (2010) Advances in viral transneuronal tracing. *Journal of neuroscience methods*, **194**, 2-20.

Vallstedt, A., Muhr, J., Pattyn, A., Pierani, A., Mendelsohn, M., Sander, M., Jessell, T.M. & Ericson, J. (2001) Different levels of repressor activity assign redundant and specific roles to Nkx6 genes in motor neuron and interneuron specification. *Neuron*, **31**, 743-755.

van Hedel, H.J. & Dietz, V. (2010) Rehabilitation of locomotion after spinal cord injury. *Restorative neurology and neuroscience*, **28**, 123-134.

van Praag, H., Kempermann, G. & Gage, F.H. (2000) Neural consequences of environmental enrichment. *Nature reviews. Neuroscience*, **1**, 191-198.

Vander Kooi, C.W., Jusino, M.A., Perman, B., Neau, D.B., Bellamy, H.D. & Leahy, D.J. (2007) Structural basis for ligand and heparin binding to neuropilin B domains. *Proceedings of the National Academy of Sciences of the United States of America*, **104**, 6152-6157.

Vanderhaeghen, P. & Cheng, H.J. (2010) Guidance molecules in axon pruning and cell death. *Cold Spring Harbor perspectives in biology*, **2**, a001859.

Vanderhorst, V.G. & Holstege, G. (1997) Organization of lumbosacral motoneuronal cell groups innervating hindlimb, pelvic floor, and axial muscles in the cat. *The Journal of comparative neurology*, **382**, 46-76.

Von Holst, E. (1935) Erregungsbildung und Erregungsleitung im Fischrückenmark [Generation and propagation of excitation in the fish spinal cord]. *Pflügers Arch Eur J Physiol*, **235**, 345-359.

Vrieseling, E. & Arber, S. (2006) Target-induced transcriptional control of dendritic patterning and connectivity in motor neurons by the ETS gene Pea3. *Cell*, **127**, 1439-1452.

Walsh, M.K. & Lichtman, J.W. (2003) In vivo time-lapse imaging of synaptic takeover associated with naturally occurring synapse elimination. *Neuron*, **37**, 67-73.

Wang, G. & Scott, S.A. (1999) Independent development of sensory and motor innervation patterns in embryonic chick hindlimbs. *Developmental biology*, **208**, 324-336.

Wang, L., Klein, R., Zheng, B. & Marquardt, T. (2011) Anatomical coupling of sensory and motor nerve trajectory via axon tracking. *Neuron*, **71**, 263-277.

Warner, S.E., Sanford, D.A., Becker, B.A., Bain, S.D., Srinivasan, S. & Gross, T.S. (2006) Botox induced muscle paralysis rapidly degrades bone. *Bone*, **38**, 257-264.

Watson, S.S., Riordan, T.J., Pryce, B.A. & Schweitzer, R. (2009) Tendons and muscles of the mouse forelimb during embryonic development. *Developmental dynamics : an official publication of the American Association of Anatomists*, **238**, 693-700.

Webster, H.d.F. & Favilla, J.T. (1984) Development of peripheral nerve fibers. In Dyck, P.J., Thomas, P.K., Lambert, E.H., Bunge, R. (eds) *Peripheral Neuropathy*. W. B. Sanders, Philadelphia, pp. 329-359.

Wernig, A., Nanassy, A. & Muller, S. (1998) Maintenance of locomotor abilities following Laufband (treadmill) therapy in para- and tetraplegic persons: follow-up studies. *Spinal cord*, **36**, 744-749.

White, F.A. & Behar, O. (2000) The development and subsequent elimination of aberrant peripheral axon projections in Semaphorin3A null mutant mice. *Developmental biology*, **225**, 79-86.

Wichterle, H., Lieberam, I., Porter, J.A. & Jessell, T.M. (2002) Directed differentiation of embryonic stem cells into motor neurons. *Cell*, **110**, 385-397.

Wiesel, T.N. & Hubel, D.H. (1963) Single-Cell Responses in Striate Cortex of Kittens Deprived of Vision in One Eye. *Journal of neurophysiology*, **26**, 1003-1017.

Wigston, D.J. & Sanes, J.R. (1982) Selective reinnervation of adult mammalian muscle by axons from different segmental levels. *Nature*, **299**, 464-467.

Winzeck, S. (2011) Neuroanatomical development of Sema3F mutant mice and influence of enriched environment housing (Internship Report) *Helmholtz Zentrum München - German Research Center for Environmental Health; Institute of Developmental Genetics*. University of Applied Sciences Munich, pp. 19.

Wolpaw, J.R. (1997) The complex structure of a simple memory. *Trends in neurosciences*, **20**, 588-594.

Wu, Y., Wang, G., Scott, S.A. & Capecchi, M.R. (2008) Hoxc10 and Hoxd10 regulate mouse columnar, divisional and motor pool identity of lumbar motoneurons. *Development*, **135**, 171-182.

Xiang, M., Zhou, L., Macke, J.P., Yoshioka, T., Hendry, S.H., Eddy, R.L., Shows, T.B. & Nathans, J. (1995) The Brn-3 family of POU-domain factors: primary structure, binding specificity, and expression in subsets of retinal ganglion cells and somatosensory neurons. *The Journal of neuroscience : the official journal of the Society for Neuroscience*, **15**, 4762-4785.

Xu, N.J. & Henkemeyer, M. (2009) Ephrin-B3 reverse signaling through Grb4 and cytoskeletal regulators mediates axon pruning. *Nature neuroscience*, **12**, 268-276.

Yamada, T., Placzek, M., Tanaka, H., Dodd, J. & Jessell, T.M. (1991) Control of cell pattern in the developing nervous system: polarizing activity of the floor plate and notochord. *Cell*, **64**, 635-647.

Yin, H.H. & Knowlton, B.J. (2006) The role of the basal ganglia in habit formation. *Nature reviews. Neuroscience*, **7**, 464-476.

Yu, W.M., Feltri, M.L., Wrabetz, L., Strickland, S. & Chen, Z.L. (2005) Schwann cell-specific ablation of laminin gamma1 causes apoptosis and prevents proliferation. *The Journal of neuroscience : the official journal of the Society for Neuroscience*, **25**, 4463-4472.

Z'Graggen, W.J., Fouad, K., Raineteau, O., Metz, G.A., Schwab, M.E. & Kartje, G.L. (2000) Compensatory sprouting and impulse rerouting after unilateral pyramidal tract lesion in neonatal rats. *The Journal of neuroscience : the official journal of the Society for Neuroscience*, **20**, 6561-6569.

Zadicario, P., Avni, R., Zadicario, E. & Eilam, D. (2005) 'Looping'-an exploration mechanism in a dark open field. *Behavioural brain research*, **159**, 27-36.

Zhou, Q., Choi, G. & Anderson, D.J. (2001) The bHLH transcription factor Olig2 promotes oligodendrocyte differentiation in collaboration with Nkx2.2. *Neuron*, **31**, 791-807.

Zlatic, M., Li, F., Strigini, M., Grueber, W. & Bate, M. (2009) Positional cues in the Drosophila nerve cord: semaphorins pattern the dorso-ventral axis. *PLoS biology*, **7**, e1000135.

VII APPENDIX

VII.1 Abbreviations

A	Adenine (Purine base)
	Ampere
aa	Amino acid
AChR	Nicotinic acetylcholine receptor
ALS	Amyotrophic lateral sclerosis
BB	*Biceps brachii*
BDA	Biotinylated dextran amine
BDNF	Brain-derived neurotrophic factor
BMC	Bone mineral content
BMP	Bone morphogenetic protein
BOS	Base of support
bp	Base pairs
°C	Celsius
C	Cytosine (Pyrimidine base)
c	Concentration
CAM	Cell adhesion molecule
cAMP	Cyclic adenosine monophosphate
cGMP	Cyclic guanosine monophosphate
clp	Claw paw
CNS	Central nervous system
CPG	Central pattern generator
CSPG	Chondroitin sulphate proteoglycan
CST	Corticospinal tract
CTB	Cholera toxin B
Cy2	Cyanine-2 (green)
Cy3	Cyanine-3 (red)
d	Day(s)
dest.	Destilled

DMEM	Dulbecco’s modified eagle medium
DMSO	Dimethylsulfoxide
DNA	Desoxyribonucleic acid
dNTP	Desoxy-nucleotide-tri-phosphate
DRG	Dorsal root ganglion
DT-A	Diphtheria toxin-A
E	Embryonic day
ECM	Extracellular matrix
ECRB	Extensor carpi radialis brevis
ECRL	Extensor carpi radialis longus
EDTA	Ethylenediaminetetraacetic acid
EE	Enriched environment
eGFP	Enhanced green fluorescent protein
EMG	Electromyogram
EtBr	Ethidium bromide
EtOH	Ethanol
ETS	E-twenty six transcription factors
FCS	Fetal calf serum
FCU	Flexor carpi ulnaris
FGF	Fibroblast growth factor
g	Gram
G	Guanine (Purine base)
GABA	Gamma-Aminobutyric acid
GDNF	Glial-cell-derived neurotrophic factor
GFP	Green fluorescent protein
h	Hour(s)
Hb9	Homeobox gene Hb9
HD	Homeodomain
HH	Hamburger-Hamilton stage
Ht-PA	Human tissue plasminogen activator
Isl1	LIM homeodomain protein Islet-1
kb	Kilobase pairs
l	Litre
Lim1	LIM homeodomain protein Lim1

LMC	Lateral motor column
LMCl	Lateral motor column lateral
LMCm	Lateral motor column medial
M	Molar (mol/l)
m	Mili
MetOH	Methanol
MIA	Multiple image alignment
min	Minute(s)
mm	Milimetre
MMC	Medial motor column
MMCl	Medial motor column lateral
MMCm	Medial motor column medial
MN	Motor neuron
mRNA	Messenger RNA
n	Nano
	Sample size
N.	Nerv
NCC	Neural crest cell
NGF	Nerve growth factor
nm	Nanometre
NMJ	Neuromuscular junction
Npn	Neuropilin
NT-3	Neurotrophin-3
OPC	Oligodendrocyte precursor
OSN	Olfactory sensory neurons
P	Postnatal day
PBS	Phosphate buffered saline
PCR	Polymerase chain reaction
PFA	Paraformaldehyde
pmn	Progressive motor neuronopathy
PNN	Perineuronal net
PNS	Peripheral nervous system
RA	Retinoic acid
RNA	Ribonucleic acid

rpm	Rounds per minute
s	Second(s)
SCI	Spinal cord injury
SD	Standard deviation
SEM	Standard error of the mean
Sema	Semaphorin
Shh	Sonic hedgehog
SHIRPA	**S**mithKline Beecham, **H**arwell, **I**mperial College, **R**oyal London Hospital, **p**henotype **a**ssessment
T	Temperature Thymine (Pyrimidine base)
TAE	Tris-acetat EDTA buffer
TB	*Triceps brachii*
TE	Tris/EDTA buffer
TEM	Transmission electron microscopy
TF	Transcription factor
Tm	Melting temperature
TrK	Tyrosine receptor kinase
UTR	Untranslated region
UV	Ultraviolet
V	Volt
Wnts	Wingless-and-Int
wt	Wildtype
µ	Micro

VII.2 Index of figures

Figure 1: Components of mono- and polysynaptic reflex circuits. 8

Figure 2: Supraspinal and local control of locomotion in vertebrates. 10

Figure 3: Induction of progenitor domains in the neural tube and subsequent generation of motor neurons. 12

Figure 4: Transcriptional network of Hox genes for columnar and pool specification of motor neurons. 14

Figure 5: Functional diversity of neuronal guidance cues. 16

Figure 6: Guidance of motor axons to dorsal and ventral limb targets. 19

Figure 7: Spontaneous sprouting in the CNS and long-distance regeneration in the PNS. 23

Figure 8: Partial genetic ablation of *Olig2-Cre*$^{+}$ motor or *Ht-PA-Cre*$^{+}$ sensory neurons upon tissue-specific DT-A^{floxed} activation. 51

Figure 9: Loss of motor neurons in *Olig2-Cre*$^{+}$;DT-A^{floxed} mice delays plexus formation of outgrowing sensory projections. 53

Figure 10: Increased variability in the formation of the plexus und spinal nerves in *Olig2-Cre*$^{+}$;*DT-A*^{floxed} mice. 54

Figure 11: Effects of early motor neuron ablation on sensory projections are maintained at E12.5. 55

Figure 12: Impaired fasciculation of motor projections in *Ht-PA-Cre*$^{+}$;DT-A^{floxed} mice. 57

Figure 13: Elimination of sensory neurons impairs the correct formation of motor projections. 58

Figure 14: *Olig2-Cre*$^{+}$;*Npn-1*$^{cond-/-}$ mutants reveal forepaw posture abnormalities and reduced body weight. 61

Figure 15: Loss of active extension in the distal forelimb of *Olig2-Cre^{+}; Npn-1$^{cond-/-}$* mutants upon stimulation of *N.radial.* 62

Figure 16: Reduced forelimb extensor muscle area in newborn *Olig2-Cre^{+}; Npn-1$^{cond-/-}$* mutants. 64

Figure 17: Gait irregularities in *Olig2-Cre^{+};Npn-1$^{cond-/-}$* mutants. 65

Figure 18: Persistent deficits in skilled locomotion in *Olig2-Cre^{+};Npn-1$^{cond-/-}$* mutants. 66

Figure 19: Distal forelimb bone malformations in *Olig2-Cre^{+};Npn-1$^{cond-/-}$* mutants. 68

Figure 20: Normal myelination of PNS forelimb nerves in *Olig2-Cre^{+};Npn-1$^{cond-/-}$* and *Npn-1^{Sema-}* mutants. 70

Figure 21: Significant changes in axon size and number of fibers in *N.radial* of *Olig2-Cre^{+}; Npn-1$^{cond-/-}$* mutants. 71

Figure 22: Motor coordination deficits improve during postnatal development in *Sema3F* mutants. 75

Figure 23: Locomotor deficits in *Npn-2* mutants. 77

Figure 24: Anatomical analysis of distal forelimb motor pools representation in the spinal cord. 79

Figure 25: Housing in enriched environments induces recovery of behavioural and anatomical deficits in *Sema3F* mutants. 82

Figure 26: Synchronous activation of antagonistic forelimb muscles in *Sema3F* mutants. 84

Figure 27: Schematic drawing of the full length Npn-1 receptor. 98

VII.3 Index of tables

Table 1: Summary of motor skills in *Sema3F* and *Npn-2* mutants tested at 4, 8 and 12 weeks. 86

VII.4 Acknowledgements

Last but not least, I want to acknowledge the people who accompanied me during my time as a graduate student and contributed to this work. I would like to express my gratitude particularly to:

Prof. Dr. Wolfgang Wurst for giving me the opportunity to do this research topic in the Institute of Developmental Genetics and present it on a regular basis in institute seminars for scientific discussions with a broad audience. Furthermore, I want to thank for his interest in my work and thesis.

Dr. Andrea Huber Brösamle for providing me fascinating and interesting research projects, for her continuous support and advice, for the freedom to also bring in and pursue my own ideas and for the opportunity to present and discuss my research data on several national and international scientific conferences. I want to thank her especially for “infecting“ me with her fascination for developmental neurobiology and immensly increasing my knowledge in this field.

Dr. Sabine Hölter-Koch & Prof. Dr. Karim Fouad, my thesis committee, for the fruitful discussions, suggestions and ideas during our meetings.

Prof. Dr. Erwin Grill for being chairman of my doctorate examination board.

Prof. Dr. Magdalena Götz for her interest in my work and volunteering as examiner of my thesis.

Prof. Dr. Karim Fouad for teaching me the technical principles to set up the electrophysiology as a new method in the institute, scientific dicussion of EMG recordings and manuscripts for publication.

Dr. Sabine Hölter-Koch and her behaviour team for fruitful discussions, suggestions and ideas as well as advice in mouse behaviour experiments.

Furthermore, I am indebted to the students (**Anja Osterwald, Anna Truckenbrodt, Tobias Gaisbauer, Christine John, Julia Sundermeier and Stefan Winzeck**) whom I supervised during my time as a graduate student for their enthusiasm and their individual contribution to this thesis. I want to thank especially:

Anna Truckenbrodt (internship and Bachelor thesis) for helping me with the analysis of postnatal *Olig2-Cre*$^{+}$*;Npn-1*$^{cond-/-}$ mutants from the beginning and

performing the analysis on the migration and maturation of newly generated OPC and myelination capabilities of mature oligodendrocytes.

Tobias Gaisbauer (Bachelor thesis) for establishing the NMJ staining with me and later on performing the analysis of NMJs in two extensor muscles of *Olig2-Cre*$^{+}$*; Npn-1*$^{cond-/-}$ mutants and controls.

Julia Sundermeier (Bachelor thesis and student assistant) for establishing the tissue processing and reconstruction of spinal motor pool representation with me. Furthermore, I want to thank her for her excellent technical help in spinal motor pool reconstruction during her time as a student assistant in the lab.

Stefan Winzeck (Internship) for establishing and performing the quantitative evaluation of spinal motor pool distribution and vGlut1 staining. In particular, I want to thank him for his valuable mathematical and informatical input and suggestions.

Prof. Dr. Fabian Theis for his expert support in mathematical spline fit analysis.

José Martínez-Hernández for starting the enriched environment housing with me and proposing BDA tracing techniques during his time as a postdoc in our lab.

Christian Brösamle for teaching me the anteriograde BDA tracing technique in the motor cortex.

Christian Cohrs (Institute of Experimental Genetics) for performing the X-ray and Alcian blue/Alizarin red experiments.

Luise Jennen & Dr. Annette Feuchtinger (Institute of Pathology) for TEM microscopy and analysis with Definiens software.

The **animal care taker of the Fieder team**, especially **Manuela Müller** and **Clarinda Hofer**, for their excellent care of the animals in the mouse facilities and their helpful technical assistance.

Former and present members of the **Neuronal circuits in Health and Disease (AHB) group** (**Corinna, Daniela, Elisa, Emre, Georg, Jana, Janice, Julia, José, Karina, Micha, Nikola, Ruth, Sandra** and **Steffi**) for advice with experiments, discussion of scientific data as well as the fun and laughter during my lab-time.

My office mates from the **Behaviour team, Lisa, Anni, Lillian, Bettina, Albert, Jan** and **Sabine** for the practical advice with mouse behaviour issues, the great atmosphere and the regular cake sessions in the office.

Finally, my **dearest ones**... my parents Barbara & Martin, my brother Benjamin, my friends and Roland S., above all for their support but also for a 1000 things more.